The University of Southern Mississippi
The Aquila Digital Community

Master's Theses

Spring 5-1-2021

How Historic Shipwrecks Influence Dispersal of Deep-Sea Microbiomes

Rachel Moseley

Follow this and additional works at: https://aquila.usm.edu/masters_theses

 Part of the Environmental Microbiology and Microbial Ecology Commons

Recommended Citation

Moseley, Rachel, "How Historic Shipwrecks Influence Dispersal of Deep-Sea Microbiomes" (2021). *Master's Theses*. 810.
https://aquila.usm.edu/masters_theses/810

This Masters Thesis is brought to you for free and open access by The Aquila Digital Community. It has been accepted for inclusion in Master's Theses by an authorized administrator of The Aquila Digital Community. For more information, please contact Joshua.Cromwell@usm.edu.

HOW HISTORIC SHIPWRECKS INFLUENCE DISPERSAL OF DEEP-SEA MICROBIOMES

by

Rachel Moseley

A Thesis
Submitted to the Graduate School,
the College of Arts and Sciences
and the School of Ocean Science and Engineering
at The University of Southern Mississippi
in Partial Fulfillment of the Requirements
for the Degree of Master of Science

Approved by:

Dr. Leila J. Hamdan, Committee Chair
Dr. Chet Rakocinski
Dr. Wei Wu

May 2021

COPYRIGHT BY

Rachel Moseley

2021

Published by the Graduate School

ABSTRACT

This thesis investigates how historic shipwrecks potentially shape dispersal of deep-sea microbiomes. Processes impacting dispersal of microbiomes around artificial structures in the ocean and how they connect to other deep-sea habitats is unknown. Dispersal processes are explained for some macroorganisms by theories in ecology, specifically the Theory of Island Biogeography and the Wooden Stepping Stone hypothesis. These have not been investigated for microorganisms, and thus this work will probe if they are applicable to microbial biogeography in this habitat. Experiments were conducted to establish new "island-like" features in near proximity (25-125 m) to wooden-hulled historic shipwrecks in the northern Gulf of Mexico (GoM). The experiments were to determine if microbiomes exhibit dispersal patterns like those seen for macroorganisms. Biofilms formed on experiments, along with sediment and water samples collected near the shipwrecks were analyzed for microbiome richness, diversity, phylogenetic composition and determination of the source of taxa to biofilms. Investigation into the source of biofilms revealed the majority source was unknown for bacteria and archaea; however, archaea at one site located at approximately 1800 m water depth had high source proportion estimates for sediment. Richness and diversity decreased with decreasing proximity to both shipwrecks revealing historic shipwrecks may function as island-like habitats. The phylogenetic composition analysis shows strong selection by wood type for bacteria, and highlights differences in bacteria, archaea, and fungi dispersal patterns. The results of this thesis show that built structures, like shipwrecks, impact microbial biogeography in the deep sea.

ACKNOWLEDGMENTS

I would like to acknowledge my thesis advisor, Dr. Leila Hamdan, for her time and energy in guiding me and assisting me through this degree. I thank my committee members, Dr. Chet Rakocinski and Dr. Wei Wu, for their time and assistance. I acknowledge the collaborators on this project, Melanie Damour, Doug Jones, Dr. Warren Wood, Max Woolsey, and Dr. Justyna Hampel for providing their time, data, and assistance. I would also like to thank my fellow lab members, Dr. Justyna Hampel, Rachel Mugge, and Anirban Ray, for their support, assistance, and encouragement throughout my degree work.

DEDICATION

I would like to dedicate this thesis to my daughter, Molly Moseley. I would like to thank my husband, Greg, for his support. I would also like to thank my parents, Jason and Deanna, and my brother, Michael, for always helping me reach my goals.

TABLE OF CONTENTS

LIST OF TABLES

LIST OF ILLUSTRATIONS

LIST OF ABBREVIATIONS

ADCP	Acoustic Doppler Current Profiler
ASV	Amplicon Sequence Variants
CTD	Conductivity, Temperature, and Depth
EPS	Extracellular Polymeric Substances
GoM	Gulf of Mexico
IMR	Integrated Microbiome Resource
ITS2	Internal Transcribe Spacer Region 2
MRE	Microbial Recruitment Experiment
NOAA	National Oceanic and Atmospheric Administration
OTU	Operational Taxonomic Unit
PCR	Polymerase Chain Reaction
QIIME2	Quantitative Insights into Microbial Ecology 2
ROV	Remotely Operated Vehicle
SCHEMA	Shipwreck Corrosion, Hydrocarbon Exposure, Microbiology, and Archaeology
TIB	The Theory of Island Biogeography
USM	The University of Southern Mississippi

CHAPTER I - INVESTIGATING THE SOURCE OF DEEP-SEA MICROBIOMES NEAR HISTORIC SHIPWRECKS

1.1 Introduction

1.1.1 Microbial Biogeography

Microbial biogeography is the study of the distribution of microorganisms across space and time (Martiny *et al*., 2006). Ideas surrounding microbial biogeography were formulated early in the field of Microbial Ecology, with the concepts posited by Marcus Beijerinck of the principal of microbial ubiquity (Beijerinck, 1913). The concept, in short, states that all microorganisms are everywhere at any time. Later, Lourens Baas-Becking postulated that with regards to environmental microorganisms, "Everything is everywhere, but the environment selects" (Baas-Becking, 1934). This statement is based on a few different aspects of microorganism biology and ecology. Microorganisms are highly abundant and small, so they have high dispersal potential. Microorganisms are also highly adaptable and metabolically diverse. Due to these traits, there is the potential for any microorganism to be anywhere at any given time. However, when a new condition arises in the environment, a certain sub-set of those microorganisms may thrive under new conditions and become dominant in the environment. In short, all microorganisms can occupy any available habitat, but different phylotypes (an observed similarity that classifies a group of organisms by their genetic similarity) will be dominant in different habitats. While neither Beijerinck nor Baas-Becking used the terminology "biogeography", their ideas provide the backbone for studies of microbial biogeography, and advancements in molecular biology through the early 2000s provide the analytical framework for study.

Arguments have been made against microorganisms exhibiting biogeographical patterns, however no arguments are clear enough to have discouraged ongoing study of microbial biogeography. In the early 2000s, theories were put forward that large microbial populations are not likely influenced by geographical barriers; thus, their high probability of dispersal and unlikely extinction allows them to be ubiquitous (Finlay, 2002, Fenchel, 2003). Another idea presented was microbial endemism, which states that while some prokaryotes are cosmopolitan, some are strictly found in only one location, attributed in many cases to evolution in isolation (Finlay, 2002, Hedlund & Staley, 2004). Support for endemism was also given by Cho and Tiedje who found genetic distance between soil *Pseudomonas* populations increased with geographical distance, suggesting bacteria continue to diversify in isolation when presented with dispersal barriers (Cho & Tiedje, 2000). Thus, biogeographical patterns may be related to the biology and habitat of the particular phylotype which would determine its dispersal.

In more recent years, studies have investigated habitats in which different microorganisms exhibited different biogeographical patterns. One study in the Antarctic, found phylotypes exhibit regional endemism while others were cosmopolitan (Jadoon *et al*., 2012). This study shows that while not all microorganisms may exhibit biogeographical patterns, there are at least some patterns evident. The arguments against the existence of microbial biogeography patterns only raised more questions and fueled further study of how biogeography could be applied to microorganisms.

In 2006, Martiny *et al*. published a paper discussing microbial biogeography in the context of how the theories concerning macroorganisms apply to microorganisms. The study concluded that microorganisms cannot be looked at exclusively with the same

rules that apply to macroorganisms in terms of biogeography. This is largely due to two key factors which make microbial dispersal different than that of macroorganisms, cell size and population density, both of which impact dispersal potential, or the ability to spread to and colonize new biogeographic provinces, regions and habitats (Martiny *et al.*, 2006, Lindstrom & Lagenheder, 2011, Zinger *et al.*, 2011). These key factors, in theory, make dispersal potential unlimited, especially in marine environments, including the deep sea.

1.1.2 Features Shaping Biogeography in the Deep Sea

The deep sea, which begins below 200 m, is the largest habitat on Earth. As this habitat accounts for approximately 1.27×10^{18} m^3 globally and is remote, it is difficult to access and thus study (Orcutt *et al*., 2011). While the deep sea may seem like an inhospitable environment, especially with cold temperatures, which can be below 0° C, and high pressure (pressure increases 1 atm per 10 m of water depth), it is an important habitat to study microbial biogeography (Orcutt *et al*., 2011). This is because 90% of Earth's microorganisms are found there (Colwell & D'Hondt, 2013). Subseafloor sediment alone may have as many as 2.9×10^{29} cells (Kallmeyer *et al.*, 2012) globally. The number of microorganisms existing here makes the deep sea a very important habitat, which is understudied in terms of microbial biogeography.

In 2012, Hanson and colleagues conducted a review of microbial biogeography studies and found a correlation between microbial community composition and at least one measured environmental or habitat feature in 92% of studies they looked at (Hanson *et al*., 2012). Habitat features in the deep ocean include hydrothermal vents, methane seeps, seamounts, and organic falls. A number of studies have looked at these features,

and hydrothermal vents have often been studied for microbial community structure. Huber and colleagues showed the geochemistry of hydrothermal vents is a factor in structuring microbial communities (Huber *et al*., 2007). Vents have also been found to host a wide diversity of archaea (Auguet *et al.*, 2010). Anderson *et al*. (2015) conducted a study into the microbial community structure of both archaea and bacteria in hydrothermal vents. This study found the community structure at the vents was heavily influenced by the location of the vent, in proximity to other vents and seamounts, rather than the chemistry of the vent. It has also been revealed that hydrothermal plumes from vents host distinct communities and that plumes function as vectors, dispersing microorganisms between chemically similar features (Dick *et al.*, 2013). Habitat features are important in shaping microbial communities and this has been seen in the deep-sea through studies involving natural seafloor features including hydrothermal vents (Huber *et al*., 2007, Dick *et al*., 2013, Anderson *et al*., 2015).

In addition to habitat features, geographic location and water circulation have also shown to be a factor to microbial communities. Similarity between deep-sea bacterial communities in the subsurface sediment decreases with increasing distance between samples, an indication that location is important (Bienhold *et al.*, 2016). Water movements in estuarine systems are known to influence microbial spatial distribution and community composition (Bell *et al.*, 2018). Circulation has also been shown to be important in arctic environments (Galand *et al*., 2010, Hamdan *et al*., 2013). However, the effect of ocean circulation on deep-sea microbial communities has not been reported.

Wood of terrestrial origin is also found on the seafloor and presents another type of habitat feature. Wood is both naturally derived as wood falls and delivered to the sea

through shipwrecks. The latter may be a more significant source of wood to the seabed than realized, considering there are over 2,000 known historic shipwrecks in the GoM, with the majority made of wood. The wood delivered in the form of shipwrecks presents another habitat feature, and thus could play a role as an anthropogenic influence on deep-sea microbial biogeography.

1.1.3 Wood and Biofilms in the Deep Sea

Wood can arrive to the deep-sea through natural processes when plant material is moved off shore by storm events. While wood falls are most common along coastlines, they have been seen in all the world's oceans and at all explored water depths (Wolff, 1979, Bienhold *et al*., 2013). Wooden shipwrecks are also a type of wood fall, although they arrive on the seabed in a more stochastic manner than materials washed out to sea, they can also be found at all explored depths. In either case, wood falls are colonized by microorganisms and create hotspots of diversity (Palacios *et al*., 2009, Fagervold *et al*., 2012, Bienhold *et al*., 2013, Kalenitchenko *et al*., 2015).

The immersion time of the wood is a significant factor dictating community composition found on wood (Fagervold *et al*., 2012). As the wood degrades it undergoes community succession processes by both macro- and microorganisms (Bienhold *et al*., 2013, Fagervold *et al*., 2012). However, this community succession process is initiated and maintained by biofilms.

Biofilms consist of a community of sessile microorganisms attached to a substrate with extracellular polymeric substances (EPS) (Garrett *et al.*, 2008). Biofilm formation occurs in three steps: 1) accumulation of macromolecules, such as lipids, on the solid surface; 2) accumulation of microorganisms on the surface; and 3) adhesion of

microorganisms to the surface (Garrett *et al.,* 2008). The adhesion of the microorganisms to the surface leads to formation of a matrix of EPS. The EPS allows other microorganisms to settle and grow. After the biofilm reaches maturation, microorganisms may disperse from it and continue spreading (Garrett *et al*., 2008, Mugge *et al.*, 2019).

The process of biofilm formation, maturation and dispersal on submersed wood provides for an opportunity to understand how wood influences biogeography processes surrounding habitat features on the seabed made of wood. Thus, the goal of this thesis was to determine how wooden shipwrecks influence biofilm dispersal to new introduced wood in proximity to wooden shipwrecks.

The objective of this chapter is to determine the source of biofilms on wood introduced to the seafloor near a historic wooden shipwreck. The potential sources of biofilms are sediment, water, and a nearby wooden shipwreck. The null hypothesis is the biofilm communities on the introduced wood do not derive from any of the potential sources. The alternative hypotheses are: (1) the biofilm communities on the introduced wood derive from the sediment, (2) the biofilm communities on the introduced wood derive from the water, and (3) the biofilm communities on the introduced wood derive from the shipwreck. These hypotheses will be tested by determining the source proportion of taxa in biofilms on wood using a source tracking algorithm called SourceTracker2 (Knights *et al.*, 2011). The analysis was used to reveal (1) the probability of the biofilm community originating from sediment, water, shipwreck, or other sources and (2) if the source of the biofilm community changes with distance from the shipwreck.

Deep-sea currents may also impact microbial dispersal on the seafloor and at or around built structures. The GoM is a stratified system with two layers, an upper layer

above approximately 800-1200 m, and the lower layer below it to the seafloor (Hamilton, 2009, Perez-Brunius *et al*., 2018). The lower layer does have depth-independent currents that fluctuate in strength over time (Hamilton *et al*., 2009). If strong prevailing currents are found at shipwreck sites used in this study, they may also impact the trajectory of biofilm dispersal to newly placed wood. Therefore, an Acoustic Doppler Current Profiler (ADCP) was placed at each shipwreck site to monitor currents for the duration of the experiment to help illustrate SourceTracker2 results.

1.2 Methods

1.2.1 Study Sites

Two sites, 15470 and 15711, were never before studied historic shipwrecks until experiments were conducted in 2019 by the Microbial Stowaways Project, supported by NOAA's Office of Ocean Exploration and Research. Both sites were identified as wooden-hulled, copper-sheathed sailing ships dating to the late 19th century.

Site 15470, discovered in 2009 during a geophysical survey, was investigated in June – July 2019. The site rests at ~1800 m water depth in the Mississippi Canyon lease area (Figure A.1). It is ~32 m long x 12 m wide, and oriented with the bow toward the West-Southwest at a bearing of ~255°. The highest vertical relief of the shipwreck is the stem and sternpost at either end of the vessel, but the average vertical relief is less than 1 m. A large artifact cluster is located on the starboard side of the vessel and contains glass bottles, ceramic dishes, and a spyglass.

Site 15711, discovered in 2013 during a geophysical survey, was investigated in June – July 2019. The site rests at ~525 m water depth in the Viosca Knoll lease area (Figure A.1). It is ~28 m long x 16 m wide, and oriented with the bow towards the West-

Southwest at a bearing of ~260°. The highest vertical relief of the shipwreck is the bow's stem ~2.5 to 3 m above the seafloor, with the majority of the site having less than 1 m vertical relief. Debris extends several meters off the bow and the starboard side of the shipwreck, indicating the vessel was listing to the starboard side upon settling on the seafloor. The bow of the vessel is mostly intact with visible copper sheathing, but overall, the hull is not well preserved.

1.2.2 Microbial Recruitment Experiments

Microbial recruitment experiments (MREs) were constructed of PVC with two main parts: a floating cover and a sample holder (Figure A.2). The cover had syntactic foam in the upper portion allowing for flotation of the cover above the sample holder when submerged. A line was tied in the rope in the top of the cover to attach it to the sample holder. The line ran through the sample holder, through a cam cleat in the base of the tower, and outside the base of the MRE where a stop was set to control cover floating height (enough to expose surfaces, but short enough to allow the cover to close without malfunction). The sample holder had 24 1.25-in holes where the wooden surfaces for collecting biofilm were placed. The wooden surfaces were cut with a miter saw from 1.25-in diameter wooden dowels and were 1.5-in long. Each MRE contained four pine surfaces and four oak surfaces. Surfaces were held in the MRE sample holder with 100% silicone water-proof sealant on the inside of the sample holder, away from the sample surface. The sample surface, which faced outward from the sample holder, was wiped clean with 70% ethanol before deployment. Each individual MRE was then connected with a 282 m line in an array with 5 total MREs, and to a lander used for recovery. On recovery (described below) the line comes under strain, thus closing the cover. The cam

cleat locks when the close event happens and serves to keep the cover down on recovery, to protect samples from disturbance during ascent through the water column.

Five MREs were arranged in an array placed in a single transect, separated by a 25 m line. The first MRE in the array was connected to a lander used for floatation during recovery. The length between the lander and first MRE was 182 m, which was greater than the distance between the shipwreck and last MRE.

For deployment, the array was placed in a rectangular cradle with a rod at each corner (Figure A.3). The 182 m line was wrapped around the exterior of the rods and secured at each point with a rubber band. The rubber bands secured the lines for descent but broke when tugged to release the line. The cradle was bolted to the remotely operated vehicle (ROV), and the 182 m line was tied to a lander. A lander was comprised of a metal frame connecting three 17-in glass spheres with a flotation of 30-50 lbs each, had a Teledyne-Benthos R2K acoustic release in the top sphere, and was attached to sacrificial weights, and, for one lander at each site, an Acoustic Doppler Current Profiler (ADCP). The ROV held the lander until it reached the drop site (Figure A.4). The shipwreck and drop site were located by ROV survey using HYPACK software and Sonar to determine the position of the shipwreck and a drop site and transects devoid of archaeological debris. At the drop site the ROV released the lander, and the lander was pulled to the seafloor by the weights. The ROV then drove forward along the predetermined transect. The line was tugged by the ROV as it drove which caused the rubber bands holding the lines on the cradle to break and the line to release. Once the 182 m line was deployed, the first MRE was pulled out and sat on the seafloor with the cover floating to expose the surfaces. An MRE was pulled out every 25 m until the fifth one. The ROV, free of all

equipment except the cradle, ascended back to the ship (Figure A.4). Two transects of MREs were deployed at both Site 15470 and 15711, and one lander at each site carried an ADCP.

The lander recovery occurred in November 2019 after a ~four-month incubation period (136 days at Site 15470, 138 days at Site 15711). The lander was outfitted with a Teledyne-Benthos R2K acoustic release prior to deployment. A hydrophone was lowered in the water above the drop site and used to send an acoustic signal to the acoustic release on the lander. The signal initiated an electrical current to a wire on the base of the lander that caused it to dissolve, subsequently dropping the arm that the sacrificial weights were attached to. Without the weight, the lander was buoyant, due to the three glass flotation spheres. As the line was tugged, the MREs closed and rose with the lander. The lander was spotted from the ship and pulled aboard with a grappling hook and crane. A capstan was used to bring in the rest of the line and MREs.

1.2.3 Transect Position

The first lander at Site 15470 was placed approximately 382 m from the shipwreck. The MREs were placed in a northeastern direction north of the shipwreck with the closest MRE approximately 100 m from the shipwreck. The remaining four MREs in the transect were 125 m, 150 m, 175 m, and 200 m from the shipwreck, respectively (Figure A.5). The second lander at Site 15470 was placed approximately 304 m from the shipwreck. The MREs were placed in a northeastern direction from the shipwreck's stern with the closest MRE approximately 22 m from the shipwreck. The remaining four MREs in the transect were 47 m, 72 m, 97 m, and 122 m away from the shipwreck, respectively (Figure A.5).

The first lander at Site 15711 was placed approximately 294 m from the shipwreck. The MREs were placed in an eastern direction from the center of the shipwreck with the closest MRE approximately 12 m from the shipwreck. The remaining four MREs in the transect were 37 m, 62 m, 87 m, and 112 m away from the shipwreck, respectively (Figure A.6). The second lander at Site 15711 was placed approximately 322 m from the shipwreck. The MREs were placed in a northeastern direction from the shipwreck's stern with the closest MRE approximately 40 m from the shipwreck. The remaining four MREs in the transect were 65 m, 90 m, 115 m, and 140 m away from the shipwreck, respectively (Figure A.6).

1.2.4 Acoustic Doppler Current Profiler

One lander at each site was modified to carry an ADCP by extending a mounting frame from the center of the lander and adding additional syntactic foam to counteract the weight of the frame and ADCP. The ADCPs monitored the current direction and velocity for the four months of incubation.

1.2.5 Biofilm Sampling

MREs were recovered during the Microbial Stowaways recovery expedition on November 14, 2019, after ~four months on the seafloor. Immediately upon recovery, the outer face (which was only in contact with the water column) of the wooden surfaces were scraped aseptically with a flame-sterilized scoopula to collect the biofilms which were placed in Lysing matrix E tubes. Lysing matrix tubes containing biofilms were stored at -80°C on the ship and transported to the USM laboratory frozen.

1.2.6 Water Sampling

Water samples were collected by CTD-Rosette at both Sites 15470 and 15711. At Site 15470, the CTD was deployed over the shipwreck to a depth of 1821 m and allowed to drift in a straight transect to the northeast. Water samples were taken directly over the center of the shipwreck, and at 50 m, 100 m, 150 m, and 200 m away from the shipwreck.

At Site 15711, the CTD was deployed over the shipwreck to a water depth of 566 m and allowed to drift in a straight transect to the west. Water samples were taken directly over the center of the shipwreck, and at 50 m, 100 m, 150 m, and 200 m away from the shipwreck. A minimum of 2 L of water was filtered through Sterivex filters (Millipore) using a peristaltic pump to concentrate microbial biomass (Hamdan *et al.*, 2013). Filters were stored at -80°C on the ship and transported to the USM laboratory frozen.

1.2.7 Sediment Sampling

Sediment samples were collected by Jason-style push cores at both Sites 15470 and 15711. The ROV used the push cores to collect sediment cores along transects beginning at the shipwreck and extending away from it. Transects were determined by ROV surveys using HYPACK software and Sonar to determine sampling areas devoid of archaeological debris.

At Site 15470, sediment cores were collected along four transects. Transect 1 began towards the bow on the starboard side of the shipwreck and ran northwest. Sediment cores were taken from this transect at 3 m, 10 m, 20 m, 40 m, and 60 m away from the shipwreck. Transect 2 began directly on the bow of the shipwreck and ran southwest. Sediment cores from this transect were taken at 6 m, 10 m, 20 m, 40 m, and

60 m away from the shipwreck. Transect 3 began directly on the stern of the shipwreck and ran northeast. Sediment cores from this transect were taken at 7 m, 10 m, 20 m, 40 m, and 61 m away from the shipwreck. Transect 4 began in the center of the port side of the shipwreck and ran southeast. Sediment cores from this transect were collected at 4 m, 10 m, 20 m, 40 m, and 60 m away from the shipwreck.

At Site 15711, sediment cores were collected along four transects. Transect 1 began near the bow on the port side of the shipwreck and ran south. Sediment cores from this transect were taken at 4 m, 10 m, 18.5 m, 41 m, and 60 m away from the shipwreck. Transect 2 began directly on the stern and ran to the east. Sediment cores from this transect were taken at 4 m, 10 m, 20 m, 40 m, and 60 m away from the shipwreck. Transect 3 began toward the stern on the starboard side of the shipwreck and ran north. Sediment cores from this transect were taken at 7 m, 10 m, 20 m, 40 m, and 57 m away from the shipwreck. Transect 4 began toward the bow on the starboard side of the shipwreck and ran west. Sediment cores from this transect were taken at 7 m, 10 m, 20 m, 40 m, and 57 m away from the shipwreck.

Sediment cores underwent destructive sampling down-core by sectioning them at 4 cm intervals using an extruder. Sediment from the center of each section was placed aseptically into sterile, PCR clean conical tubes, frozen on the ship at -80°C, and transported to the USM laboratory frozen.

1.2.8 DNA Extraction and Quantitation

Biofilms in Lysing matrix E tubes underwent DNA extraction with the FastDNA® SPINKit for Soil (MP Biomedicals LLC, Santa Ana, CA, USA). Sediment samples were processed and analyzed as previously described in Hamdan *et al*., 2013.

For water samples, the filter barrels were cracked, and the filter was aseptically removed and processed as above. Quantitation of total extracted DNA (ng/mL) was performed on Qubit 2.0 Fluorometric Quantitation system (Invitrogen, Carlsbad, CA, USA) to assess quantity, and a NanoDrop spectrophotometer (ThermoFisher, Waltham, MA, USA) was used to assess purity.

1.2.9 16S rRNA Sequencing of Bacteria and Archaea

For 16S rRNA gene amplification and sequencing of bacteria and archaea, ~2 ng/μL for each sample was used at the Integrated Microbiome Resource (IMR) facility at Dalhousie University (Halifax, Nova Scotia, Canada). Gene amplification was carried out as in Comeau *et al*. (2011), using fusion primers B969F/BA1406R to target the V6-V8 variable regions of the bacterial 16S rRNA gene, and fusion primers A956F/A1401R to target the V6-V8 variable regions of the archaeal 16S rRNA gene. The primers used in this analysis have been successfully used before in microbial biogeography studies (Comeau *et al.*, 2011, Comeau *et al.*, 2016, Comte *et al.*, 2016).

1.2.10 Bioinformatics Analysis

Bioinformatics was performed using Quantitative Insights into Microbial Ecology 2 (QIIME2) (Caporaso *et al.*, 2012). DADA2 was used to trim and truncate forward and reverse reads, dereplicate sequences, denoise, merge paired end reads and identify any chimeras (Callahan *et al*., 2016). DADA2 outputs amplicon sequence variants (ASVs) which are sequences with only single nucleotide differences. VSEARCH de novo clustering was used for operational taxonomic unit (OTU) clustering of the feature table output from DADA2 at 97% similarity. A table containing the abundance of OTUs in samples was generated and used for taxonomic identification and phylogenetic

alignment. The phylogenetic tree was built using FastTree with a mid-point root and incorporated mafft, a denovo multiple sequence alignment, and mask to remove highly variable positions. Core metrics were obtained using phylogeny. For taxonomic analysis, the SILVA database (v. 132) was used for archaea and bacteria.

1.2.11 Statistical Techniques

To determine outliers for the archaeal dataset, the median absolute deviation (MAD) was determined using the "mad" command available in the "Stats" package in RStudio (v. 1.3.959) (Leys *et al.*, 2013). A coefficient of 0.5 was used to determine the threshold for outliers. For archaea, the minimum threshold was 216 non-chimeric reads, meaning samples with fewer than 216 non-chimeric reads were eliminated from SourceTracker2 analyses.

In addition, there were 3 MREs that surfaced at recovery open: 140 m MRE from Transect 1 at Site 15711, and 100 m and 150 m MREs from Transect 1 at Site 15470. Since they were exposed to outside water, the biofilms may have been compromised. Therefore, the samples from these MREs were excluded from all SourceTracker2 analyses.

1.2.12 SourceTracker2 Analyses

SourceTracker2 was created to estimate the proportion of contaminants in high throughput metagenomic studies from possible sources (Knights *et al*. 2011). It uses a Bayesian approach that models contamination as a mixture of source communities into a sink community. In this study, SourceTracker2 was used to identify sources of bacteria and archaea OTUs to biofilms. Biofilm samples were treated as sink communities, and sediment and water samples were treated as source communities. Analyses were run on

sites and wood types separately, but all distances of sediment, water, and biofilm samples were included. Therefore, a sediment or water community from any distance was treated as a potential source for any biofilm community. Results are reported as proportion estimates grouped by distance from the shipwreck.

1.3 Results

SourceTracker2 analyses indicated the source of all bacterial OTUs to biofilms on both pine and oak was more than 99% unknown and 0.005% was the highest proportion estimate attributed to sediment (Figure A.7). The SourceTracker2 analyses for bacteria did not indicate any bacteria found in the biofilm was sourced from water. However, a general trend of higher sediment proportion estimates is seen in the first 75 m from the shipwreck for all sites and wood types except 15470 oak samples (Figure A.8).

SourceTracker2 analysis indicated the source of archaeal OTUs to biofilms at Site 15711 for pine samples was more than 99% unknown with less than 1% of the archaea in biofilms sourcing from sediment. SourceTracker2 analysis for Site 15711 oak samples also indicated more than 99% of bacteria in biofilms was unknown, but the remaining 1% was sourced from both sediment and water (Figure A.9). Both pine and oak proportion estimates for sediment and water declined to zero at distances greater than 100 m for Site 15711 (Figure A.10). SourceTracker2 proportion estimates for Site 15470 archaea, both pine and oak, were majority from unknown sources and less than 1% from water but indicated proportion estimates up to 42% for sediment (Figure A.9). The unknown proportion estimates for both pine and oak at Site 15470 peak at 75-99 m from the shipwreck (Figure A.10). The highest proportion estimate for sediment (42.7%) is seen at 175-200 m away from the shipwreck in the 15470 pine samples; however, this distance

category only contains one sample for this site and wood type. Therefore, similar to bacteria, for both sites and wood types, proportion estimates for sediment are generally greater in the first 75 m from the shipwreck (Figure A.10).

The ADCP at Site 15711 indicated the currents had a velocity ranging from 0-1 knot with no prevailing current direction during the time of deployment (Figure A.11). The ADCP at Site 15470 indicates the currents had a velocity ranging from 0-0.5 knot with a prevailing Southward current, but West to Southwest currents also frequently occurred (Figure A.12). These current directions mean the flow of water was moving over the MREs first before reaching the shipwreck for a majority of the deployment time (Figure A.5).

1.4 Discussion

The objective of using a source tracking tool in this study was to determine the source of biofilms on wood introduced to the seafloor near a deep-sea historic wooden shipwreck. SourceTracker2 (Knights *et al*., 2011) was used to estimate the proportion of taxa that water, sediment, and unknown sources were contributing to the wood biofilm samples. It has been used in aquatic environmental studies to estimate sources of dispersal in different habitats (Hamdan *et al*., 2013, Storesund *et al*., 2017, Comte *et al*., 2018, Mugge *et al*., 2019). This information was aimed at providing insight into how shipwrecks promote the dispersal of microorganisms from shipwrecks. The null hypothesis stated the biofilm communities on the introduced wood do not derive from any of the potential sources. Alternatively, the biofilm communities on the introduced wood derive from the sediment, the water, or the shipwreck. The current information from the sites was intended to help verify the source of taxa to biofilms. A current would

be a factor in the movement of microorganisms and could either positively or negatively impact their ability to settle on a biofilm.

At Site 15711, current velocity was low, but always non zero, and there was no prevailing current. This indicates heterogeneous current around the site during the experimental period. Accordingly, microorganisms were not being influenced one prevailing current direction, and thus could passively disperse. At Site 15470, the current velocity was low, but ranged up to half a knot, and had prevailing currents. The main current direction was Southward, with West to Southwest currents also frequently occurring. This indicates the current was traveling over the MREs before reaching the shipwreck for a majority of the experiment. However, currents measured in all directions, meaning the water column could have been homogenizing, so the potential for the shipwreck to be a source of taxa to the wood surfaces should not be ruled out based on the prevailing currents.

Source proportion estimates for sediment being a source for both bacteria and archaea in biofilms were low (< 0.005% for bacteria and < 1% for archaea) at Site 15711. SourceTracker2 proportion estimates for sediment being a source to bacterial biofilms at Site 15470 are also low (< 0.005%). While water proportion estimates were nonexistent for bacteria and extremely low for archaea (< 0.01%), there were fewer water samples taken, so SourceTracker2 may not have had enough input to determine if water was a source of taxa to biofilms. However, a previous study investigating the source contribution of sediment and water to biofilms on metal surfaces near metal shipwrecks also saw very little contribution from water, but higher contributions from sediment, up to 22% (Mugge *et al*., 2019). Since the shipwrecks are historic, no direct samples of

wood could be taken from them, thus the specific microorganisms dispersing from the shipwreck could lie in the "unknown" portion of the microorganisms in the SourceTracker2 proportion estimates.

The archaea dataset evidenced more variable sediment proportion estimates across distances than bacteria. At Site 15711 for archaea, for both pine and oak samples, the estimates decreased to zero for samples greater than 75 m from the shipwreck. At Site 15470 for both pine and oak samples, archaea unknown proportion estimates peak at 75-99 m. This pattern could be an indication of an ecotone around the shipwreck, where the influence of dispersal from the shipwreck converges with the influence of the surrounding ambient environment (Levin *et al*., 2016). Whale falls, which are also organic falls and exhibit similarities to wood falls, have also been shown to exhibit a sphere of influence in fauna on the sea floor at a standoff distance from the actual fall environment (Smith *et al*., 2015). In the current study, the peak of dispersal is observed more clearly for archaea, indicating that either dispersal patterns for archaea differ from bacteria, which seems unlikely, or the selection process for biofilms on wood for archaea differ from bacteria.

For the archaea, proportion estimates for unknown sources are greater at Site 15711 than at Site 15470. One explanation as to why the proportion estimates for unknown sources were greater at Site 15711, is due to the location of the site, in shallower water nearer to the Mississippi River plume. Depth and proximity to land are known to be important drivers on community composition in sediments (Kallmeyer *et. al*., 2012, Mason *et al*., 2016, Sanchez-Soto *et al*., 2018) In the case of Site 15711, proximity to land and to the Mississippi River plume likely provides greater nutrient and

carbon deposition at the site relative to Site 15470, which is located in a deeper, more oligotrophic setting. The increased nutrient availability at Site 15711 allows for a community that is not solely based on the presence of the shipwreck. The influx of nutrients may allow a more diverse and rich community of microorganisms to exist there. Whereas at Site 15470, in more oligotrophic waters, the presence of a shipwreck is a greater influence on community composition.

This work shows that microbial dispersal patterns in the deep sea are different for archaea and bacteria, and the source signature is stronger in deep water than it is in shallower water. These conclusions are evidence that microbial dispersal in the deep sea is complex and further studies are needed.

CHAPTER II - HISTORIC SHIPWRECK INFLUENCE ON DIVERSITY, RICHNESS, AND PHYLOGENETIC COMPOSITION OF DEEP-SEA MICROBIOMES

2.1 Introduction

2.1.1 Island Theory

The Theory of Island Biogeography (TIB) first published by MacArthur and Wilson in 1967 focused exclusively on macroorganisms and explained the mechanisms of biogeography relative to islands (MacArthur & Wilson, 1967). There are three main considerations in the TIB: size of an island, distance of an island from the mainland (isolation), and immigration and extinction rates of colonists. The size of an island is important because the number of organisms that can survive there is dictated, in part, by space and resource availability. According to TIB, increasing island size decreases the rate of species extinction on the island. The distance from the mainland is also important because the mainland is the source of new taxa, so increasing distance from that source will decrease immigration to the island. According to the TIB, these coupled features of island size and isolation impact immigration and extinction rates. The TIB introduces a biotic equilibrium model in which the number of species present is plotted against species number vs. time. Species richness of an island reaches a steady state when the rate of immigration equals the rate of extinction. When an island reaches equilibrium, it can be determined through a species extinction plot showing a decrease in species richness and diversity with distance from an individual island. When such a distance effect is discernable, it can be an indicator of an island or island-like system.

Some studies have shown aquatic microorganisms to exhibit biogeographic patterns in island-like habitats (Bell *et al*., 2005, van der Gast *et al*., 2005, Darcy *et al*.,

2018). Bacterial communities in water-filled tree holes and metal cutting machine sump tanks were found to exhibit less diversity with decreasing "island" size, so the size of the hole or the tank had an effect on microbial diversity (Bell *et al.*, 2005, van der Gast *et al.*, 2005). Similarly, cryoconite holes, water filled holes on glaciers, also show the relationship between hole size and bacterial diversity as well as distance effects between holes (Darcy *et al*., 2018). So, microorganisms exhibit island biogeographical patterns in habitats that are not islands in the traditional sense.

Natural habitat features in the marine environment, including whale falls, vents, and seeps are known to structure seafloor communities. Whale falls were found to be an island-like system for bacteria by exhibiting a distance effect-with species richness being higher at whale fall sites than reference sites (Smith & Baco, 2003, Goffredi & Orphan, 2010). Anderson *et al*. (2015) found the community structure at vents was heavily influenced by the location of the vent, in proximity to other vents and seamounts. Methane seeps were found to be island-like habitats as they harbor distinct microbial communities from other seafloor ecosystems (Ruff *et al*., 2015).

Anthropogenic structures, including historic shipwrecks, could also be considered as island-like systems. This has been investigated for steel hulled shipwrecks (Hamdan *et al*., in revision) but has yet to be explored for wooden-hulled shipwrecks. However, wood falls naturally occuring on the seafloor have been investigated as habitat features for seafloor microbiomes and research into the factors influencing microbial community composition have commenced. Geographic location and depth have been shown to be important in structuring bacterial communities on submerged wood (Palacios *et al*., 2009, Ristova *et al*., 2017). Different conditions of the wood including wood type and length of

immersion were also shown to be important in both bacterial and archaeal submerged wood communites (Palacios *et al*., 2009, Fagervold *et al*., 2012, Kalenitchenko *et al*., 2015).

2.1.2 Seafloor Habitat Features and the Wooden Stepping Stone Hypothesis

The stepping stone hypothesis was first posited in 1989 with the first discovered whale fall off the coast of California. Smith *et al*. 1989 hypothesized whale skeletons act as stepping stones for dispersal of organisms that rely on chemoautotrophic bacteria endosymbionts. The biogeochemistry connected to a whale fall, and their progressive mineralization by microorganisms, results in similar geochemical regimes to sulfur rich deep-sea habitats (e.g., hydrothermal vents) (Smith & Baco, 2003). Whale falls can become biologically formed, but geochemically similar, specialized habitats interspersed between geologically formed, but geochemically similar, vent habitats. When located at intermediate distances between vents, chemosynthetic whale falls create a link for organismal dispersal and range expansion for vent taxa.

Since sediment biogeochemistry surrounding wood falls and whale falls bears similarity to hydrothermal vents, Distel and colleagues evaluated the concept of stepping stones by looking at symbiont-containing mussels in wood and bone rich marine systems (Distel *et al*., 2000). Their results indicated wood and bone acted as dispersal steps to allow for the transport of these mussels between vents, seeps, or other chemically similar habitats. They also suggested wood and bone could be an evolutionary step toward vent habitats for species not previously found at vents by providing a habitat where endosymbionts could evolve from a heterotrophic endosymbiosis to an autotrophic one. In another study, more evidence was provided for the wooden stepping stone hypothesis

by studying the shipworm *Kuphus polythalamia* (Distel *et al*., 2017). Most shipworms have microbial cellulolytic endosymbionts that allow the worms to obtain nutrition from the wood they bore into, through a heterotrophic endosymbiosis. *Kuphus polythalamia* has sulfur-oxidizing chemotrophic endosymbionts and burrows into marine sediments. This chemosynthetic endosymbiosis likely evolved, displacing the ancestral heterotrophic endosymbiosis. It is proposed that the evolutionary stepping stone from heterotrophy to chemoautotrophy was submerged wood on the seabed. Accordingly, it is taken to mean that *K. polythalamia* shipworms are no longer confined to a wooden environment because of the evolutionary 'step' they have employed. This study indicates that microorganisms associated with wood on the seabed can use the wood to move between habitats and may evolve in the process. It is thus possible to consider that other bacteria, including those not associated with hosts, use wood as a both a dispersal and an evolutionary stepping stone.

Prior studies show microbial communities at wood falls are associated with chemosynthetic environments similar to those at whale-falls and hydrothermal vents (Bienhold *et al*., 2013, Fagervold *et al*., 2012). To date, no study has investigated how natural or artificial wood falls support dispersal of free-living or biofilm associated microorganisms. Sunken wood on the seafloor hosts diverse microbial communities with free-living sulfate reducers, methanogens, and sulfide oxidizers commonly observed (Wolff, 1979, Fagervold *et al.*, 2012, Bienhold *et al.*, 2013). If free-living microorganisms use wood falls as stepping stones, a community response should be evident, with a change in phylogenetic composition across distance away from and between "steps". While wood falls are ordinarily considered natural deposits of forest

material to the seabed, historic wooden shipwrecks would also provide a source of wood to the seafloor similar to that seen at natural wood falls. Accordingly, microorganisms, like macroorganisms, could use wooden shipwrecks to support both dispersal and evolution across the seafloor.

The objective of this chapter is to investigate how the dispersal of wood colonizing microbiomes changes as a function of distance from historic wooden shipwrecks, and how this influences diversity, richness and phylogenetic composition in the shipwreck's surrounding environment. The null hypothesis of this work is that diversity, richness, and community composition of wood colonizing microbiomes (bacteria, archaea, and fungi) are not impacted by proximity to wooden shipwrecks. This leads to two alternative hypotheses. First, diversity and richness of wood colonizing microbiomes increases with increased proximity to wooden shipwrecks. Second, the community composition of wood colonizing microbiomes changes as a function of distance from shipwrecks.

2.2 Methods

2.2.1 Study Sites

In addition to the two sites from the Microbial Stowaways Project described in Chapter I (15470 and 15711), two other sites were included in this work. These two sites, the *Mica* and *Ewing Bank* shipwrecks, are historic shipwrecks previously explored by the Gulf of Mexico-Shipwreck Corrosion, Hydrocarbon Exposure, Microbiology and Archaeology (GoM-SCHEMA) project in 2014 (Damour *et al.,* 2016, Hamdan *et al.,* 2018, Mugge *et al*., 2019). Data from experiments in 2014 at the *Mica* and *Ewing Bank* shipwrecks were analyzed and integrated into this study. These shipwrecks are similar to

the shipwrecks at Sites 15470 and 15711, as they are also wooden-hulled, copper-sheathed sailing ships dating to the 19th century.

The *Ewing Bank* shipwreck, first surveyed in 2006, was investigated by the GoM-SCHEMA project in 2014 as reported in previous studies (Damour *et al.*, 2016, Hamdan *et al.*, 2018, Mugge *et al.*, 2019). It is a 19th century shipwreck ~45 m long x 12 m wide. The site rests at ~600 m water depth in the Viosca Knoll lease area (Figure A.1).

The *Mica* shipwreck, first surveyed in 2001, was investigated by the GoM-SCHEMA project in 2014 as reported in previous studies (Damour *et al*., 2016, Hamdan *et al*., 2018, Mugge *et al*., 2019). It is a 19th century shipwreck ~20 m long x 6 m wide. The site rests in ~800 m water depth in the Mississippi Canyon lease area (Figure A.1).

2.2.2 Microbial Recruitment Experiments and Transect Positions

The same MREs and transect positions as described in Chapter I for Microbial Stowaways Sites 15470 and 15711 were used for the analyses described in this chapter.

Mica and *Ewing Bank* both had a single MRE placed 2 m from the shipwreck. The single MREs were placed and recovered by ROV in immediate proximity (within 2 m) to the *Mica* and *Ewing Bank* shipwrecks. The single MREs had the same dimensions and sampling materials as used in the more recent experiment, but they were not connected to a lander/array and were inserted directly into the sediment. The height above the seafloor of experimental surfaces is the same in both experiments, and the single MREs were recovered inside of a cover which protected biofilms from washing off surfaces. The single MREs at *Mica* and *Ewing Bank* contained 3 pine surfaces and 3 oak surfaces for colonization.

2.2.3 Biofilm Sampling

MREs from Sites 15711 and 15470 were recovered during the Microbial Stowaways recovery expedition on November 14, 2019, after four months on the seafloor. Immediately upon recovery, wooden surfaces were scraped aseptically with a flame-sterilized scoopula to collect the biofilms which were placed in Lysing matrix E tubes. Lysing matrix tubes containing biofilms were stored at -80°C on the ship and transported to the USM laboratory frozen.

MREs from *Mica* and *Ewing Bank* were collected by the GoM-SCHEMA project in 2014 after four months on the seafloor. Biofilms were collected in the same way as above.

2.2.4 DNA Extraction and Quantitation

Biofilms in Lysing matrix E tubes underwent DNA extraction with the FastDNA® SPINKit for Soil (MP Biomedicals LLC, Santa Ana, CA, USA). Quantitation of total extracted DNA (ng/mL) was performed on Qubit 2.0 Fluorometric Quantitation system (Invitrogen, Carlsbad, CA, USA) to assess quantity, and a NanoDrop spectrophotometer (ThermoFisher, Waltham, MA, USA) was used to assess purity.

2.2.5 16s Sequencing of Bacteria and Archaea

For 16S rRNA gene amplification and sequencing of bacteria and archaea, ~2 ng/μL for each sample was used at the Integrated Microbiome Resource (IMR) facility at Dalhousie University (Halifax, Nova Scotia, Canada). Gene amplification was carried out as in Comeau *et al*. (2011), using fusion primers B969F/BA1406R to target the V6-V8 variable regions of the bacterial 16s rRNA gene, and fusion primers A956F/A1401R to target the V6-V8 variable regions of the archaeal 16S rRNA gene. The primers used in

this analysis have been successfully used before in microbial biogeography studies (Comeau *et al.*, 2011, Comeau *et al.*, 2016, Comte *et al.*, 2016).

2.2.6 ITS2 Sequencing of Fungi

For fungal analysis, amplification and sequencing of the internal transcribed spacer region 2 (ITS2) was performed at IMR with primers ITS86F/ITS4. These primers have been shown to be suitable for studying both diversity and community structures of fungi (Op De Beeck *et al*., 2014).

2.2.7 Bioinformatics Analysis

Bioinformatics was performed using Quantitative Insights into Microbial Ecology 2 (QIIME2) (Caporaso *et al.*, 2012). DADA2 was used to trim and truncate forward and reverse reads, dereplicate sequences, denoise, merge paired end and identify any chimeras (Callahan *et al*., 2016). DADA2 outputs amplicon sequence variants (ASVs) which are sequences with only single nucleotide differences. VSEARCH de novo clustering was used for operational taxonomic unit (OUT) clustering of the feature table output from DADA2 at 97% similarity. A table containing the abundance of OTUs in samples was generated and used for taxonomic identification and phylogenetic alignment. The phylogenetic tree was built using FastTree with a mid-point root and incorporated mafft, a denovo multiple sequence alignment, and mask to remove highly variable positions. Core metrics were obtained using phylogeny. For taxonomic analysis, the SILVA database (v. 132) was used for archaea and bacteria, and the UNITE database (v. 8.0) was used for fungi.

2.2.8 Statistical Techniques

To determine outliers for archaeal and fungal datasets, the median absolute deviation (MAD) was determined using the "mad" command available in the "Stats" package in RStudio (v. 1.3.959) (Leys *et al.*, 2013). A coefficient of 0.5 was used to determine the threshold for outliers. For archaea from the Microbial Stowaways data (Sites 15711 and 15470), the minimum threshold was 216 non-chimeric reads, meaning samples with fewer than 216 non-chimeric reads were eliminated from statistical analysis. For archaea from the GoM-SCHEMA data (*Mica* and *Ewing Bank*), the minimum threshold was 43 non-chimeric reads. For fungi from the Microbial Stowaways data, the minimum threshold was 2494 non-chimeric reads. For fungi from the GoM-SCHEMA data, the minimum threshold was 701 non-chimeric reads. In addition, there were 3 MREs that came up open: 140 m MRE from transect 2 at Site 15711, and 100 m and 50 m MREs from transect 1 at Site 15470. Since they were exposed to outside water, the biofilms may have been compromised. Therefore, the samples from these MREs were excluded from all statistical analyses. After removing compromised MREs and outliers from the Microbial Stowaways data, 136 bacterial biofilm samples, 103 archaeal biofilm samples, and 110 fungal biofilm samples remained for statistical analyses. After removing outliers from the GoM-SCHEMA data, 6 bacterial biofilm samples, 4 archaeal biofilm samples, and 4 fungal biofilm samples remained for statistical analyses.

Shannon index was calculated from 16S rRNA amplicons in QIIME2. OTU Richness was determined by the number of non-chimeric reads output by QIIME2. This data was used to plot both Shannon index and OTU richness for each individual biofilm sample as a function of distance from the shipwreck for each site and wood type.

Creation of nMDS plots for each site was carried out using PRIMER v. 6.1.13 13 (PRIMER-E Ltd., Plymouth, UK). Sequence abundance data was used to generate Bray-Curtis dissimilarities to determine relatedness between samples. Non-metric multidimensional scaling (nMDS) of Bray-Curtis dissimilarities was performed on non-transformed data to yield a 2-and 3-dimensional representation of microbiome structure. This resulted in a nMDS plot with a cluster overlay at 60% similarity to visually explain the similarity in terms of community composition and abundance between samples. Since Bray-Curtis data was used, the analysis did not reveal similarity as a result of phylogeny. A permutational analysis of variance (PERMANOVA, 999 unique permutations) was conducted to understand how the three factors in this study (site, wood type, proximity to shipwreck) impact community composition patterns.

To analyze the phylogenetic composition of the bacterial biofilms, a weighted UniFrac analysis was performed. QIIME2 core metrics, obtained using phylogeny, output the weighted UniFrac distance matrix. This analysis differs from the Bray-Curtis dissimilarity matrix because it takes the branch lengths of the phylogenetic tree into account and thus measures the phylogenetic distance between the taxa, resulting in information on similarity derived from abundance, composition and phylogeny (Lozupone & Knight, 2005). The UniFrac results were displayed visually as a Principal Coordinates Analysis (PCoA) which were obtained through QIIME2. The UniFrac distance matrix was also used in PERMANOVA (999 unique permutations) analyses to identify differences in phylogeny between samples.

QIIME2 also output the relative abundance of each OTU in the community (for each domain separately). This output was used in constructing bar plots at the highest

level of taxonomic classification possible. Notably, some OTUs can only be annotated to the phylum level, but they represent individual phylotypes in the dataset, not a collection of phylotypes under that phylum.

2.3 Results

2.3.1 Diversity and Richness

The Shannon index revealed a general decrease in bacterial diversity as a function of distance from Site 15711 for biofilms on oak samples and Site 15470 for both pine and oak samples (Figure A.13). However, the trend was only significant ($p < 0.05$) at Site 15470 for pine samples. Distance from the shipwreck explained up to 23% of variance in bacterial diversity data. For pine samples at both 15711 and 15470, diversity is highest near the shipwreck, but exhibits a secondary peak at 125 m away from the shipwreck. Bacterial OTU richness also declined as a function of distance for all sites and wood types except for Site 15711 pine samples (Figure A.14). This trend was significant ($p < 0.05$) for Site 15711 oak and Site 15470 pine and oak samples. Richness was also highest near the shipwreck but exhibited a secondary peak at 125 away from the shipwreck for pine samples at both sites and oak samples at Site 15470.

Archaeal Shannon index decreased significantly ($p < 0.05$) as a function of distance at Site 15470 for both pine and oak (Figure A.15), explaining up to 20% of the variance in data at that site. However, it increased significantly ($p < 0.05$) as a function of distance at Site 15711 for pine samples and did not indicate a significant relationship or a trend for oak samples at this site (Figure A.15). A secondary peak in diversity was observed for both wood types at site 15470. Due to compromised sample recovery and the MAD analyses for archaea, Site 15711 had very different numbers of samples in each

transect. As a result, the Shannon index and OTU richness plotted as function of distance from the shipwreck for this site were examined in individual transects (Figure A.16), and revealed results were driven by the only complete transect for that site. Archaeal OTU richness decreases as a function of distance at both locations and on both wood types, however, this relationship was only significant ($p < 0.05$) at Site 15470 for oak samples (Figure A.17). A secondary peak in richness was again observed at 125 m for samples from both wood types at Site 15470.

The fungal Shannon index decreased slightly or exhibited a flat trend with distance from the shipwreck for all sites and wood types except Site 15711 pine samples where the relationship was significant (Figure A.18). Diversity in Site 15711 pine samples significantly increased with distance from the site ($p < 0.05$). When Site 15711 pine samples were looked at as individual transects, no significant differences were seen between transects for diversity or richness (Figure A.19, $p \geq 0.05$). There were no significant trends in fungal OTU richness with distance in any samples (Figure A.20). However, the trends did decrease slightly with distance.

2.3.2 Community Structure and Phylogenetic Composition of Bacteria

The nMDS plot revealed bacterial communities grouped by two main criteria, wood type and site location (Figure A.21). The clustering did not reveal a clear grouping of samples by distance from the shipwrecks (Figure A.22). Although not evident from the nMDS, the PERMANOVA provided that wood type, site, and proximity (listed from greatest to least influence on community composition) are all significant in determining bacteria biofilm composition on wood (Table A.1, $p < 0.05$).

An individual nMDS for Site 15711 again confirmed wood type is the strongest influencing factor on community composition in this study. In this analysis, however, the effect of distance on community composition was seen, as samples from 0-24 m formed a small cluster and samples from 100-124 m formed a small cluster (Figure A.23). The PERMANOVA results revealed wood type, proximity to the shipwreck, and transect (which indicates different directions and distances around the site) are all significant in bacteria biofilm community composition (Table A.2, $p < 0.05$). An individual nMDS for Site 15470 also confirmed wood type is the strongest influencing factor on bacterial biofilm community composition, but again, the effect of distance on composition was seen (Figure A.24). The PERMANOVA results revealed all three factors were significant (Table A.3, $p < 0.05$), with wood type being the most influential driver followed by transect (position and proximity), and then proximity to the shipwreck.

An nMDS plot was created to place bacteria samples from the previous GoM-SCHEMA study in context with samples from this study. It revealed *Mica* and *Ewing Bank* grouped more closely together with Site 15470 (Figure A.25). With the *Mica and Ewing Bank* data included, the PERMANOVA results again showed that wood type, site, and proximity to a shipwreck are significant (Table A.4, $p < 0.05$).

The UniFrac ordination for both sites and wood types explained 60.5% of variance in the data, with clear grouping by wood type (Figure A.26). When this PCoA was viewed by distance, there were some groupings seen, but there is overlap between all distance categories (Figure A.27). A PERMANOVA performed on the UniFrac distance matrix was in line with the one performed on the Bray-Curtis dissimilarity matrix. Wood type, site, and proximity were all significant (Table A.5, $p < 0.05$).

The UniFrac PCoA for Site 15711 pine samples explained 47.5% of the variance in the data (Figure A.28). A clear separation of samples based on distance from the shipwreck is evident along the two main axes. Axis 1 showed 23.74% of the variance is explained by distance category as the groupings were seen mainly along this axis. The UniFrac PCoA for Site 15470 pine samples explained 46% of variance in the data, but with less clear separation by distance groups (Figure A.29). However, distance category still explains the highest percentage seen (17.91%). This contribution of distance categories to the variance in the data is an indication that proximity to a shipwreck is a driver in phylogenetic composition of pine biofilm communities.

The UniFrac PCoA for Site 15711 oak samples explained 55% of the variance in the data (Figure A.30). A clear separation of samples based on distance from the shipwreck was again seen along Axis 1, explaining 27% of variance. The UniFrac PCoA for Site 15470 oak samples explained 58% of the variance in the data (Figure A.31). Distance category separations were not as clear at this site, but the separation along Axis 1 did still appear to be driven by distance (30.16%). These results indicate proximity to a shipwreck is also a driver in phylogenetic composition of oak biofilm communities.

The top 25 most relatively abundant bacterial OTUs were selected to visualize which OTUs were most abundant at different distances from the shipwreck (Figure A.32). For pine samples, Myxococcales (Blrii41) dominated at intermediate distances, dropping in abundance at the closer and farther distances. This trend for Myxococcales (Blrii41) was also seen in oak, but in much lower abundances. Rhodobacteraceae(uncultured) also followed a trend of peaking at intermediate distances for pine samples but dominated Site 15711 oak samples across distances. For Site 15470

oak samples, another Rhodobacteraceae OTU was seen in higher abundances at farther distances. Colwellia and Roseobacter (clade NAC11-7 linkage) are also seen at 15470 oak samples with a decrease in the middle of the transect. Flavobacteriaceae and Flavobacteriaceae(uncultured) were seen in steady abundances across all sites and wood types, as is Gammaproteobacteria. Proteobacteria remained in stable abundances across pine samples but fluctuated with a slight peak at intermediate distances for oak samples.

2.3.3 Community Structure and Phylogenetic Composition of Archaea

The nMDS for archaea at both sites showed archaeal communities were not grouped exclusively by wood type (Figure A.33). A second nMDS revealed samples were mainly grouped by site, and to some extent, by distance (Figure A.34). There was a cluster with mainly samples between 75 and 124 m. Another cluster contained largely samples between 0 and 74 m with a few samples from farther distances. The PERMANOVA results indicated site and proximity to a shipwreck were highly significant ($p < 0.05$) to structuring these communities (Table A.6). Unlike bacterial communities, archaeal composition was not primarily driven by the wood type that biofilms formed on, as the PERMANOVA results confirmed wood type is the weakest factor structuring archaeal community composition. Since site is the most significant factor in archaea biofilm composition, sites were analyzed separately.

The nMDs for Site 15711 showed that a few samples at distances greater than 50 m from the shipwreck did not cluster with the majority of samples from the study (Figure A.35). The PERMANOVA for Site 15711 revealed wood type and proximity to the shipwreck were both significant to archaea biofilm composition (Table A.7, $p < 0.05$). For Site 15470, the nMDS depicted a separate cluster containing samples from 75-99 m

and 100-124 m, while most samples from 125-149 m and 175-200 m fell into a cluster with samples from closer distances (Figure A.36). The PERMANOVA for Site 15470 indicated proximity, transect, and wood type were all significant ($p < 0.05$, Table A.8).

An nMDS plot was created to place archaea samples from the previous GoM-SCHEMA study in context with samples from this study (Figure A.37). This nMDS showed samples from *Ewing Bank* and *Mica* grouping in the cluster in the lower left that previously consisted of largely samples between 75 and 124 m. However, samples from these GoM-SCHEMA sites appeared in all of the other clusters. The PERMANOVA results indicated site and proximity were significant in archaea biofilm composition ($p < 0.05$, Table A.9).

The UniFrac ordination for both sites and wood types explained 63.95% of variance in the data (Figure A.38). The PCoA reveals Axis 1 and Axis 2 are both largely driven by distance with samples between 75 - 124 m clustering together on both axes (Figure A.38). When the UniFrac is labeled by wood type, it appeared that Axis 1 is driven by this feature (Figure A.39). A PERMANOVA on the UniFrac results indicated site is still the most significant factor in archaea biofilm composition, but distance and wood type are both significant shaping features on phylogenetic composition ($p < 0.05$, Table A.10). These results indicated that there were differences in archaea phylotypes that colonize wood, and that distance from the shipwreck also influences phylogenetic composition.

The UniFrac PCoA for Site 15711 pine samples explained 76% of the variance in the data and showed distance groupings along Axis 1 which indicated distance from the shipwreck explained 51.88% of variance (Figure A.40). The UniFrac PCoA for Site

15470 pine samples explained 91% of variance in the data, and Axis 1 showed distance from the shipwreck explained 78.26% of variance (Figure A.41).

The UniFrac PCoA for Site 15711 oak samples explained 62% of the variance in the data and showed distance groupings primarily along Axis 1, which revealed distance from the shipwreck explained 38% of variance (Figure A.42). The UniFrac PCoA for Site 15470 oak samples explains 86% of variance in the data, and Axis 1 revealed distance from the shipwreck explained 69.56% of variance (Figure A.43).

OTUs with representation greater than 1% relative abundance of the total community were selected to visualize which OTUs were most abundant at different distances from the shipwreck (Figure A.44). For Site 15711 pine and oak samples, one OTU, Ca. *Nitrospumilus*, dominated sequence relative abundance for all sample groups (average of all distance categories 49% for pine and 55% for oak). For Site 15470 pine and oak samples, both Ca. *Nitrospumilus* (average of all distance categories 25% for pine and 34% for oak) and an ambiguous taxon from Nitrospumilaceae (average of all distance categories 19% for pine and 21% for oak) dominated sequence relative abundance. Since the two most abundant OTUs, Ca. *Nitrospumilus* and Nitrospumilaceae, are of a group known to be ubiquitous in both marine sediments (Overholt *et al*., 2019) and the water column (Tolar *et al*., 2020), and were dominating the visual representation of the archaeal community, they were removed from all plots to better view the remainder of the community (Figure A.45). Three OTUs of Crenarcheota found in pine samples had variable abundances across the transects. Bathyarchaeia(uncultured archaeon) peaked at intermediate distances for 15711 pine, but another OTU from the group labeled as Bathyarchaeia declined . This trend was reversed

for 15711 oak as Bathyarchaeia(uncultured archaeon) declined and Bathyarchaeia peaked at intermediate distances. Euryarchaeota Marine Group II peaked at intermediate distances for pine samples at both sites but peaked at the closer distances for oak samples at both sites. Another ambiguous taxon from Euryarchaeota Marine Group II also peaked at intermediate distances for oak samples, and to some extent, pine samples. Thaumarcheota Nitrospumilaceae peaked at intermediate distances for all sites and wood types except 15711 oak samples. In 15711 oak samples, it was not found in the samples from 0-24 m, then declined for samples from 75-99 m. An ambiguous taxon from Thaumarcheota Nitrospumilaceae declined at intermediate distances for both pine and oak at Site 15470.

2.3.4 Community Structure and Phylogenetic Composition of Fungi

The nMDS for fungi at both sites showed an ordination of fungal samples that was not clearly explained by wood type (Figure A.46), site, or distance (Figure A.47). The majority of samples from both sites formed one large group with samples from both wood types and all distances. The samples outside of this group also represented both sites and wood types and varying distances. PERMANOVA results, revealed that neither site, distance, nor wood type are significant structuring features on fungal biofilm composition (Table A.11, $p > 0.05$). This was also the case when sites were visualized separately (data not shown).

The nMDS analysis of fungi from all sites, including GoM-SCHEMA sites *Mica* and *Ewing Bank*, also did not reveal any patterns for site, wood type, or distance (Figure A.48). However, the PERMANOVA indicated that site is significant (Table A.12, $p < 0.05$).

The UniFrac ordination for both sites and wood types explains 50.65% of variance in the data (Figure A.49). The UniFrac PCoA showed mainly a large cluster with samples, but some samples, especially 0-24 m, 25-49 m, and 75-99 m, were found on the outside of this larger cluster. When the UniFrac is labeled by wood type, it appeared that the separation along both Axes 1 and 2 were driven in part by wood type, but also by distance from the shipwreck (Figure A.50). A PERMANOVA on the UniFrac results indicated all three factors are significant, with site closely followed by wood type as the most significant factor ($p < 0.05$, Table A.13).

The UniFrac PCoA for Site 15711 pine samples explained 68% of the variance in the data, but no one axis had a much higher percentage (Figure A.51). Distance groupings appeared to be along both Axis 1 and Axis 2. The UniFrac PCoA for Site 15470 pine explained 75.2% of the variance, and distance groupings along Axis 1 showed 42.26% of the variance was explained by distance from the shipwreck (Figure A.52).

The UniFrac PCoA for Site 15711 oak samples explained 76.6% of the variance, and Axis 1 showed 40.58% was explained by distance from the shipwreck (Figure A.53). The UniFrac PCoA for Site 15470 oak samples explained 87.6% of the variance, and Axis 1 showed 43.56% was attributed to distance from the shipwreck (Figure A.54).

OTUs with representation greater than 1% relative abundance of the total community were selected to visualize which OTUs were most abundant at different distances from the shipwreck (Figure A.55). The majority of fungal OTUs were not assigned taxonomic classifications (average of unassigned OTUs in all samples of 89%). Ascomycota was found in variable abundances across transects regardless of site or wood type. For 15711 pine, it peaked at 75-99 m, for 15711 oak it peaked at 0-24, for 15470

pine it peaked at 175-200 m, and for 15470 oak it peaked greatly at 75-99 m. Ascomycota Tetrapisispora peaked at the farthest distance from the shipwreck for 15711 pine and at the closest distance for 15711 oak. It had variable abundances across the transect for both wood types at Site 15470 but declined at intermediate distances. Basidomycota Agaricomycetes abundance peaked at intermediate distances for pine samples from both sites but declined at intermediate distances for oak samples at both sites. Basidiomycota Agaricales peaked at 0-24 m for 15711 pine and 15470 oak and peaked at 75-99 m for 15470 pine. Glomeromycota *Rhizophagus clarus* had a peak at 75-99 m for 15711 oak samples. This OTU dominated sequence relative abundance at 100-124 m and 124-149 m categories for 15470 oak samples. It was also seen in high abundances at 0-24 m and 25-49 m categories for 15470 pine samples and dominated sequence relative abundance at 124-149 m for this site and wood type.

2.4 Discussion

The main focus of this work was to determine how proximity to shipwrecks influenced diversity, richness, and phylogenetic composition of biofilms formed on wood. In terms of diversity and richness, this study shows that both do change as a function of distance from both Site 15711 and 15470 for bacteria and archaea. However, the same trends are not seen for diversity and richness, or for each site.

While not always statistically significant, diversity consistently exhibits a negative trend for Site 15470 for bacteria and archaea. However, richness consistently exhibits a negative trend for bacteria and archaea at both sites. Richness and diversity also both have a secondary peak at ~125 m away from the shipwreck for several sites and wood types. Richness being more consistent and richness and diversity exhibiting a

secondary peak may be due to the presence of an ecotone. An ecotone is a convergence zone between two ecosystems that connects them along an environmental gradient, and it can function as a diversity hotspot (Levin *et al*., 2016). If the shipwreck ecosystem converging with the background deep-sea ecosystem creates an ecotone, there will be a higher diversity and richness of organisms here because there are phylotypes present from both types of ecosystems. Since the Shannon Diversity index takes into account relative abundance, evenness, and richness, the diversity score may be masking the richness trend seen, due to the increased diversity when reaching the ecotone. The secondary peak of both richness and diversity at 125 m indicates this is where the convergence zone, or ecotone, between the shipwreck environment and the surrounding ambient deep-sea environment is found. The presence of an ecotone is evidence that the shipwreck has its own diverse community that is different from the background habitat and is thus functioning as an island-like system, and that microorganisms dispersing from the shipwreck are using the introduced wood as dispersal stepping stones to reach the background environment.

The overall pattern of decreasing diversity and richness is more evident at Site 15470 for both bacteria and archaea as, overall, there are more significant and negative trends (3 for diversity, 3 for richness) seen here than at Site 15711 (1 for richness). The two sites are separated by 111 km of seafloor and 1275 m of vertical depth. Both location and depth are important factors driving marine sediment community composition (Kallmeyer *et al*., 2012, Hoshino *et al*., 2020), and thus these may also influence biofilm composition. Site 15711 is nearer to the coast and to discharge from the Mississippi River which is also known to influence community composition (Mason *et al*., 2016, Sánchez-

Soto *et al*., 2018). Since Site 15711 is only 76 km from the Mississippi River delta, it is likely that this site recieves more nutrient and carbon deposition relative to 15470. It is, therefore, also likely that 15711 has higher rates of immigration because of its proximity to a source of new taxa, or a "mainland" in the terms of TIB. If the immigration remains high, is connected to a 'mainland' source, and does not equal the extinction rate on the proposed shipwreck island, the distance effect created by organisms dispersing from the shipwreck would not be as evident as would be seen at an island further from the mainland and at equilibrium. Since Site 15470 is in deeper, more oligotrophic waters further from the mainland source of taxa, it is more likely to be at equilibrium and therefore exhibit the stronger distance effect. The increased nutrient availibilty at Site 15711 can also be thought of in terms of island-size. A larger island has higher species richness because it has more resources. In this case, while 15711 is not actually larger, it does have more resources and thus could have more species richness than 15470.

To summarize the findings for diversity and richness in this study, the differences in richness and diversity trends and the secondary peaks in richness and diversity seen at 125 m reflect an ecotone being present between the shipwreck and background environment, which is an indication of the shipwrecks functioning as islands and as dispersal stepping stones. However, the extent to which a distance effect may be seen for a shipwreck functioning as an island is influenced by its geographic location in proximity to a source of taxa and nutrients. In conclusion, while differences in richness and diversity and between sites are seen, these results indicate both diversity and richness change as a function of distance from a shipwreck.

In addition to diversity and richness, this study also investigated how community composition of biofilms on wood was influenced by proximity to a shipwreck. This was done in 3 ways: UniFrac PCoAs, PERMANOVAs on the UniFrac distance matrix results, and taxonomic bar plots. These results showed that community composition is affected by site location, type of wood used, and proximity to a shipwreck.

The differences in geographic location between sites explained above can explain the statistically significant effect of site in structuring the communities of all three domains observed in this study. Geographic location has been found to be important in wood associated bacterial communities before as a study by Ristova *et al.* found that sunken wood communities were more similar within one geographic location than between different seas (Ristova *et al*., 2017). However, studies that take wood type into account show it to be a strong influence on bacterial communities, and more important in bacterial community composition than geographic location or depth (Palacios *et al*., 2009, Fagervold *et al*., 2012, Kalenitchenko *et al*., 2015). An important finding of the current study is that wood type is a selective force on phylogenetic composition for bacteria, archaea, and fungi. Wood type is a selective force on all communities, but it is not as strong as a driver for archaeal or fungal communities as site is. Therefore, the wood type results of this study for bacteria are in line with previous studies, but the results also show that wood type does matter, if to a lesser extent than geographic location, to archaeal and fungal communities.

Along with wood type, proximity to historic wooden shipwrecks also shaped the community composition of biofilms on wood for all three domains. The OTU richness – extinction curves show that there is evidence of an island effect surrounding the two

shipwrecks studied. This indicated that the shipwrecks are a source of taxa to biofilms on other wood surfaces, and thus shape dispersal of the seabed. This feature can also be viewed through the lens of changes to phylogenetic composition and help explore if members of the community use shipwrecks as wooden steps to facilitate their evolution. Previous studies have shown specific phylotypes have an affinity for forming biofilms on different types of sunken marine wood (Palacios *et al*., 2009, Fagervold *et al*., 2012, Kalenitchenko *et al*., 2015). The order Myxococcales has been found in association with sunken pine submerged for 20 months in the South Pacific (Fagervold *et al*., 2012). In the current study, one OTU associated with the Myxococcales (Blrii41) was abundant, in most samples, but changed in abundance as an apparent function of distance. To visualize these changes across distances, a taxonomic bar plot containing this OTU, along with other Myxococcales found in the study that were not present in the top 25 most relative abundant OTUs, was created (Figure A.56). This figure depicts both Sites 15711 and 15470 combined; the only separation is wood type. The abundance for Myxococcales Blrii41 on pine begins at 5% for 0-24 m, peaks at 20% and 19% for 50-74 m and 75-99 m, respectively, and ends at 8% for 175-200 m samples. This pattern of peak abundance at intermediate distances is also seen in oak, but in lower abundances. For oak, the OTUs abundance begins at 1.5% for 0-24 m, peaks at 4.5% and 5% for 50-74 m and 75-99 m, respectively, and ends at 0.7% for 175-200 m samples. There are other OTUs in this study for all three domains that exhibit this pattern of peak abundance at intermediate distances and are in groups known to be associated with marine submerged wood. For bacteria this also includes Rhodobacteraceae on oak samples (Kalenitchenko *et al*., 2015). For archaea this includes Euryarcheaota Marine Group II (2 OTUs) and

Thaumarchaeota Nitrospumilaceae for pine and oak samples (Fagervold *et al*., 2012, Kalenitchenko *et al*., 2015). For fungi this includes Basidiomycota Agaricomycetes for pine samples (Pedersen, 2020). There are 3 scenarios that could lead to this peak in abundance at intermediate distances: (1) fluid dynamics leading to a chance encounter, (2) microorganisms sourcing from the sediment microbiome, and (3) dilution of microorganisms resulting in less competition at intermediate distances allowing for more wood associated taxa to survive.

The first scenario involves fluid dynamics around the shipwreck creating more dispersal of microorganisms to intermediate distances. In Chapter I, Acoustic Doppler Current Profiler data was presented that indicated there was no prevailing current direction at Site 15711 during the deployment time of the experiments. At Site 15470, there was a prevailing Southward current, but other West to Southwest currents were also frequently occurring. These heterogeneous current directions in all directions could cause MREs closer to the shipwreck to receive less taxa than those at intermediate distances. The currents cause more wood associated taxa to be carried from the shipwreck to the MREs at intermediate distances. This is the least likely scenario as it relies mainly on a chance encounter, but because of the various currents at the sites, cannot be ruled out.

The second scenario involves microorganisms at intermediate distances sourcing from the sediment more than at other distances. In Chapter I, SourceTracker2 results were presented that revealed sediment was a source to biofilms, particularly for archaea. For Site 15711, bacteria and archaea proportion estimates for sediment peaked at intermediate distances. Site 15470 sediment proportion estimates were more variable but did peak at intermediate distances for 15470 pine bacteria. If the sediment was a greater

source at intermediate distances, there would be a greater abundance of taxa at those distances as well. However, if this was the case, the taxa at the intermediate distances would not necessarily be wood associated. Those taxa associated specifically with wood would be expected to be in higher abundances at the MRE closest to the main wood source (the shipwreck) than at an intermediate distance from it. Since we see the peak abundance at intermediate distances for taxa known to be associated with wood as well, the sediment as a source does not explain the full story.

The third scenario involves dilution of microorganisms resulting in less competition at intermediate distances allowing for taxa more suited to utilizing wood to thrive there. This study has shown through OTU richness – extinction curves that there is evidence of an island effect surrounding the two shipwrecks and the richness of organisms decreases as a function of distance. Therefore, as distance from the shipwreck increases, competition on the wood surfaces decreases. This decreasing competition allows the microorganisms better suited to utilizing wood to thrive in the environment. However, eventually they will be diluted, too. So, at close distances to the shipwreck they are less abundant due to competition, they peak at intermediate distances where there's less competition and thus more resources and are diluted to lesser abundances at greater distances. This finding comes back to Baas-Becking's statement from 1934, "Everything is everywhere, but the environment selects" (Bass-Becking, 1934). All OTUs are still present at the intermediate distances, but the environment has selected for those taxa that are best suited to it. The microorganisms are using the wood as stepping stones, but they are not stepping in isolation. It takes an amount of distance from the source of taxa to optimize the concentration of the wood associated taxa relative to the concentration of all

taxa. The abundances change across distances as the environment selects for these taxa. In order to be selected, microbes will need to diversify and change, and the wooden stepping stones provides them a link to do so (Distel *et al*., 2017). Wooden shipwrecks could function in this same way. Their presence on the seafloor provides microorganisms with a stepping stone between two environments.

To summarize community composition results of this study, the proximity of the shipwreck to a mainland source of taxa and wood type of the shipwreck will affect the microbiome of the shipwreck and will influence community composition to a different extent for different domains. Wood type is a stronger driver than location for bacteria. While not as strong as location, wood type is a driver for archaeal and fungal biofilm communities. The community composition of biofilms on marine submerged wood also changes as a function of distance from the shipwreck for all three domains. The pattern of peak abundance at intermediate distances for wood associated taxa indicates that the environment does select for taxa best suited to it, and that those taxa could use wooden shipwrecks as a stepping stone between environments.

The combined diversity, richness, and community composition results of this study indicate that wood colonizing microbiomes are impacted by historic wooden shipwrecks. Therefore, proximity to these anthropogenic structures should be considered in studies of marine microbial biogeography.

APPENDIX A – Tables and Figures

Table A.1 *PERMANOVA conducted on Bray-Curtis similarity matrix of bacteria samples from Sites 15711 and 15470.*

Source	Degrees of Freedom	Sum of Squares	Mean Sum of Squares	Pseudo-F	significance (ρ)	Unique Permutations
Site	1	37910	37910	65.629	0.001	999
Wood Type	1	47405	47405	82.066	0.001	998
Distance Category	6	2.53E+03	2532.8	4.3847	0.001	995
Residuals	112	64696	577.64			
Total	135	2.0059E+o5				

Permutational multivariate analysis of variance (PERMANOVA) conducted on bacteria 16s samples to determine differences in community similarity based on site, wood type, and proximity to a shipwreck (distance category). PERMANOVA was run using Type I (sequential) sum of squares, fixed effects summed to zero with permutation of residuals under a reduced model and 999 permutations.

Table A.2 *PERMANOVA conducted on Bray-Curtis similarity matrix of bacteria samples from Site 15711.*

Source	Degrees of Freedom	Sum of Squares	Mean Sum of Squares	Pseudo-F	significance (ρ)	Unique Permutations
Transect	1	1387.3	1387.3	3.0323	0.007	999
Wood Type	1	35909	35909	78.487	0.001	999
Distance Category	4	8.60E+03	2150	4.6992	0.001	998
Residuals	54	24706	457.52			
Total	71	8.11E+04				

Permutational multivariate analysis of variance (PERMANOVA) conducted on bacteria 16s samples to determine differences in community similarity based on wood type, proximity to Site 15711, and transect position. PERMANOVA was run using Type I (sequential) sum of squares, fixed effects summed to zero with permutation of residuals under a reduced model and 999 permutations.

Table A.3 *PERMANOVA conducted on Bray-Curtis similarity matrix of bacteria samples from Site 15470.*

Source	Degrees of Freedom	Sum of Squares	Mean Sum of Squares	Pseudo-F	significance (ρ)	Unique Permutations
Transect	1	3207.8	3207.8	5.6312	0.001	999
Wood Type	1	32981	32981	57.896	0.001	999
Distance Category	5	8.14E+05	1628.3	2.8584	0.001	998
Residuals	50	28483	569.66			
Total	63	7.97E+04				

Permutational multivariate analysis of variance (PERMANOVA) conducted on bacteria 16s samples to determine differences in community similarity based on wood type, proximity to Site 15470, and transect position. PERMANOVA was run using Type I (sequential) sum of squares, fixed effects summed to zero with permutation of residuals under a reduced model and 999 permutations.

Table A.4 *PERMANOVA conducted on Bray-Curtis similarity matrix of bacteria samples from Sites 15711 and 15470 and Mica and Ewing Bank.*

Source	Degrees of Freedom	Sum of Squares	Mean Sum of Squares	Pseudo-F	significance (ρ)	Unique Permutations
Site	3	52396	17465	31.555	0.001	999
Wood Type	1	43930	43930	79.372	0.001	998
Distance Category	6	2.50E+03	2498.4	4.5139	0.001	997
Residuals	120	66417	553.48			
Total	147	2.21E+05				

Permutational multivariate analysis of variance (PERMANOVA) conducted on biofilm samples to determine differences in bacteria microbiome community similarity based on site, wood type and proximity to a shipwreck (distance category). PERMANOVA was run using Type I (sequential) sum of squares, fixed effects summed to zero with permutation of residuals under a reduced model and 999 permutations.

Table A.5 *PERMANOVA conducted on UNIFRAC distance matrix of bacteria samples from Sites 15711 and 15470.*

Source	Pseudo-F	significance (ρ)	Unique Permutations
Site	28.4395	0.001	999
Wood Type	46.747	0.001	999
Distance Category	3.13531	0.001	999

Permutational multivariate analysis of variance (PERMANOVA) conducted on a UNIFRAC distance matrix of bacterial biofilm samples to determine differences in bacteria microbiome community similarity based on site, wood type and proximity to a shipwreck (distance category).

Table A.6 *PERMANOVA conducted on Bray-Curtis similarity matrix of archaea samples from Sites 15711 and 15470.*

Source	Degrees of Freedom	Sum of Squares	Mean Sum of Squares	Pseudo-F	significance (ρ)	Unique Permutations
Site	1	18567	18567	31.857	0.001	999
Wood Type	1	926.27	926.27	1.5892	0.185	998
Distance Category	6	3.17E+04	5290.5	9.0772	0.001	998
Residuals	80	46627	582.84			
Total	102	1.17E+05				

Permutational multivariate analysis of variance (PERMANOVA) conducted on archaea 16s samples to determine differences in community similarity based on site, wood type, and proximity to a shipwreck (distance category). PERMANOVA was run using Type I (sequential) sum of squares, fixed effects summed to zero with permutation of residuals under a reduced model and 999 permutations.

Table A.7 *PERMANOVA conducted on Bray-Curtis similarity matrix of archaea samples from Site 15711.*

Source	Degrees of Freedom	Sum of Squares	Mean Sum of Squares	Pseudo-F	significance (ρ)	Unique Permutations
Transect	1	1861.6	1861.6	1.7151	0.128	999
Wood Type	1	1193.8	2293.8	2.1132	0.067	998
Distance Category	4	8.27E+03	2067.7	1.9049	0.025	998
Residuals	38	41247	1085.4			
Total	54	6.46E+04				

Permutational multivariate analysis of variance (PERMANOVA) conducted on archaea 16s samples to determine differences in community similarity based on wood type, proximity to Site 15711, and transect position. PERMANOVA was run using Type I (sequential) sum of squares, fixed effects summed to zero with permutation of residuals under a reduced model and 999 permutations.

Table A.8 *PERMANOVA conducted on Bray-Curtis similarity matrix of archaea samples from Site 15470.*

Source	Degrees of Freedom	Sum of Squares	Mean Sum of Squares	Pseudo-F	significance (ρ)	Unique Permutations
Transect	1	4466.3	4466.3	11.615	0.001	999
Wood Type	1	1397.2	1397.2	3.6335	0.02	999
Distance Category	5	31417	6.28E+03	16.341	0.001	999
Residuals	35	13458	384.52			
Total	47					

Permutational multivariate analysis of variance (PERMANOVA) conducted on archaea 16s samples to determine differences in community similarity based on wood type, proximity to Site 15470, and transect position. PERMANOVA was run using Type I (sequential) sum of squares, fixed effects summed to zero with permutation of residuals under a reduced model and 999 permutations.

Table A.9 *PERMANOVA conducted on Bray-Curtis similarity matrix of archaea samples from Sites 15711 and 15470 and Mica and Ewing Bank.*

Source	Degrees of Freedom	Sum of Squares	Mean Sum of Squares	Pseudo-F	significance (ρ)	Unique Permutations
Site	3	21888	7295.9	11.437	0.001	998
Wood Type	1	165.3	265.3	0.41586	0.702	998
Distance Category	6	3.17E+04	5280.3	8.277	0.001	998
Residuals	87	55502	637.95			
Total	113	1.33E+05				

Permutational multivariate analysis of variance (PERMANOVA) conducted on archaea biofilm samples to determine differences in community similarity based on site, wood type, and proximity to a shipwreck (distance category). PERMANOVA was run using Type I (sequential) sum of squares, fixed effects summed to zero with permutation of residuals under a reduced model and 999 permutations.

Table A.10 *PERMANOVA conducted on UNIFRAC distance matrix of archaea samples from Sites 15711 and 15470.*

Source	Pseudo-F	significance (ρ)	Unique Permutations
Site	31.9512	0.001	999
Wood Type	4.31825	0.002	999
Distance Category	2.22786	0.001	999

Permutational multivariate analysis of variance (PERMANOVA) conducted on a UNIFRAC distance matrix of bacterial biofilm samples to determine differences in archaea microbiome community similarity based on site, wood type and proximity to a shipwreck (distance category).

Table A.11 *PERMANOVA conducted on Bray-Curtis similarity matrix of fungi samples from Sites 15711 and 15470.*

Source	Degrees of Freedom	Sum of Squares	Mean Sum of Squares	Pseudo-F	significance (ρ)	Unique Permutations
Site	1	988.12	988.12	2.5705	0.051	999
Wood Type	1	705.98	705.98	1.8365	0.122	999
Distance Category	6	3.73E+03	621.13	1.6158	0.072	999
Residuals	84	32291	384.42			
Total	107	4.69E+04				

Permutational multivariate analysis of variance (PERMANOVA) conducted on fungal biofilm samples to determine differences in community similarity based on site, wood type, and proximity to a shipwreck (distance category). PERMANOVA was run using Type I (sequential) sum of squares, fixed effects summed to zero with permutation of residuals under a reduced model and 999 permutations.

Table A.12 *PERMANOVA conducted on Bray-Curtis similarity matrix of fungi samples from Sites 15711 and 15470 and Mica and Ewing Bank.*

Source	Degrees of Freedom	Sum of Squares	Mean Sum of Squares	Pseudo-F	significance (ρ)	Unique Permutations
Site	3	9425.6	3141.9	7.2207	0.001	999
Wood Type	1	887.73	887.73	2.0402	0.094	999
Distance Category	6	3.66E+03	610.24	1.4025	0.145	998
Residuals	89	38726	435.12			
Total	116	6.54E+04				

Permutational multivariate analysis of variance (PERMANOVA) conducted on fungal biofilm samples from *Sites 15711 and 15470 and* Mica *and* Ewing Bank to determine differences in community similarity based on site, and proximity to a shipwreck (distance category). PERMANOVA was run using Type I (sequential) sum of squares, fixed effects summed to zero with permutation of residuals under a reduced model and 999 permutations.

Table A.13 *PERMANOVA conducted on UNIFRAC distance matrix of fungi samples from Sites 15711 and 15470.*

Source	Pseudo-F	significance (ρ)	Unique Permutations
Site	9.57768	0.001	999
Wood Type	8.67313	0.001	999
Distance Category	1.68039	0.006	999

Permutational multivariate analysis of variance (PERMANOVA) conducted on a UNIFRAC distance matrix of bacterial biofilm samples to determine differences in fungal microbiome community similarity based on site, wood type and proximity to a shipwreck (distance category).

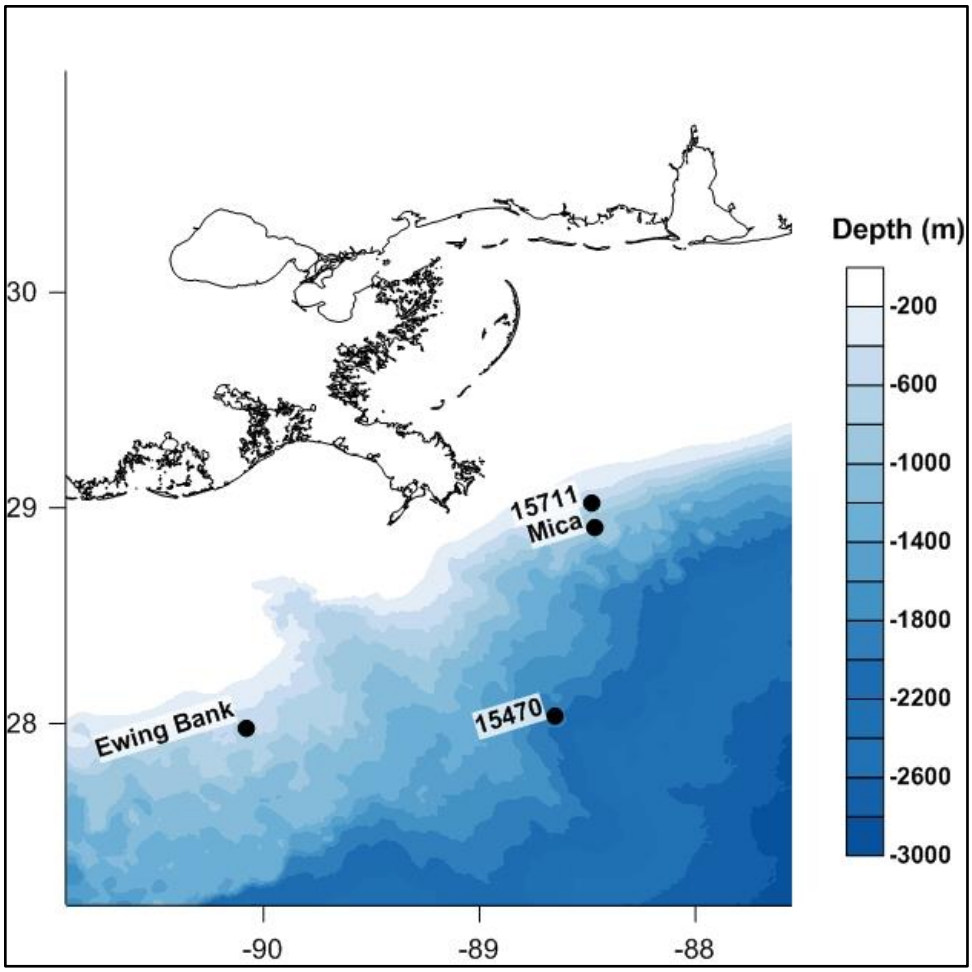

Figure A.1 *Site Map*

Map depicts location of Sites 15711 and 15470 described in Chapter One. Sites Ewing Bank and Mica will be described in Chapter Two.

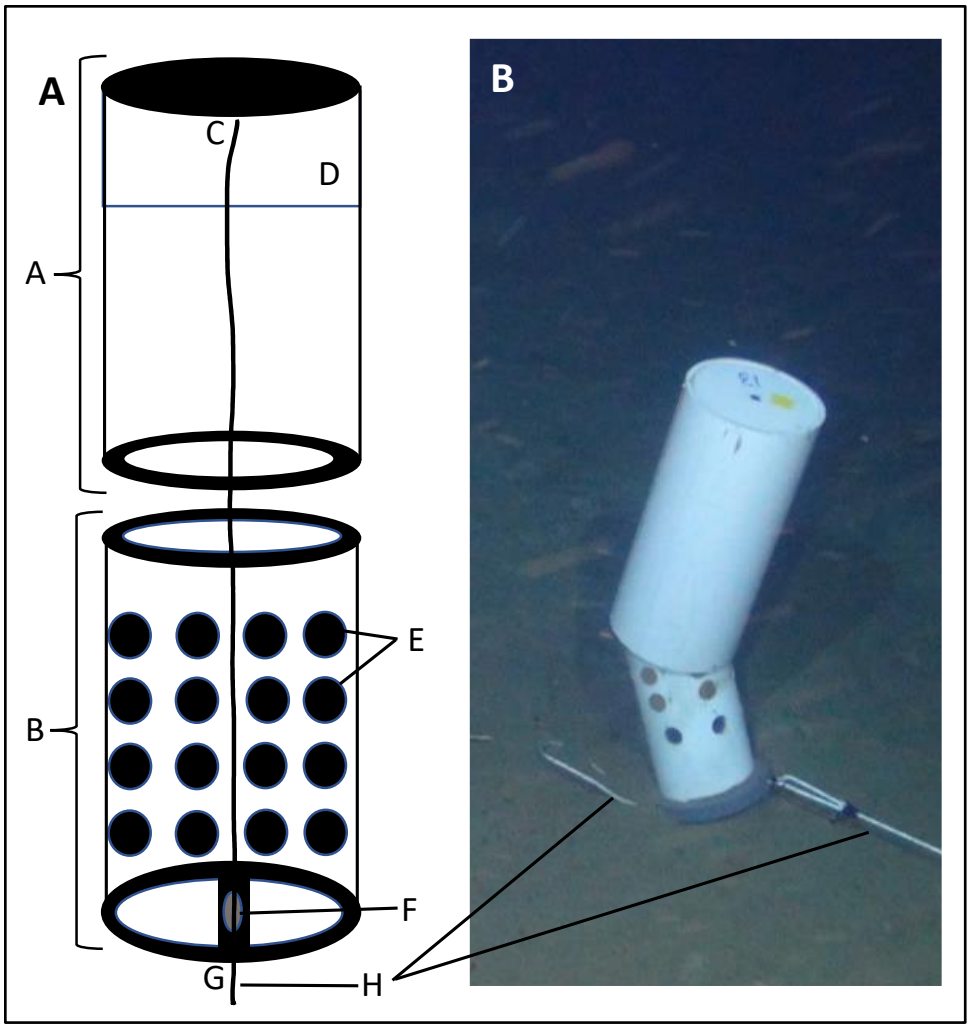

Figure A.2 *Diagram of an MRE*

A. Diagram of an MRE: (A) cover (B) sample holder (C) knot attaching cover to sample holder (D) syntactic foam (E) 1.25-in holes (F) cleat (G) knot determining cover floating height (H) lines connecting MREs. **B.** Actual MRE deployed on the seafloor.

Figure A.3 *MRE array placed in cradle*

The cradle is bolted to the ROV for deployment.

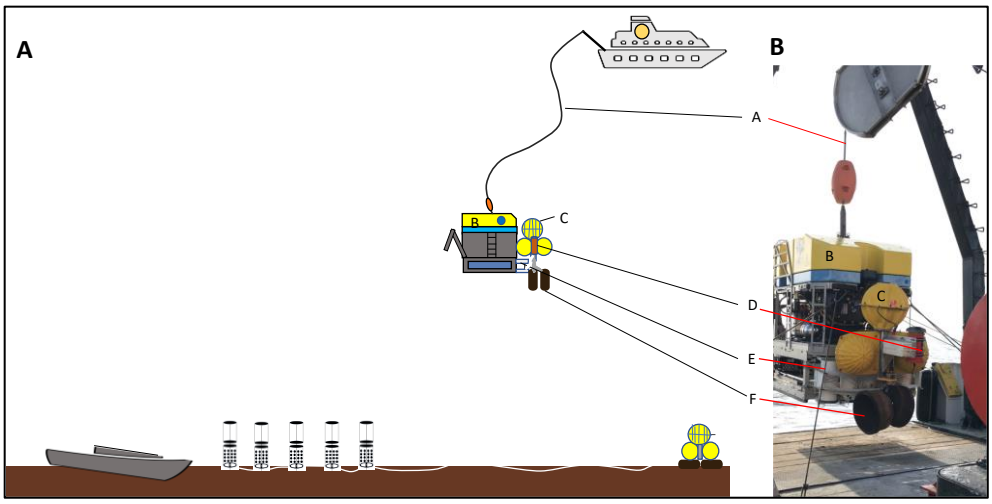

Figure A.4 *MRE deployment by ROV*

A. Diagram of lander and MRE deployment (A) ROV tether (B) ROV (C) lander (D) ADCP (E) MREs in cradle attached to ROV (F) sacrificial weights (G) ROV navigates to lander drop zone and releases lander (H) ROV travels along the transect and MREs are deployed (I) ROV returns to ship. **B**. Actual ROV prepped for deployment.

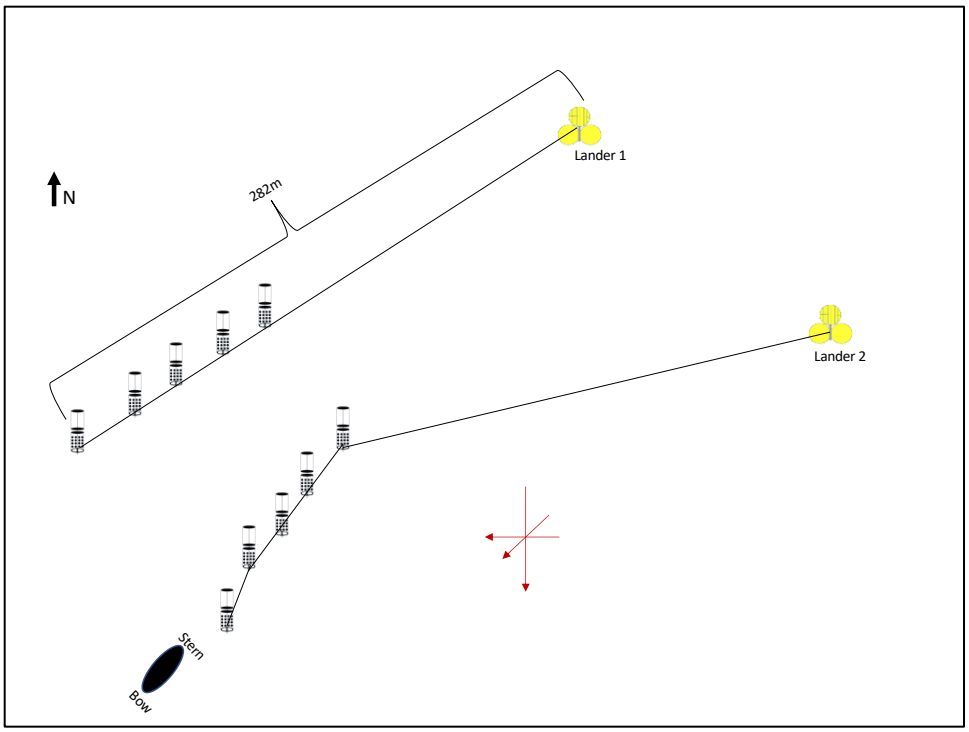

Figure A.5 *Transects at Site 15470*

The ADCP was located on Lander 2. Red arrows indicate the directions of prevailing currents.

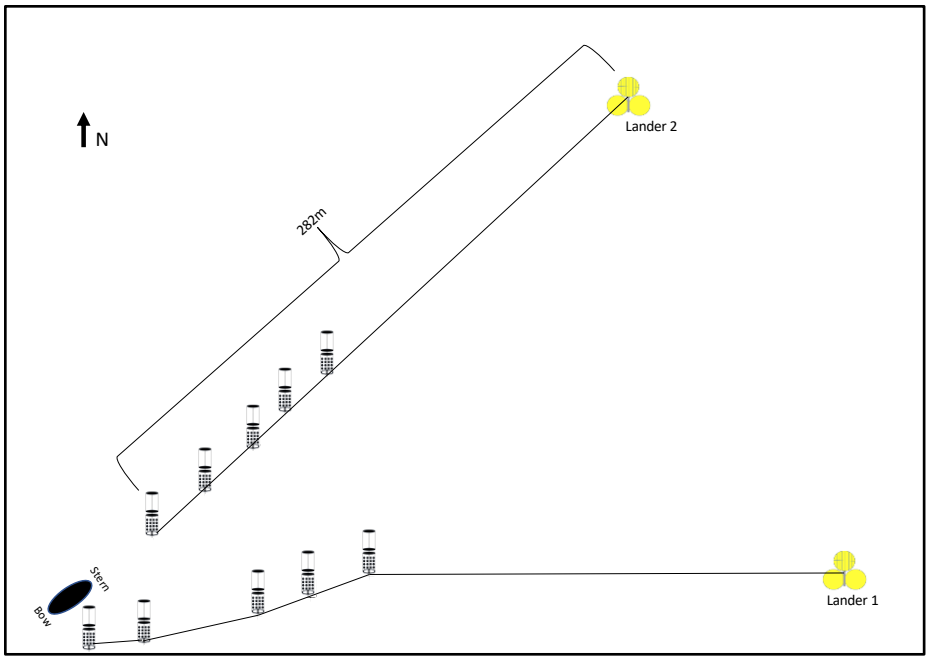

Figure A.6 *Transects at Site 15711*

ADCP was located on Lander 2.

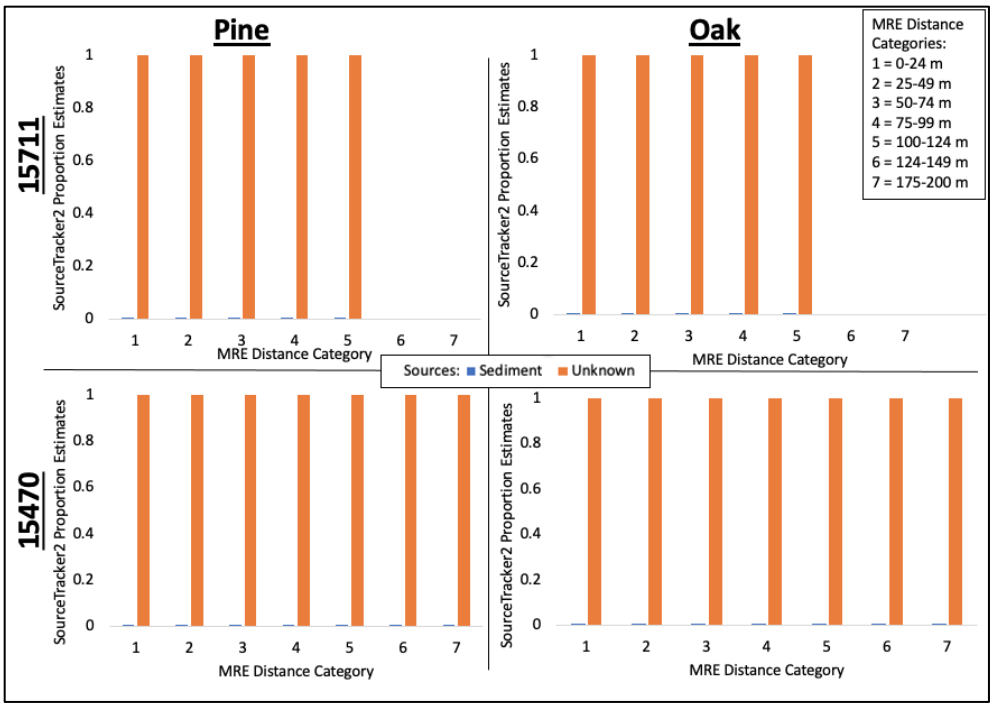

Figure A.7 *Bacteria SourceTracker2 Proportion Estimates*

SourceTracker2 analyses were conducted on each site and wood type separately. Bacteria biofilms were treated as a sink community while sediment and water were treated as a source community. Results are reported as proportion estimates. Water proportion estimates were not reported in any of the bacteria analyses.

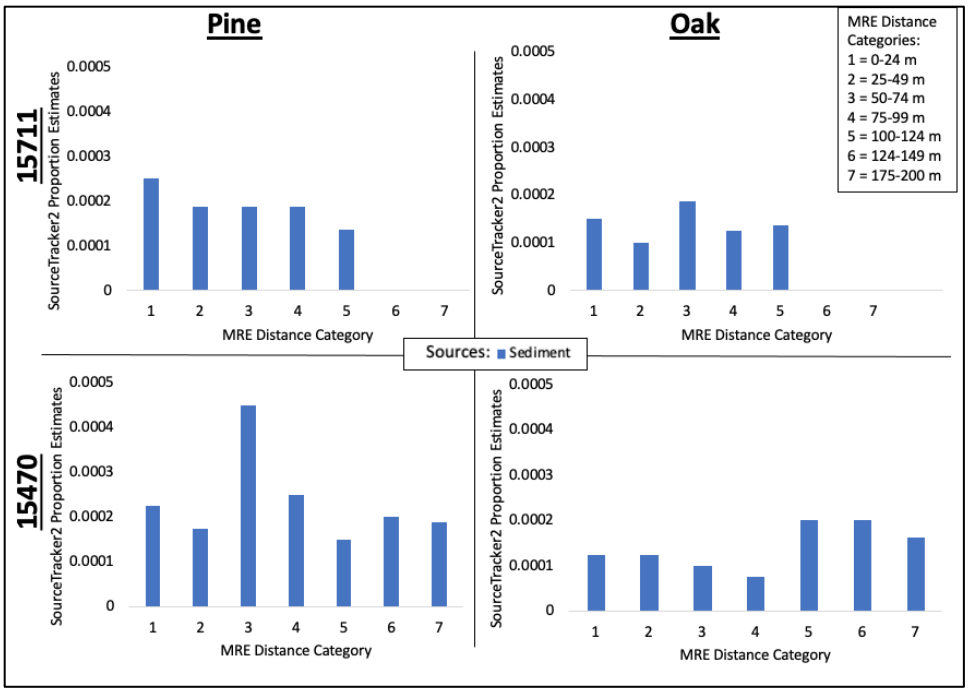

Figure A.8 *Bacteria SourceTracker2 proportion estimates for sediment only*

The unknown sources bar was removed in order to visualize the sediment proportion estimates for bacteria more closely.

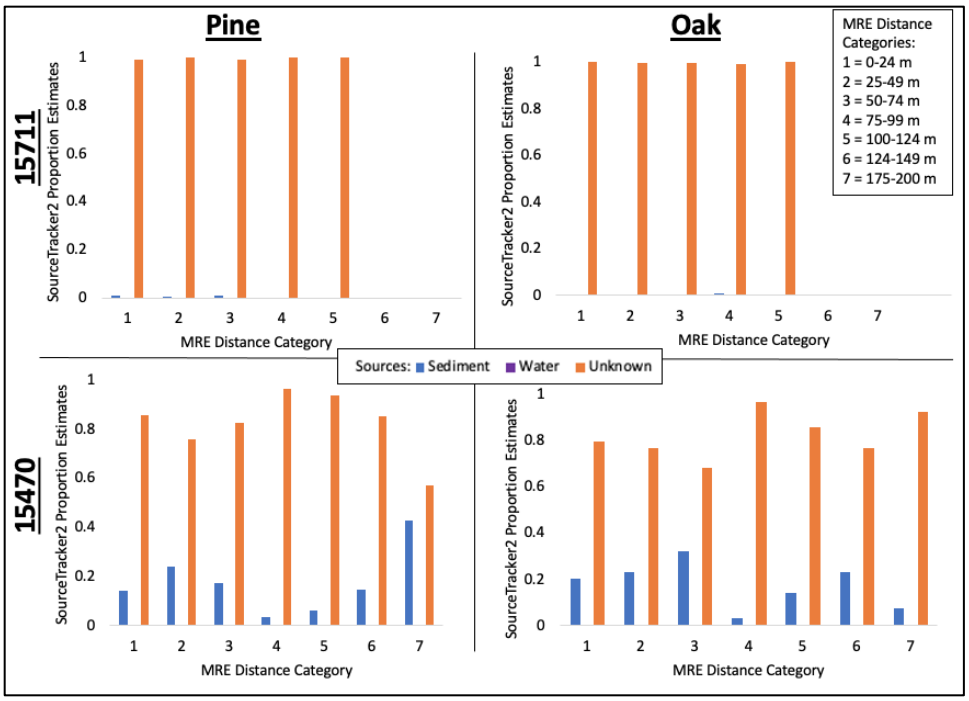

Figure A.9 *Archaea SourceTracker2 proportion estimates*

SourceTracker2 analyses were conducted on each site and wood type separately. Archaea biofilms were treated as a sink community while sediment and water were treated as source communities. Results are reported as proportion estimates.

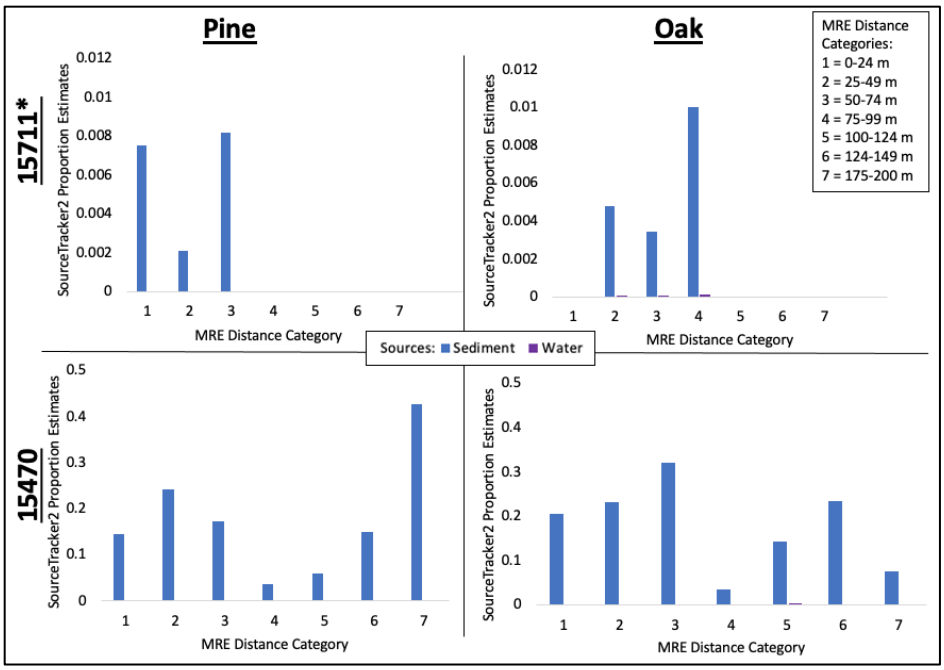

Figure A.10 *Archaea SourceTracker2 proportion estimates for sediment and water only*

Asterisk denotes the scale for Site 15711 is different from that of Site 15470. The unknown sources bar was removed in order to visualize the sediment and water proportion estimates for archaea more closely.

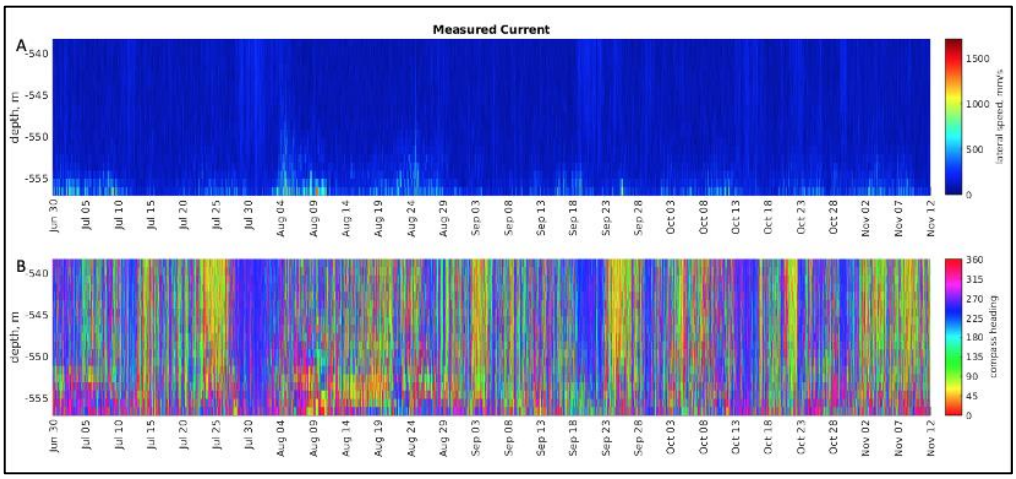

Figure A.11 *Acoustic Doppler Current Profiler data from Site 15711*

A. Speed of current in mm/s at depths 540 m to 560 m from June 30, 2019 to November 12, 2019. **B.** Direction of the current at depths 540 m to 560 m for the same time period.

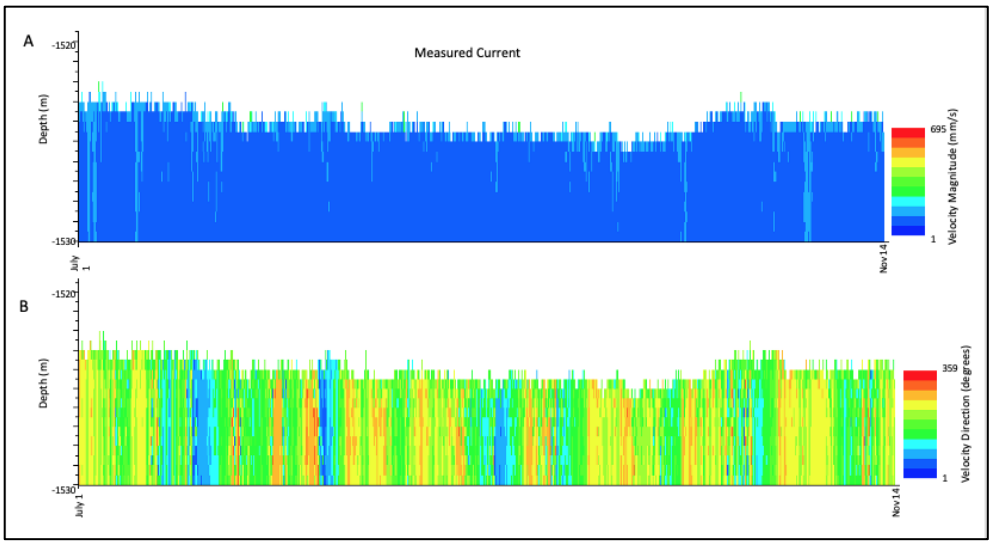

Figure A.12 *Acoustic Doppler Current Profiler data from Site 15470*

A. Speed of current in mm/s at depths 1520 m to 1530 m from July 1, 2019 to November 14, 2019. **B.** Direction of the current at depths 1520 m to 1530 m for the same time period.

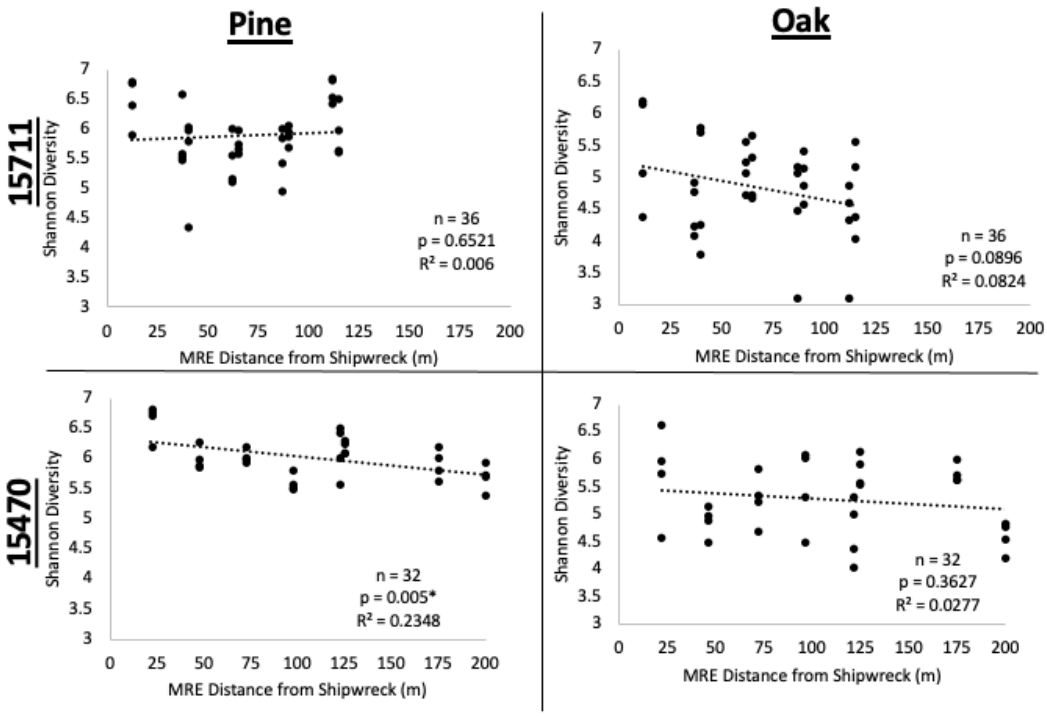

Figure A.13 *Bacteria Shannon Diversity for Sites 15711 and 15470.*

Shannon diversity of 16s rRNA bacteria reveals diversity does significantly decrease as a function of distance from the shipwreck for Site 15470 pine ($p < 0.05$). While not significant, the trends for oak at both sites are negative.

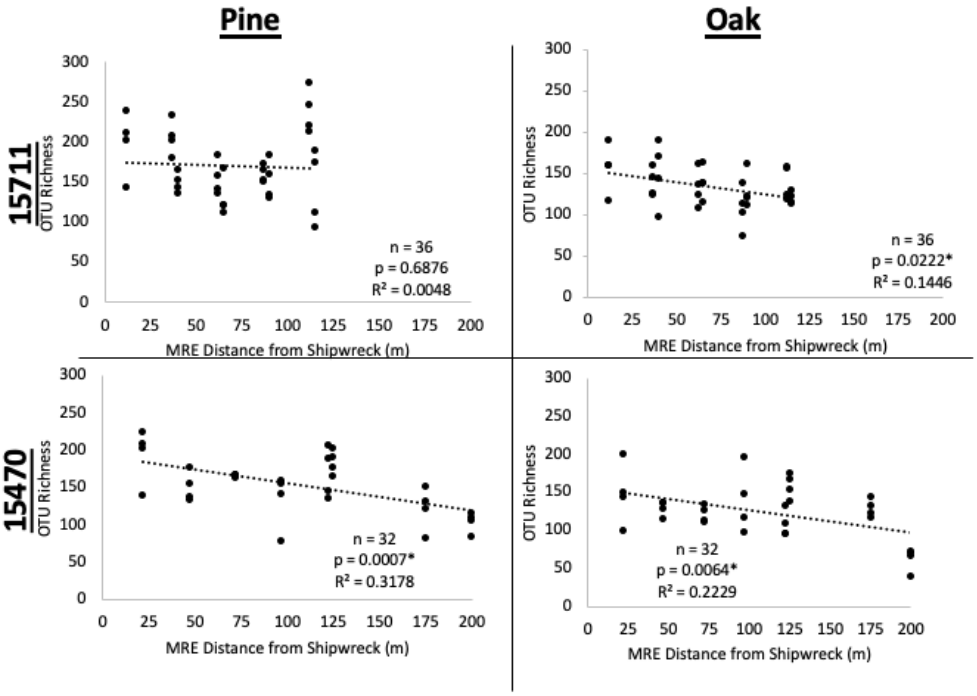

Figure A.14 *Bacteria OTU Richness for Sites 15711 and 15470.*

OTU richness of 16s rRNA bacteria reveals richness does significantly decrease as a function of distance from the shipwreck for all sites and wood types except 15711 pine. Asterisk denotes statistical significance of $p < 0.05$.

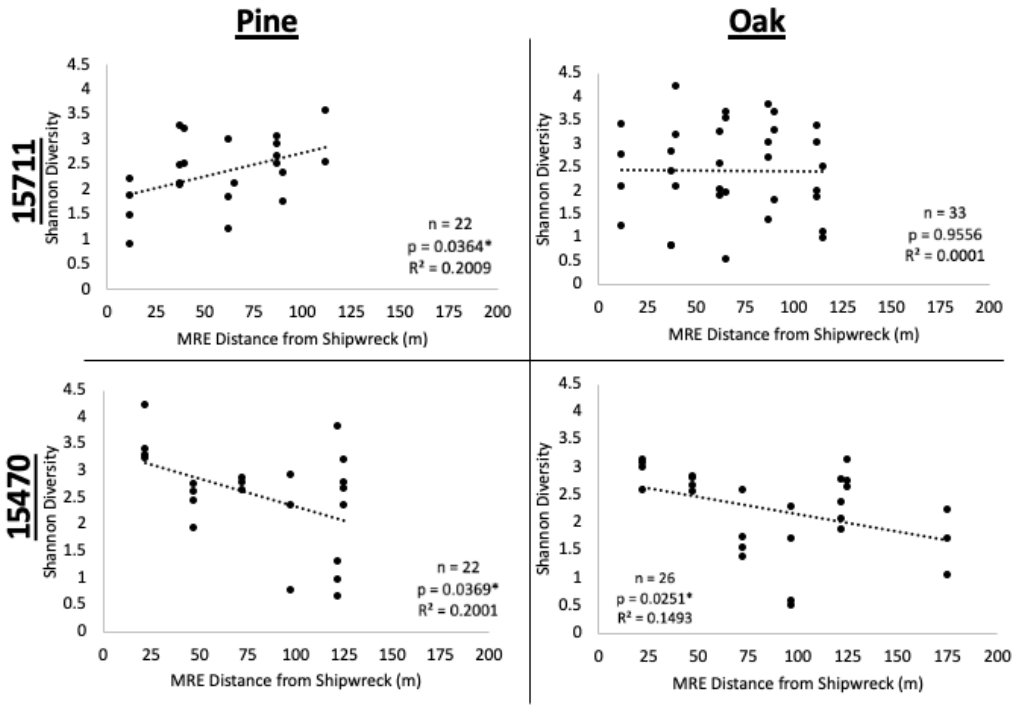

Figure A.15 *Archaea Shannon Diversity for Sites 15711 and 15470.*

Shannon diversity of 16s rRNA archaea reveals diversity does significantly decrease as a function of distance from the shipwreck at Site 15470 for both wood types. Shannon diversity at Site 15711 significantly increases with distance for pine samples and remains stable for oak samples. Asterisk denotes statistical significance of $p < 0.05$.

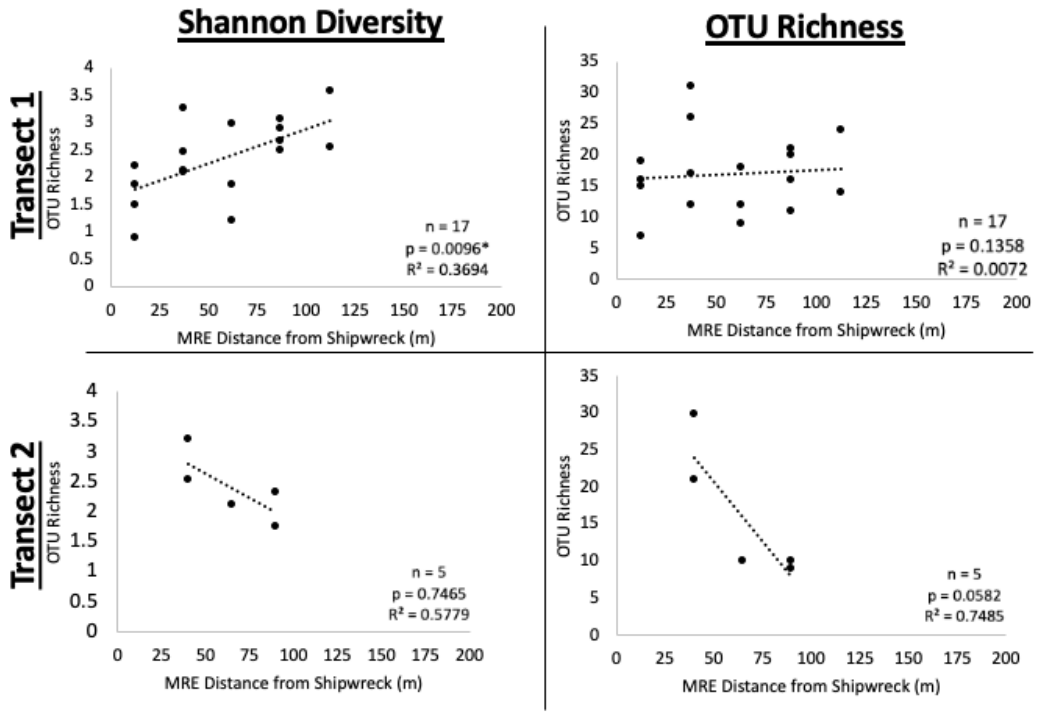

Figure A.16 *Archaea Shannon Diversity and OTU richness for Site 15711 pine samples.*

16s rRNA for archaea at Site 15711 for pine samples are separated by transect to show there were many samples removed from transect 2 and only Shannon diversity for transect one is statistically significant ($p < 0.05$).

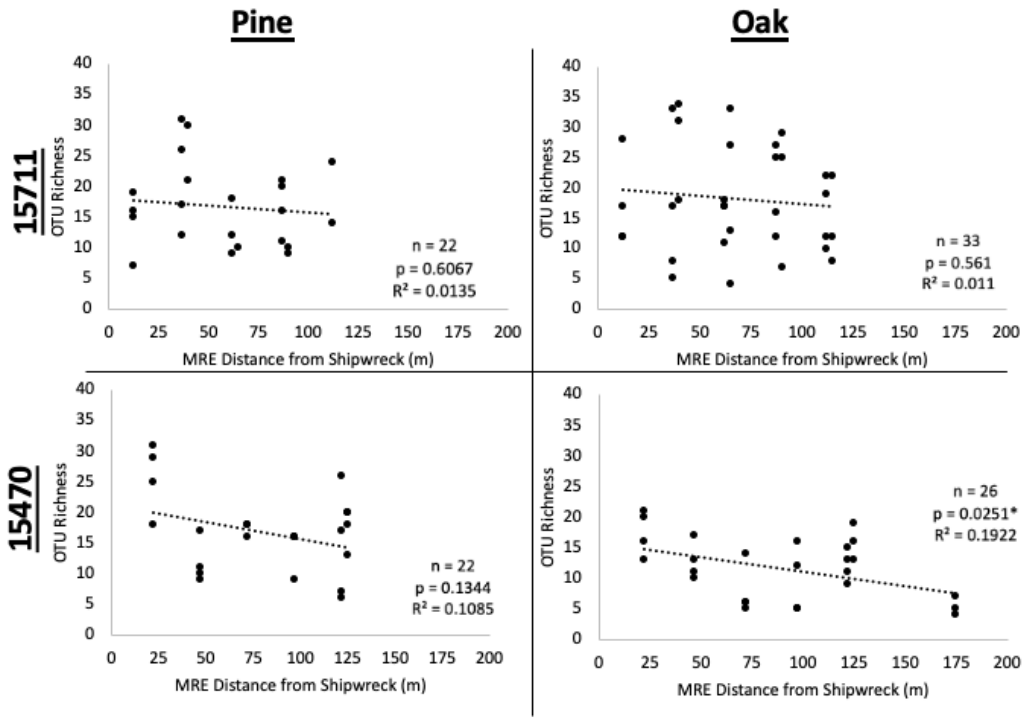

Figure A.17 *Archaea OTU Richness for Sites 15711 and 15470.*

OTU richness of 16s rRNA archaea reveals richness does decrease as a function of distance from the shipwreck at Site 15470 for oak samples ($p < 0.05$).

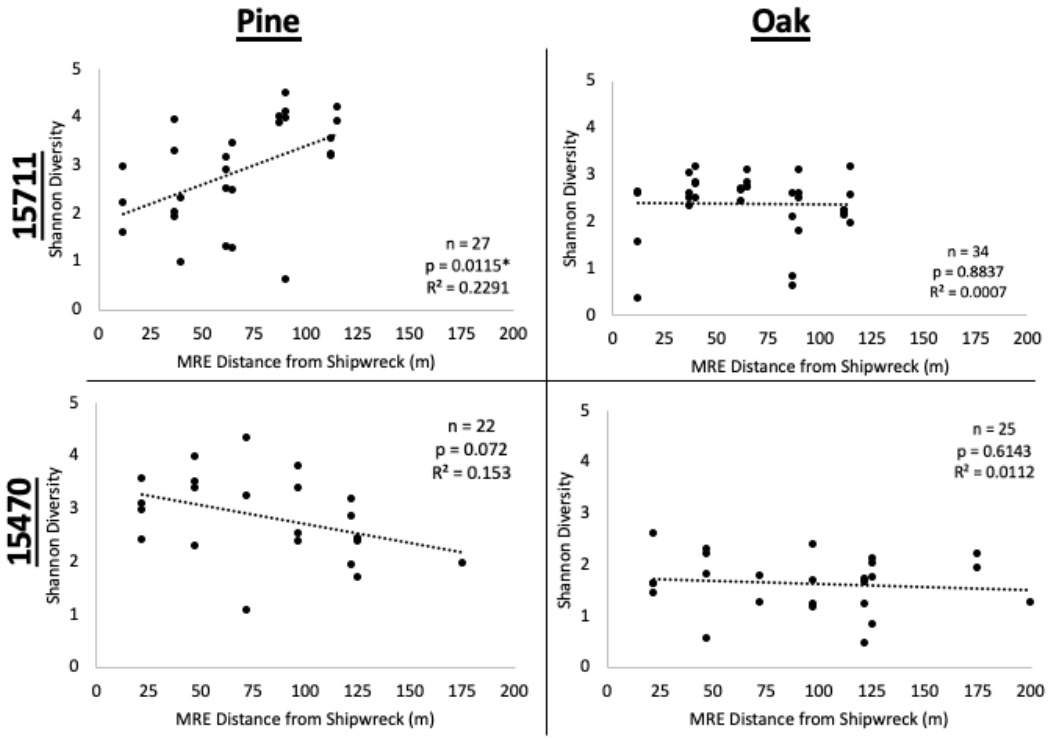

Figure A.18 *Fungi Shannon Diversity for Sites 15711 and 15470.*

Shannon diversity for ITS2 fungi show no significant relationships decreasing with decreased proximity to the shipwreck. Only 15711 pine samples depict a significant relationship, and it shows an increase in diversity with decreased proximity. Asterisk denotes statistically significant relationship of $p < 0.05$.

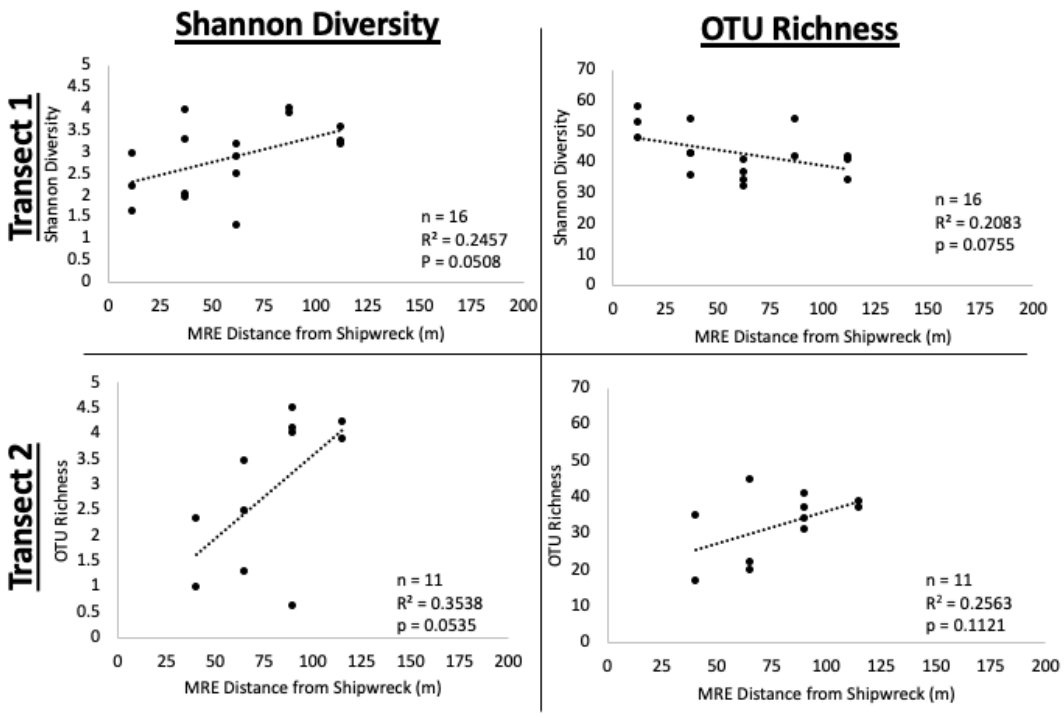

Figure A.19 *Fungi Shannon Diversity and OTU Richness for Site 15711 pine samples.*

Shannon diversity and OTU richness of ITS fungi for individual transects of Site 15711 pine samples do not reveal any significant relationships of one transect over the other.

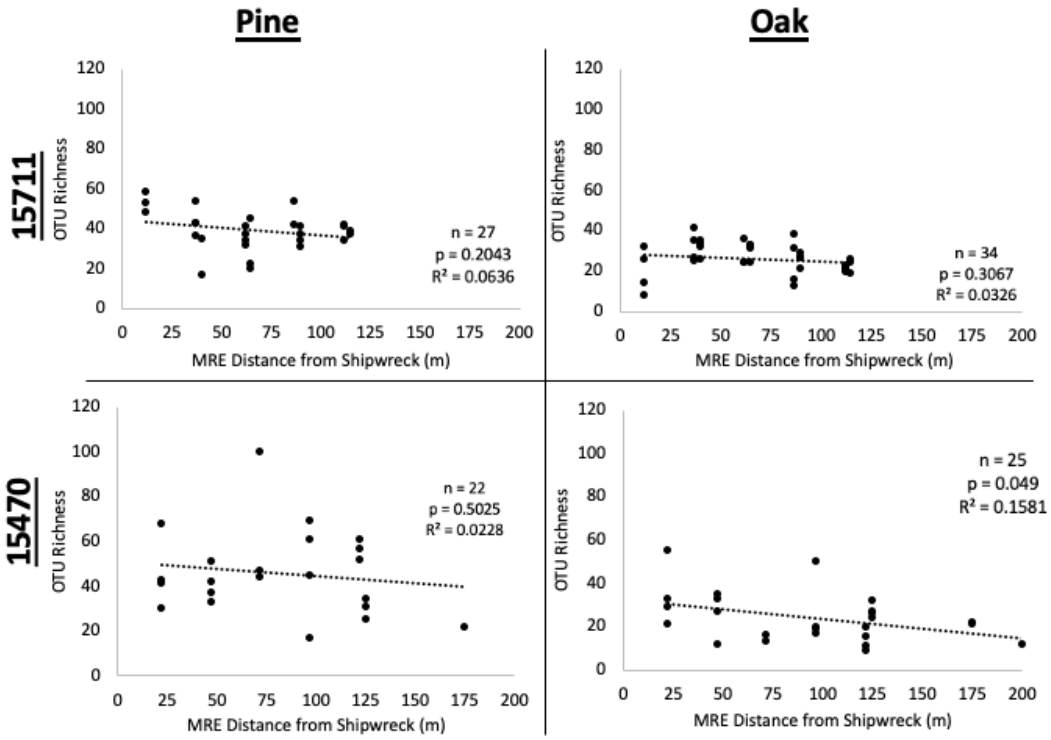

Figure A.20 *Fungi OTU Richness for Sites 15711 and 15470.*

OTU richness for ITS2 fungi does not reveal any significant relationships.

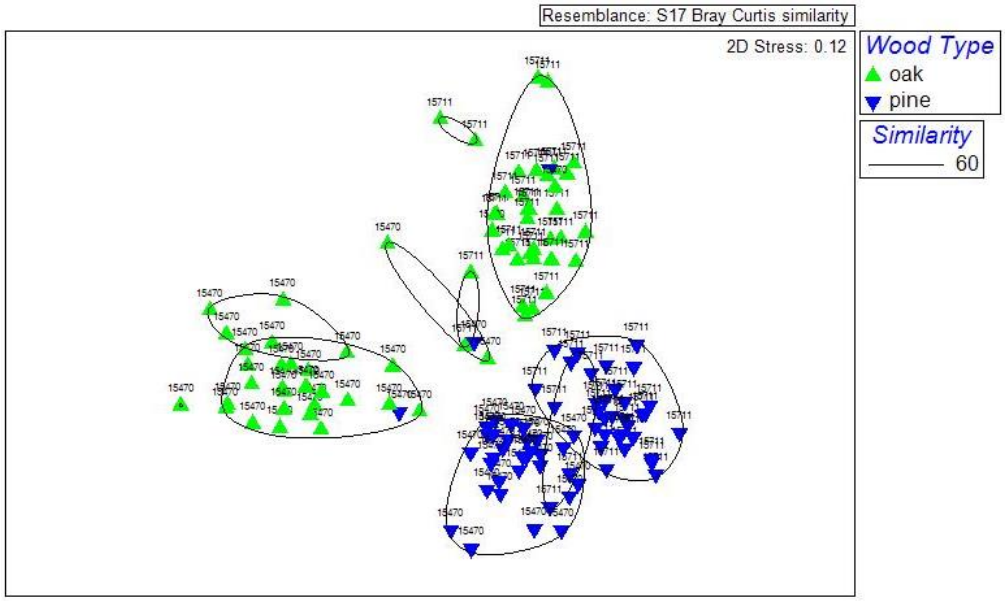

Figure A.21 *Bacteria nMDS for Sites 15711 and 15470 labeled by wood type and site.*

nMDS of 16s rRNA bacteria depicts samples grouping out by wood type and site (label) at 60 percent Bray-Curtis similarity. Samples fall into four main groupings: Site 15470 pine, Site 15470 oak, Site 15711 pine, and Site 15711 oak.

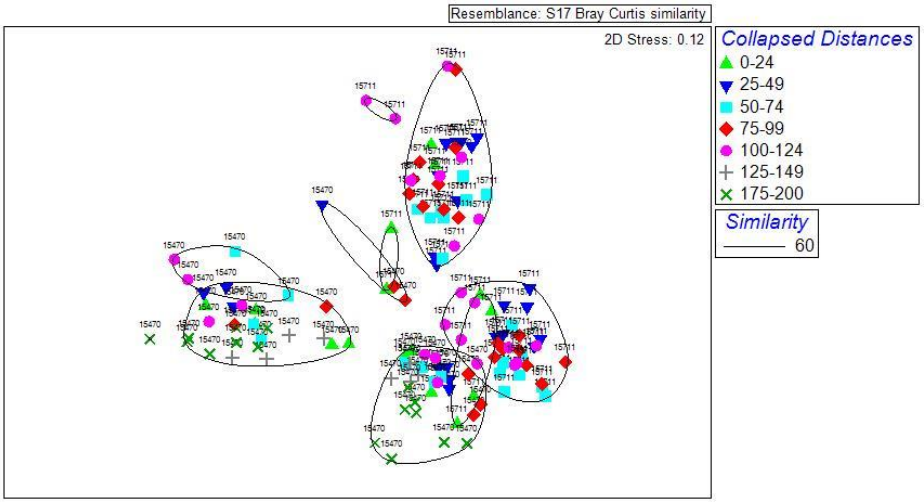

Figure A.22 *Bacteria nMDS for Sites 15711 and 15470 labeled by collapsed distances and site.*

nMDS of 16s rRNA bacteria depicts samples grouping out by wood type and site (label) at 60 percent Bray-Curtis similarity. Samples fall into four main groupings: Site 15470 pine, Site 15470 oak, Site 15711 pine, and Site 15711 oak.

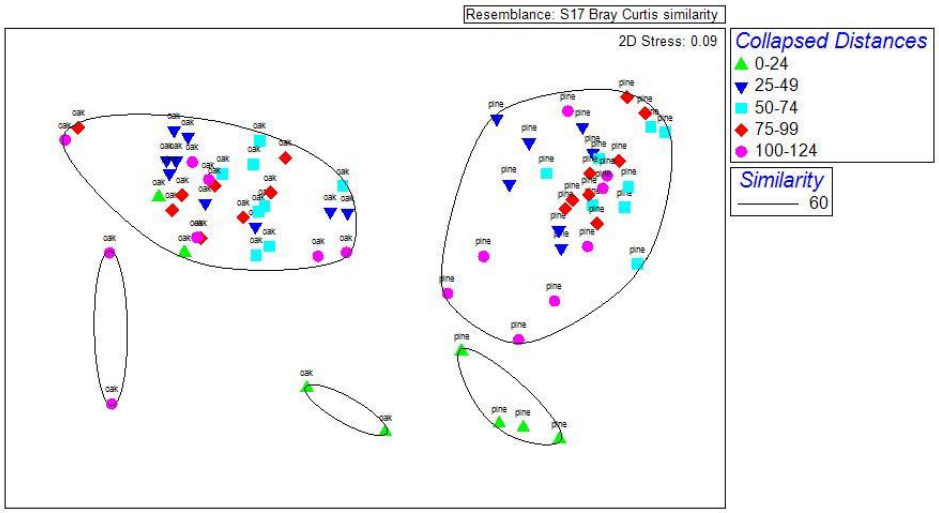

Figure A.23 *Bacteria nMDS for Site 15711.*

nMDS for 16s rRNA bacteria at Site 15711 at 60 percent Bray-Curtis similarity indicates strong grouping by wood type (label), but some distance groupings can be seen.

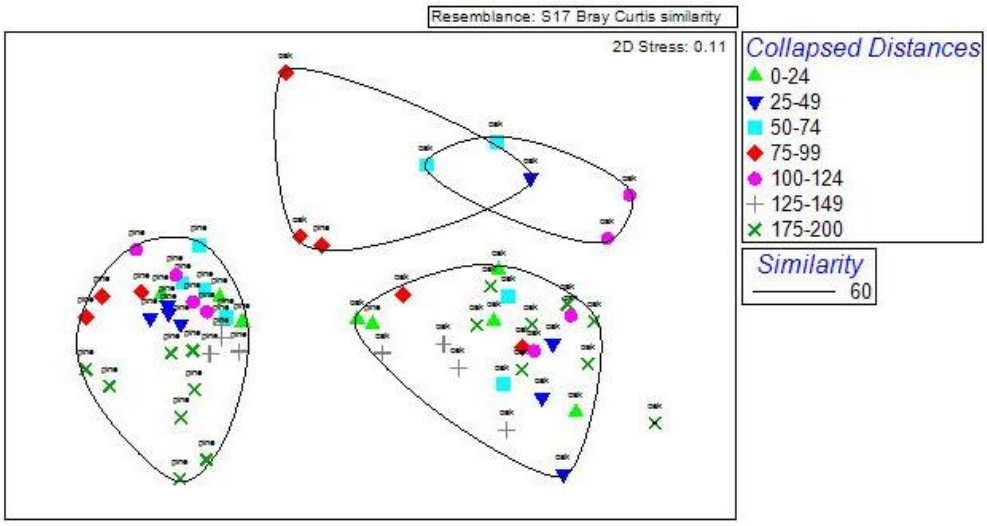

Figure A.24 *Bacteria nMDS for Site 15470.*

nMDS for 16s rRNA bacteria at Site 15470 at 60 percent Bray-Curtis similarity indicates strong grouping by wood type (label), but some distance groupings can be seen.

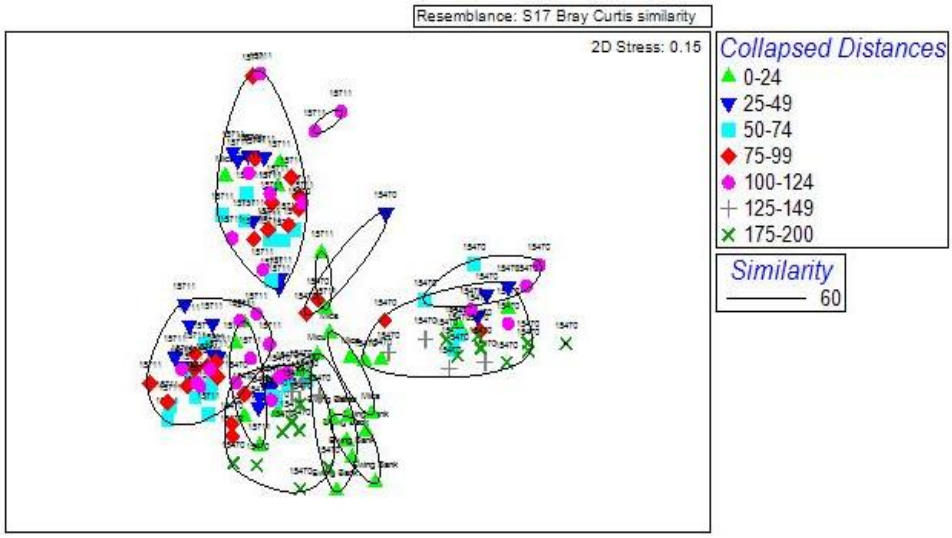

Figure A.25 *Bacteria nMDS for Sites 15711, 15470, Mica, and Ewing Bank.*

nMDS for 16s rRNA bacteria at all four sites at 60 percent Bray-Curtis similarity indicates GoM-SCHEMA sites grouping together despite wood type.

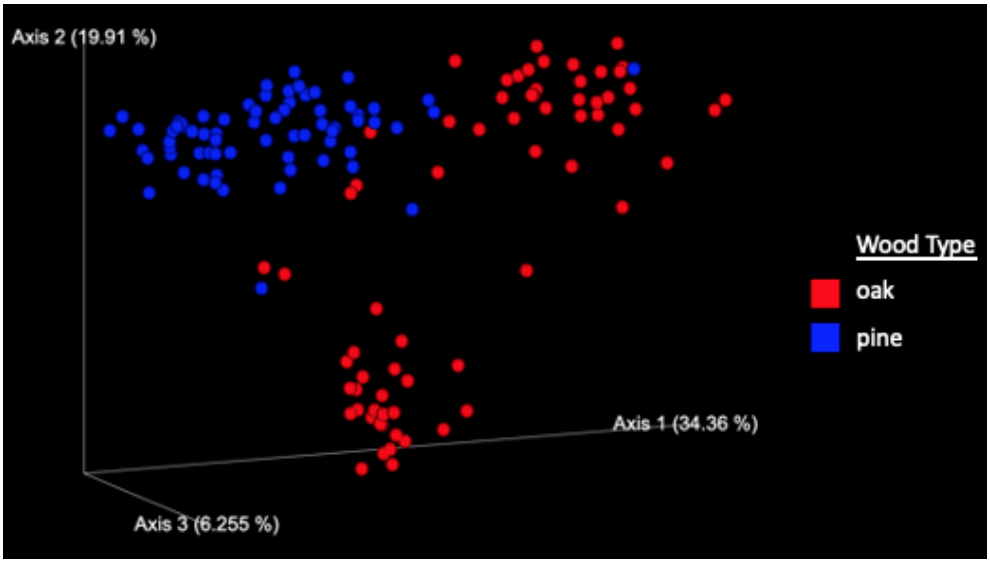

Figure A.26 *UniFrac PCoA for bacteria from Sites 15711 and 15470 labeled by wood type.*

UniFrac PCoA reveals grouping by wood type.

.

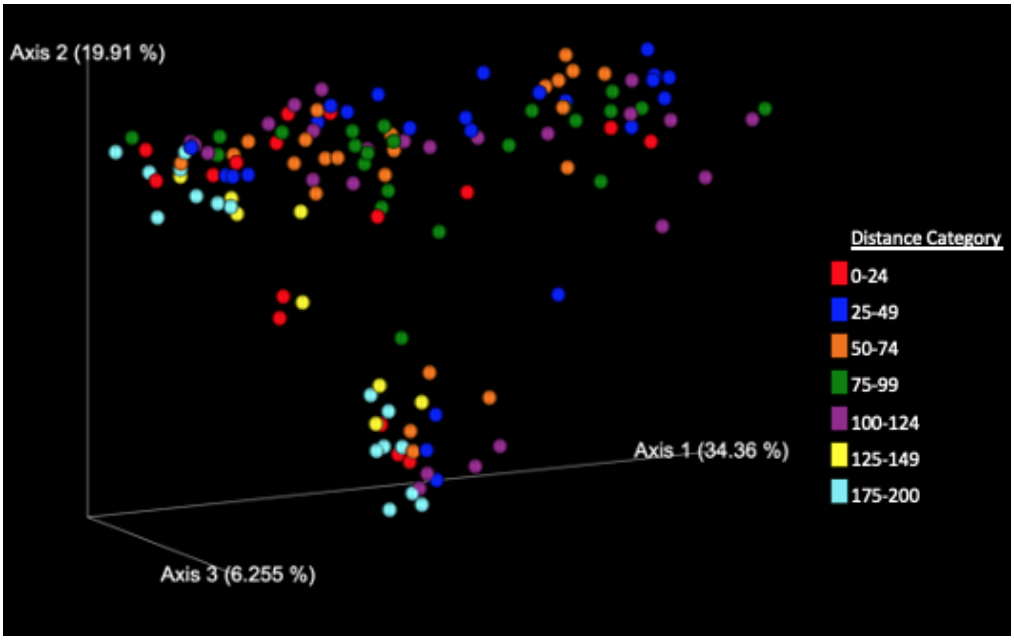

Figure A.27 *UniFrac PCoA for bacteria from Sites 15711 and 15470 labeled by distance category.*

UniFrac PCoA reveals grouping by distance category is driven by Axis 1.

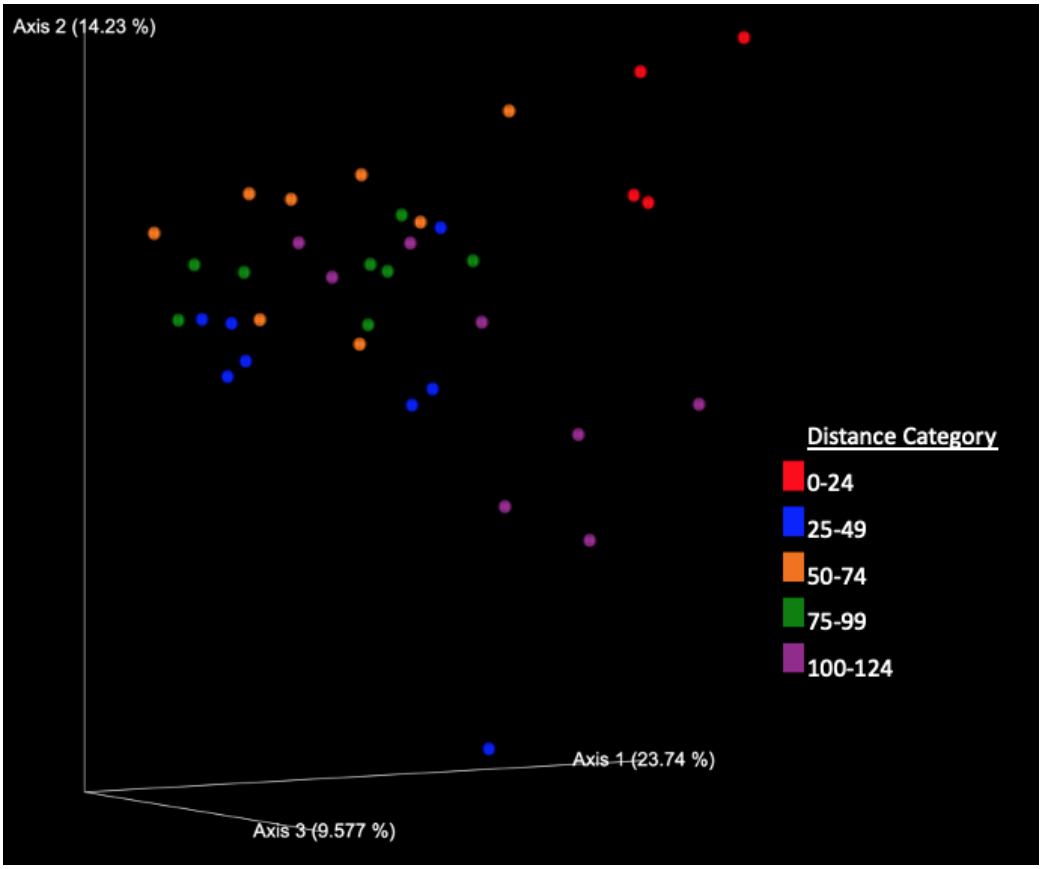

Figure A.28 UniFrac PCoA for bacteria from Site 15711 pine samples.

UniFrac PCoA reveals grouping by distance category is driven by Axis 1.

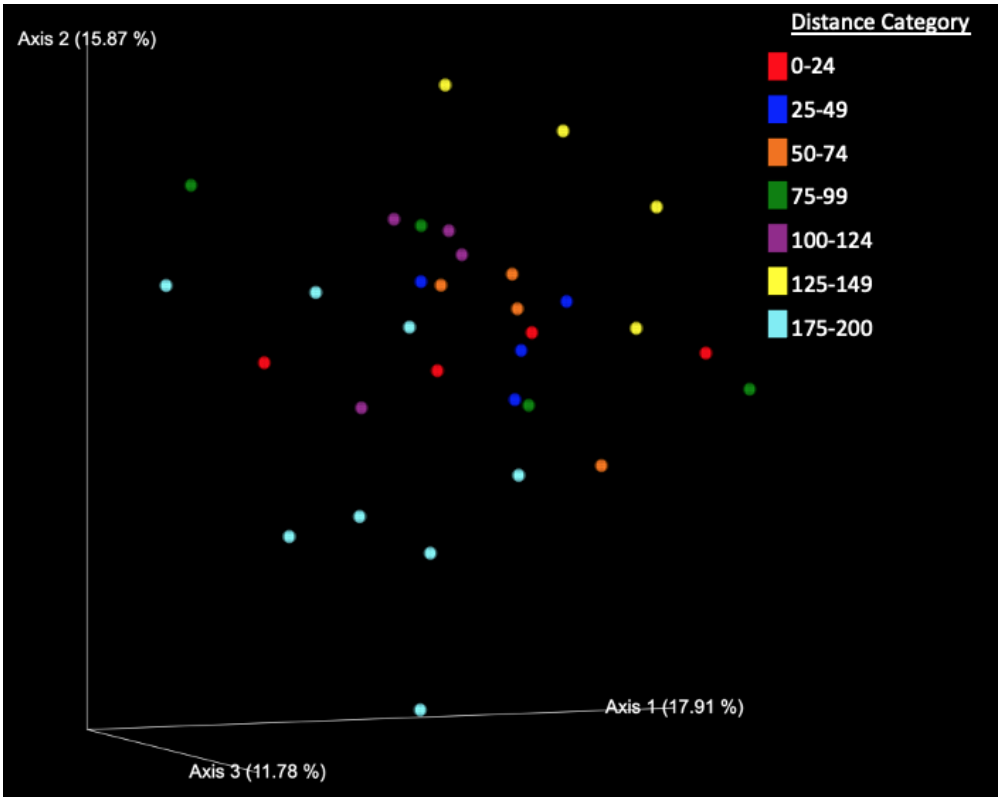

Figure A.29 *UniFrac PCoA for bacteria from Site 15470 pine samples.*

UniFrac PCoA reveals grouping by distance category is driven by Axes 1 and 2.

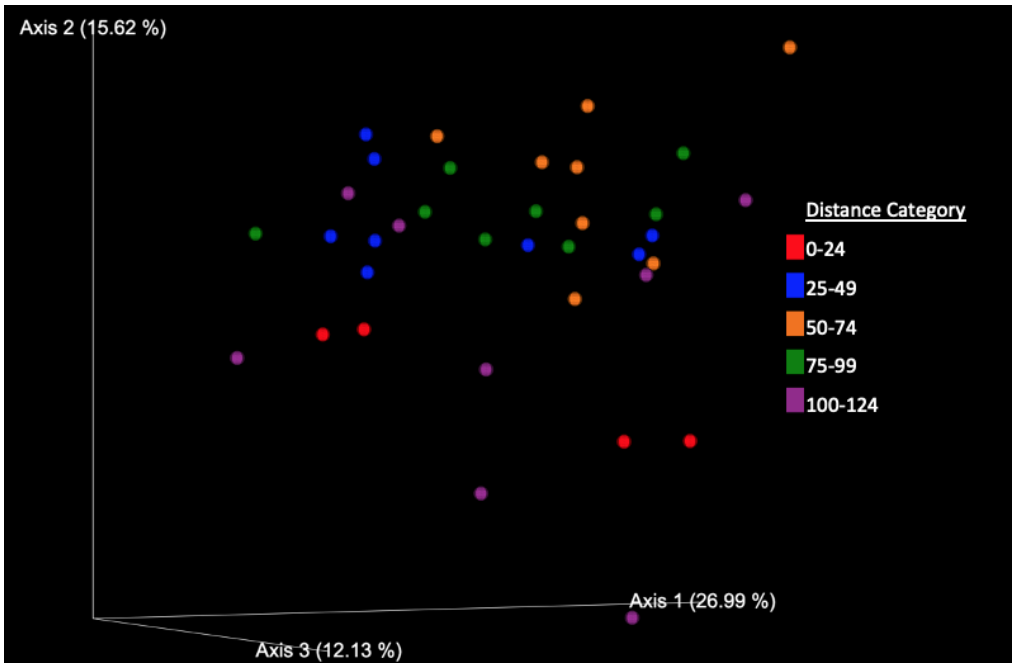

Figure A.30 *UniFrac PCoA for bacteria from Site 15711 oak samples.*

UniFrac PCoA reveals grouping by distance category is driven by Axis 1.

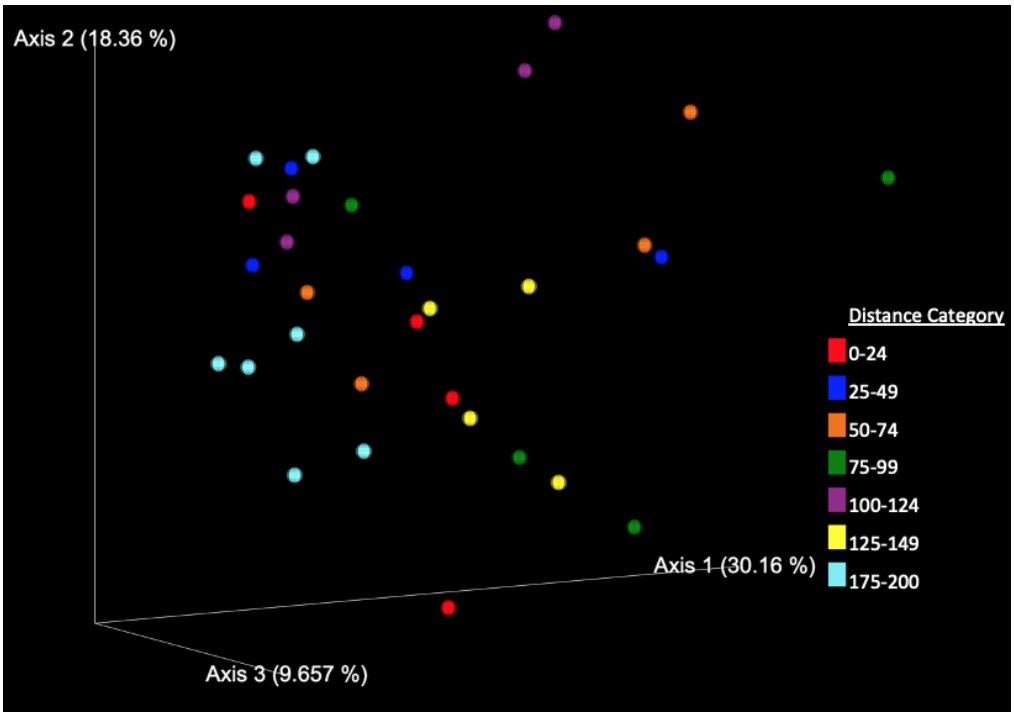

Figure A.31 *UniFrac PCoA for bacteria from Site 15470 oak samples.*

UniFrac PCoA reveals grouping by distance category is driven by Axis 1.

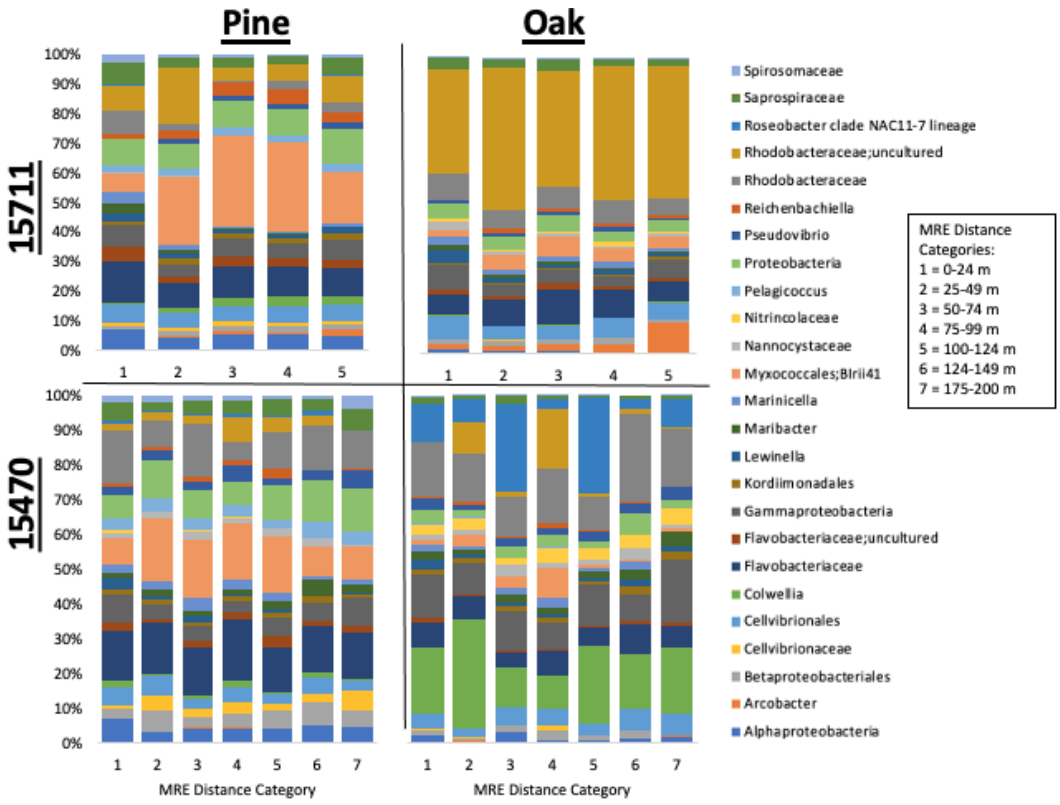

Figure A.32 *Top 25 most relative abundant bacterial OTUs at Level 7 classification for Sites 15711 and 15470.*

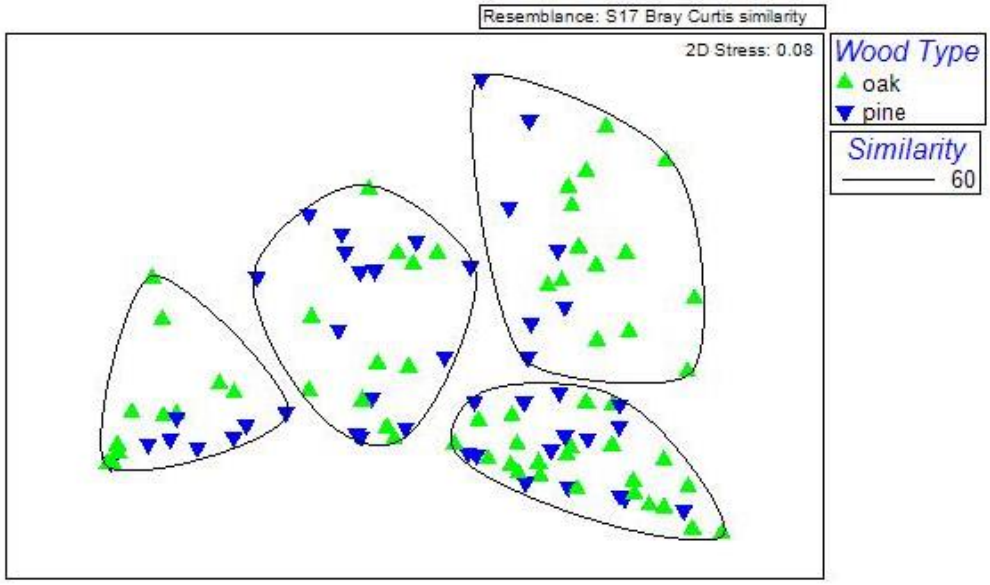

Figure A.33 *Archaea nMDS for Sites 15711 and 15470 labeled by wood type.*

nMDS of 16s rRNA archea depicts samples grouping out slightly by wood type within clusters.

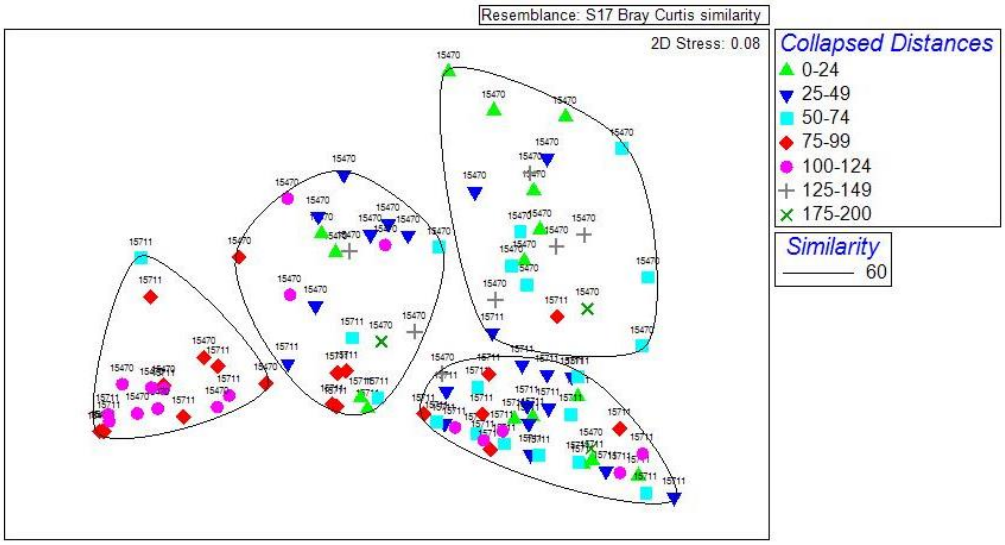

Figure A.34 *Archaea nMDS for Sites 15711 and 15470 labeled by collapsed distances.*

nMDS of 16s rRNA archaea at Sites 15711 and 15470 at 60 percent Bray-Curtis similarity depicts samples grouping out slightly by site (labels) and by distance category.

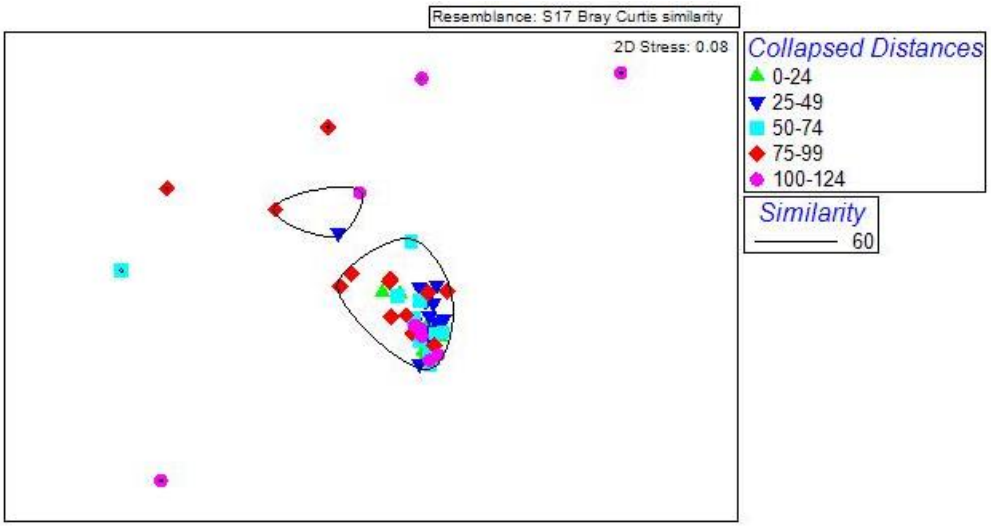

Figure A.35 *Archaea nMDS for Site 15711.*

nMDS of 16s rRNA archaea at Site 15711 at 60 percent Bray-Curtis similarity depicts samples grouping out by distance category.

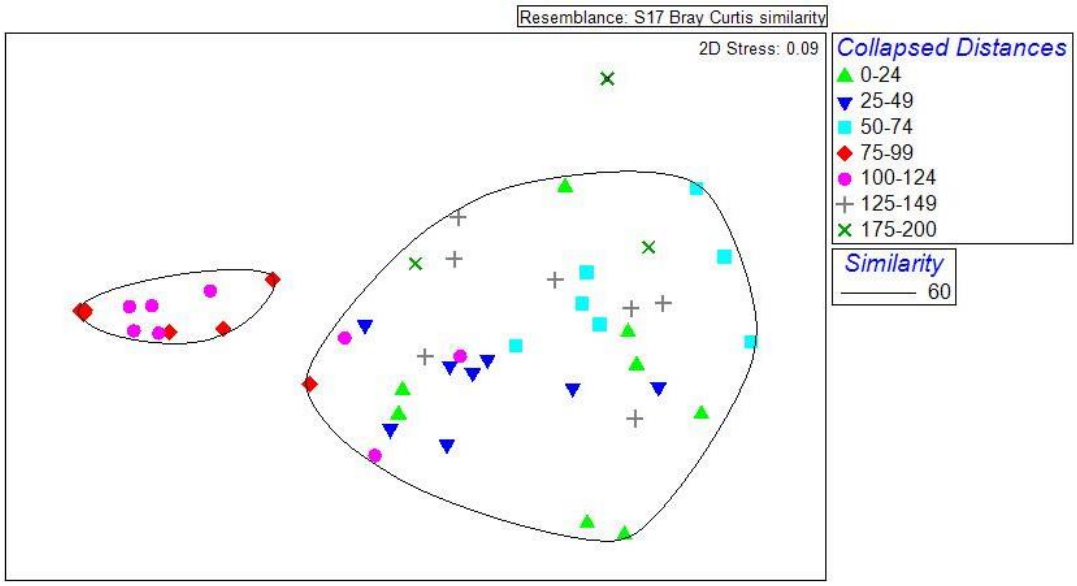

Figure A.36 *Archaea nMDS for Site 15470.*

nMDS of 16s rRNA archaea at Site 15470 at 60 percent Bray-Curtis similarity depicts samples grouping out by distance category.

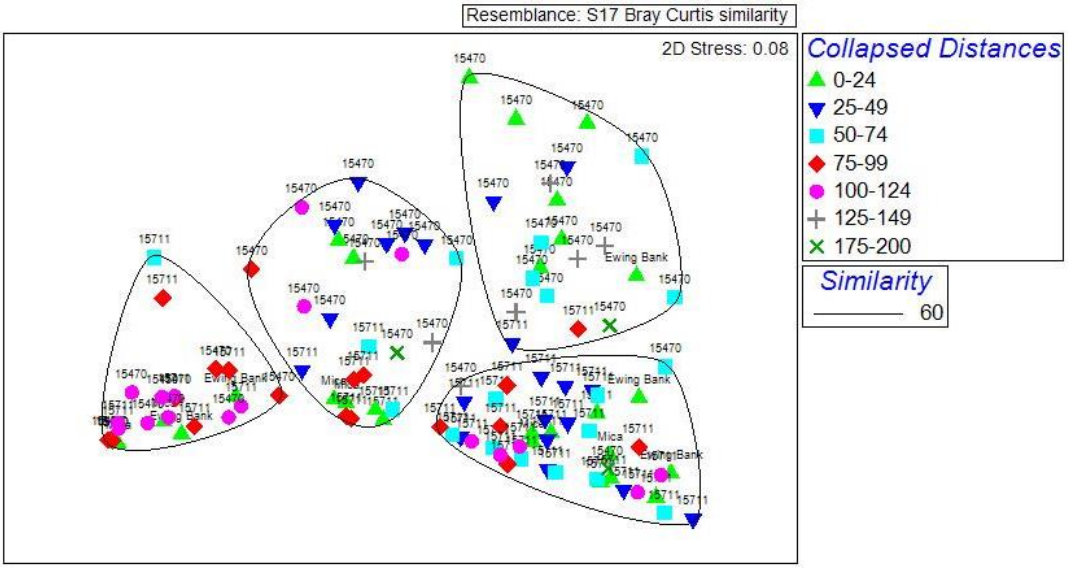

Figure A.37 *Archaea nMDS for Sites 15711, 15470, Mica and Ewing Bank.*

nMDS of 16s rRNA archaea for Sites 15711 and 15470 and *Mica* and *Ewing Bank* reveals samples from *Mica* and *Ewing Bank* in all clusters, including several in the left most one.

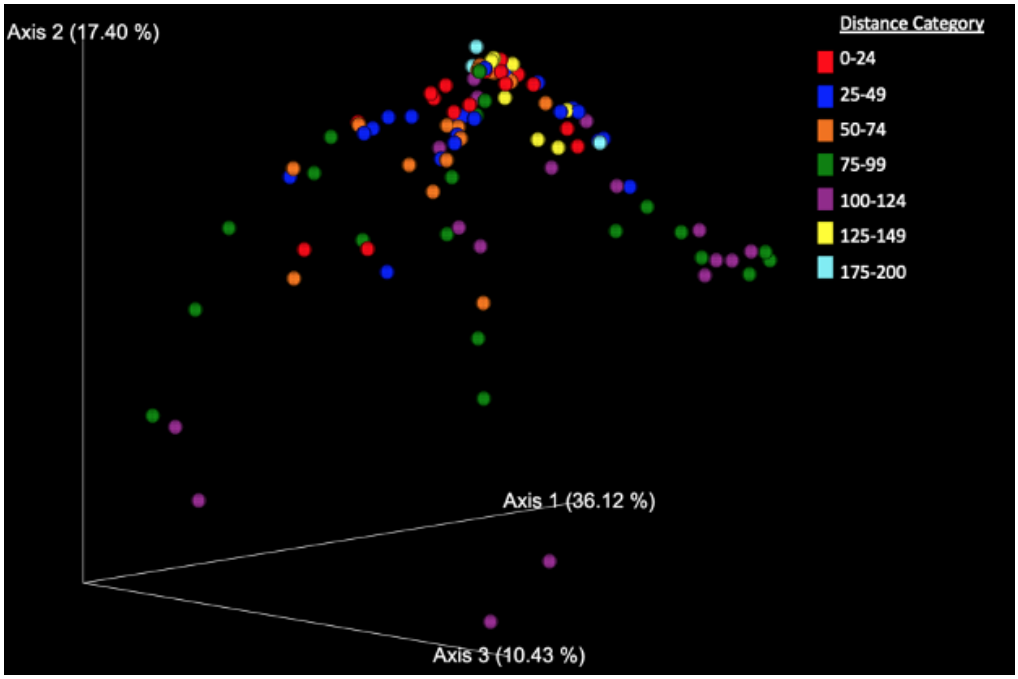

Figure A.38 *UniFrac PCoA for archaea at Sites 15711 and 15470 labeled by collapsed distance.*

UniFrac PCoA reveals grouping by distance category along Axis 1.

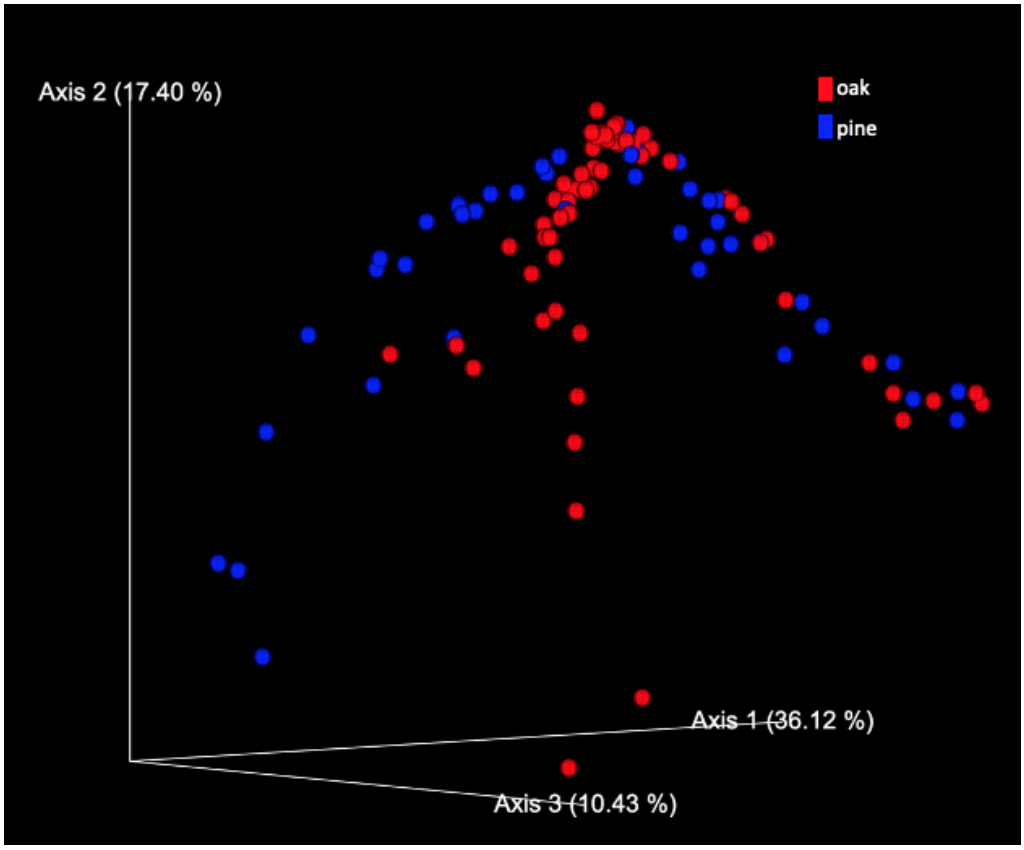

Figure A.39 *UniFrac PCoA for archaea both Sites 15711 and 15470 labeled by wood type.*

UniFrac PCoA reveals grouping by wood type along Axis 2.

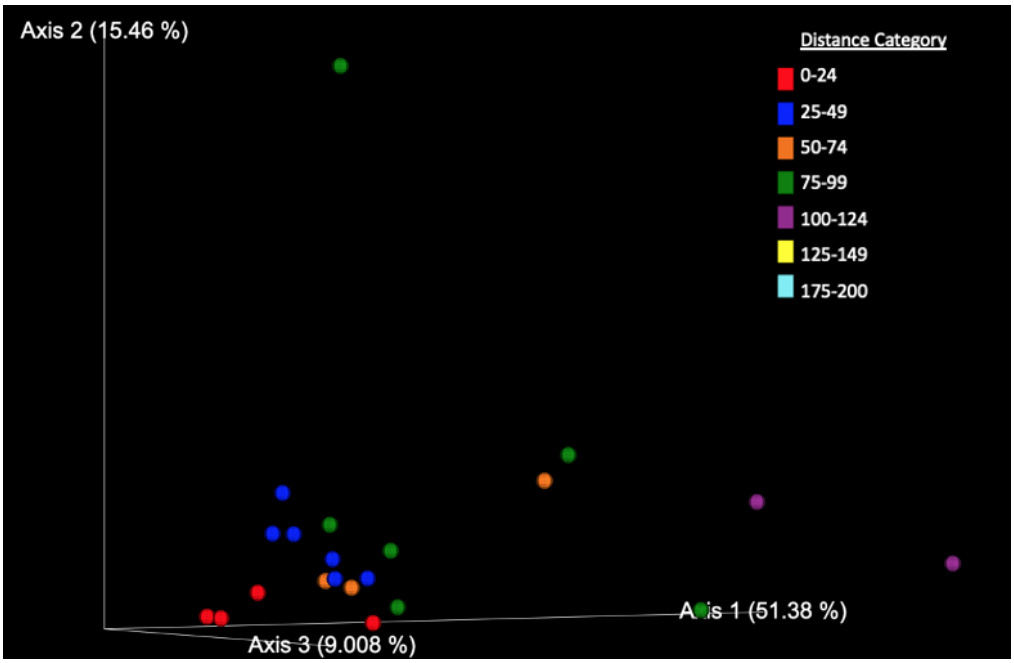

Figure A.40 *UniFrac PCoA for archaea at Site 15711 pine samples.*

UniFrac PCoA reveals grouping by distance category along Axis 1.

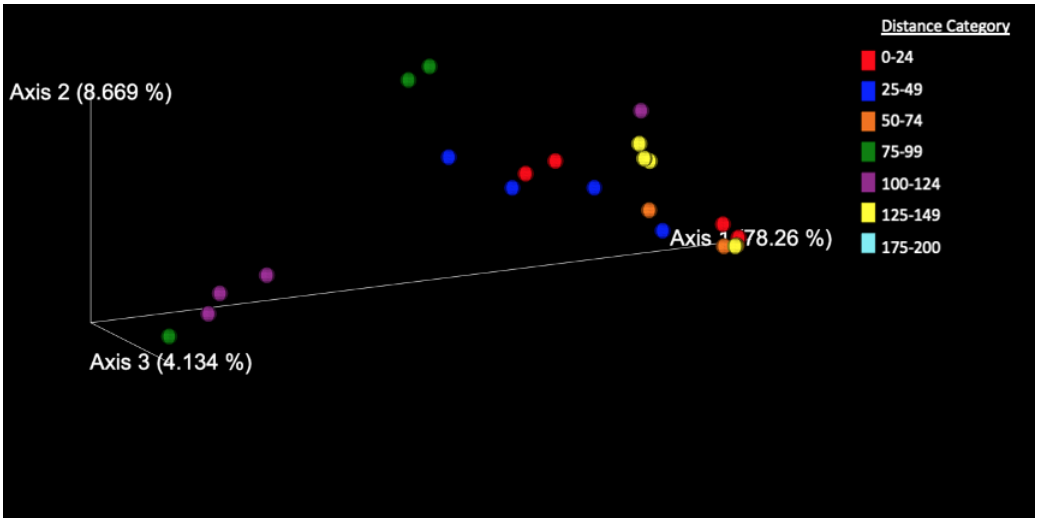

Figure A.41 UNIFRAC PCoA for archaea at Site 15470 for pine samples.

UniFrac PCoA reveals grouping by distance category along Axis 1.

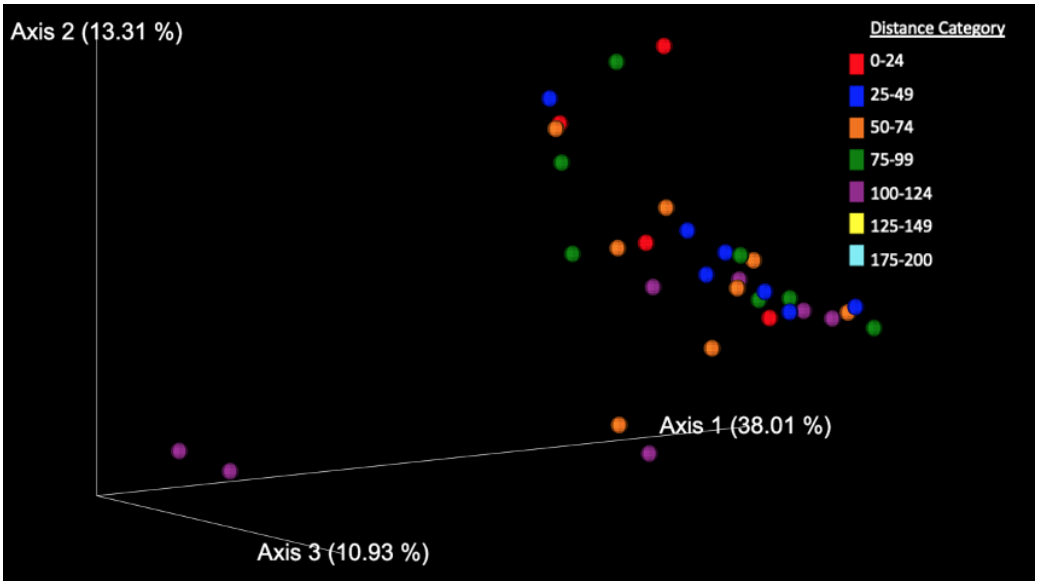

Figure A.42 UniFrac PCoA for archaea at Site 15711 oak samples.

UniFrac PCoA reveals grouping by distance category along Axis 1.

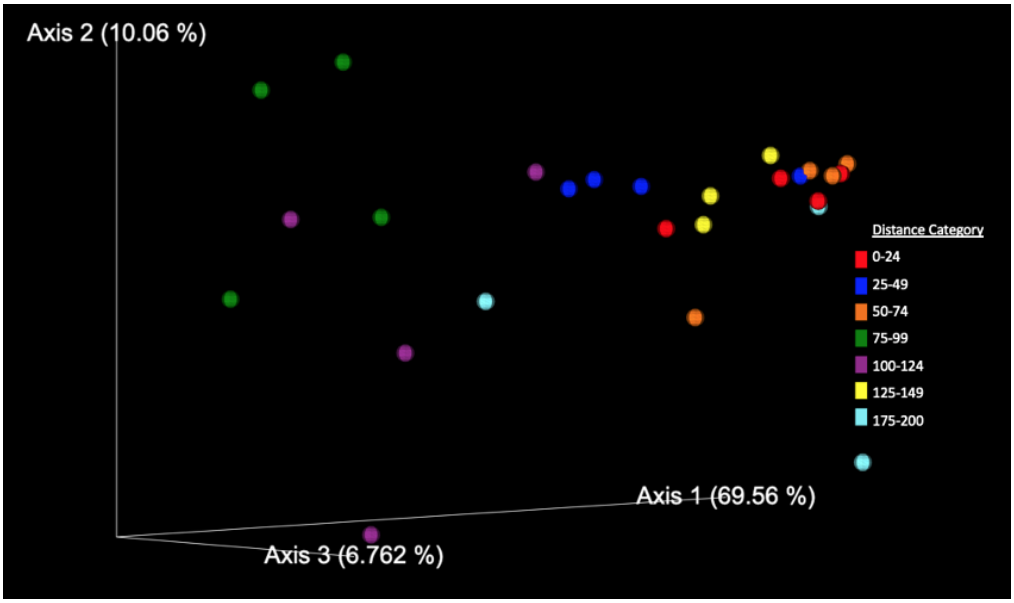

Figure A.43 UNIFRAC PCoA for archaea at Site 15470 oak samples.

UniFrac PCoA reveals grouping by distance category along Axis 1.

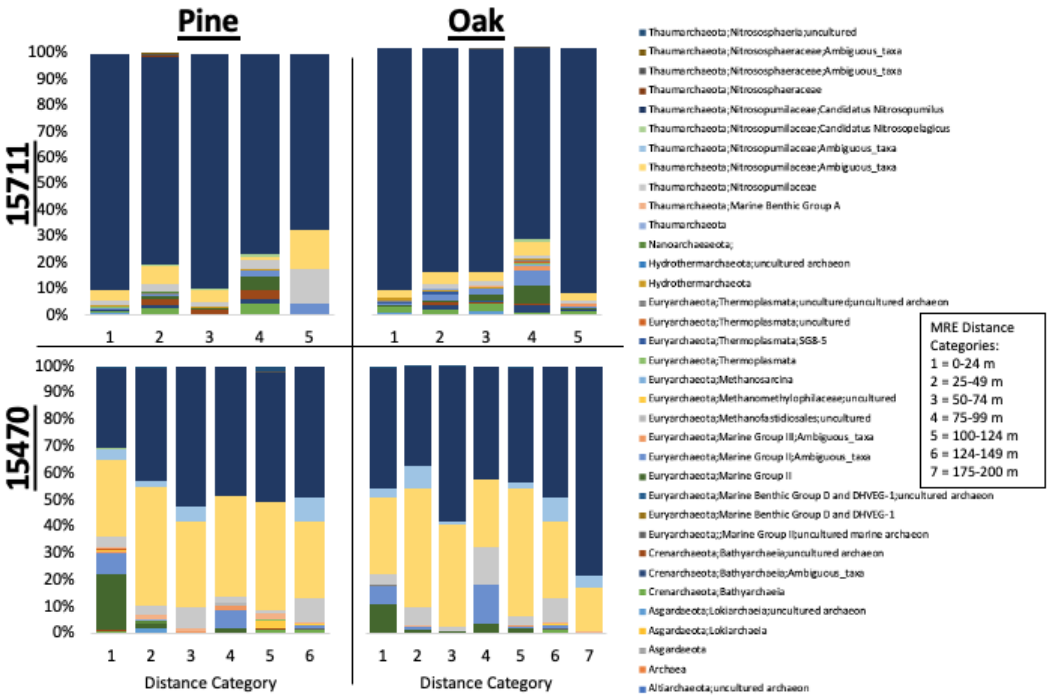

Figure A.44 *OTUs with greater than 1% relative abundance of the total archaea community at Level 7 classification for Sites 15711 and 15470.*

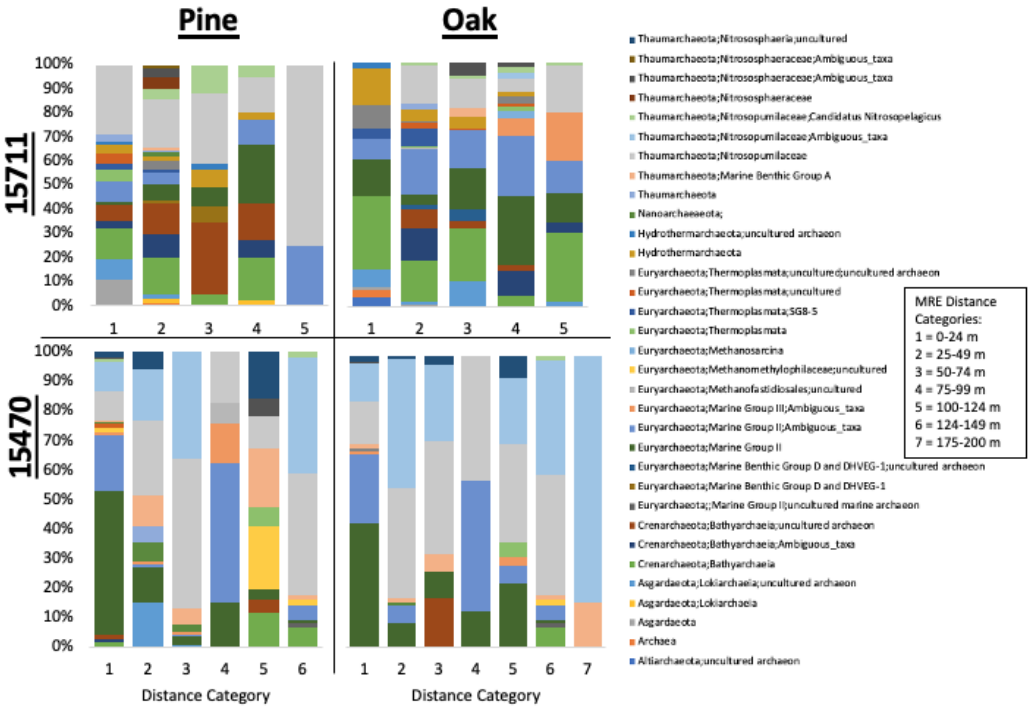

Figure A.45 *OTUs with greater than 1% relative abundance of the total archaea community at Level 7 classification for Sites 15711 and 15470 with the top 2 most relatively abundant OTUs removed.*

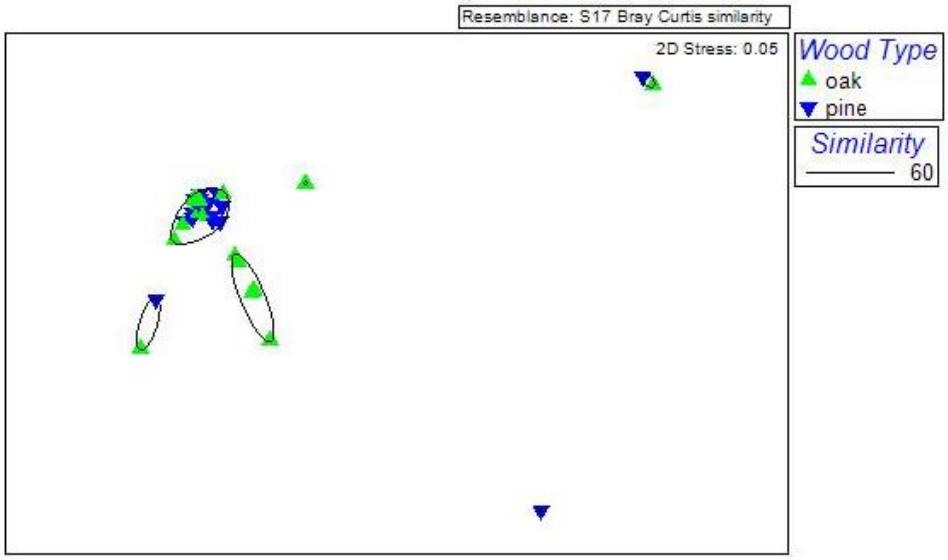

Figure A.46 *Fungi nMDS for Sites 15711 and 15470 labeled by wood type.*

nMDS of ITS2 fungi for Sites 15711 and 15470 at 60 percent Bray-Curtis similarity reveal no patterns for site, wood type, or distance.

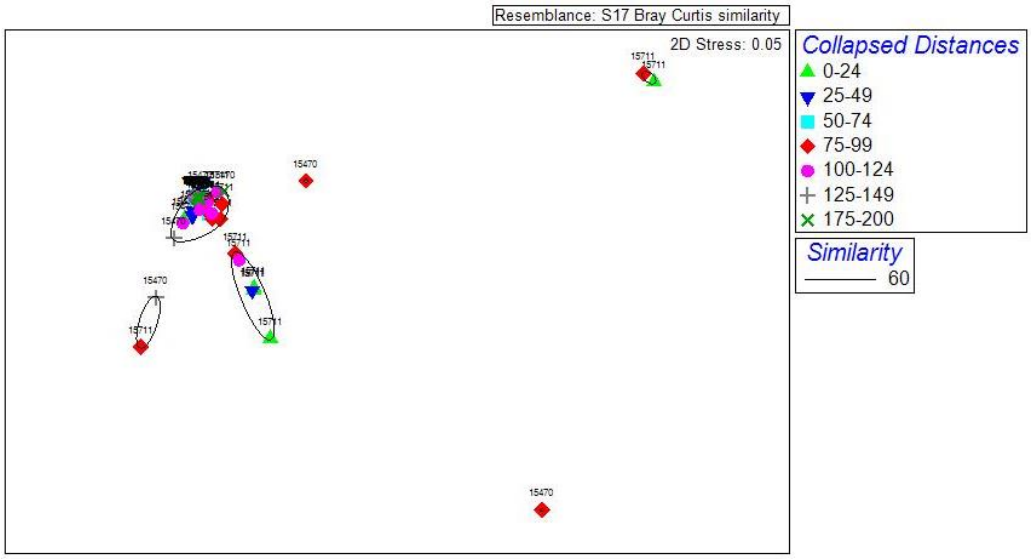

Figure A.47 *Fungi nMDS for Sites 15711 and 15470 labeled by collapsed distances.*

nMDS of ITS2 fungi for Sites 15711 and 15470 at 60 percent Bray-Curtis similarity reveal no patterns for site, wood type, or distance.

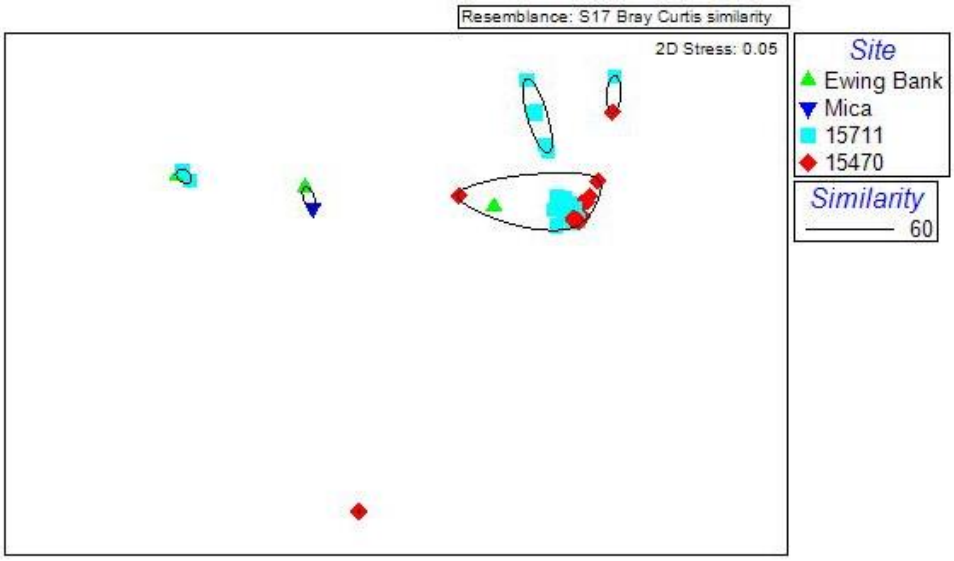

Figure A.48 *Fungi nMDS for Sites 15711 and 15470, Mica, and Ewing Bank.*

nMDS of ITS2 fungi for Sites 15711 and 15470 and *Mica* and *Ewing Bank* at 60 percent Bray-Curtis similarity reveal no patterns for site, wood type, or distance.

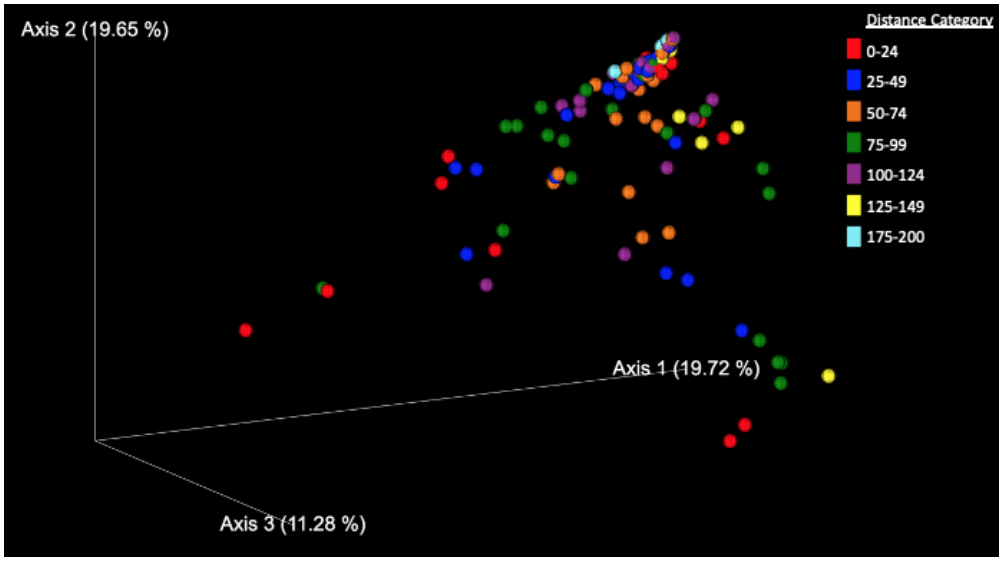

Figure A.49 *UniFrac PCoA for fungi from Sites 15711 and 15470 labeled by distance category.*

UniFrac PCoA results reveal distance category groupings along Axes 1 and 2.

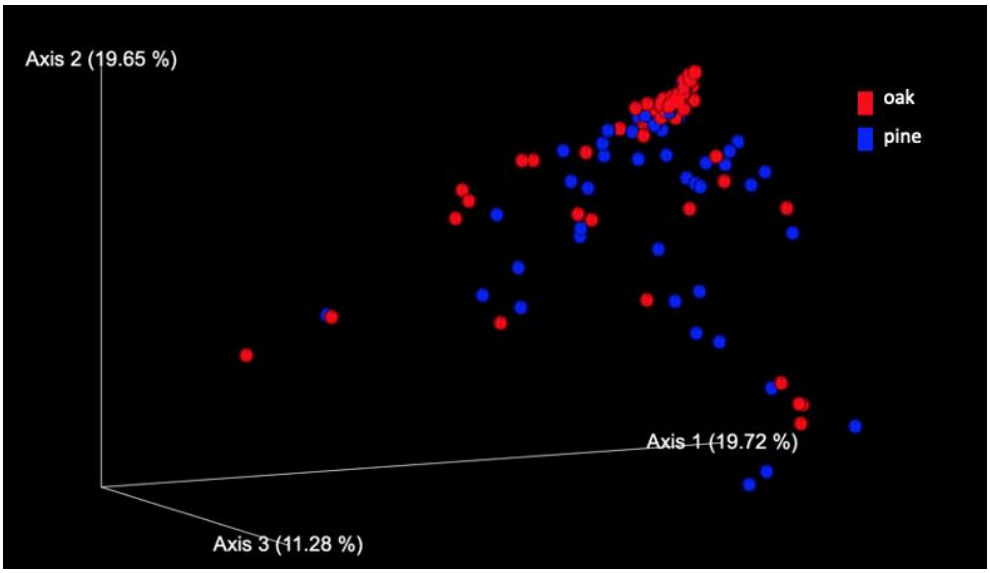

Figure A.50 UniFrac PCoA for fungi from Sites 15711 and 15470 labeled by wood type.

UniFrac PCoA results reveal distance category groupings along Axis 2.

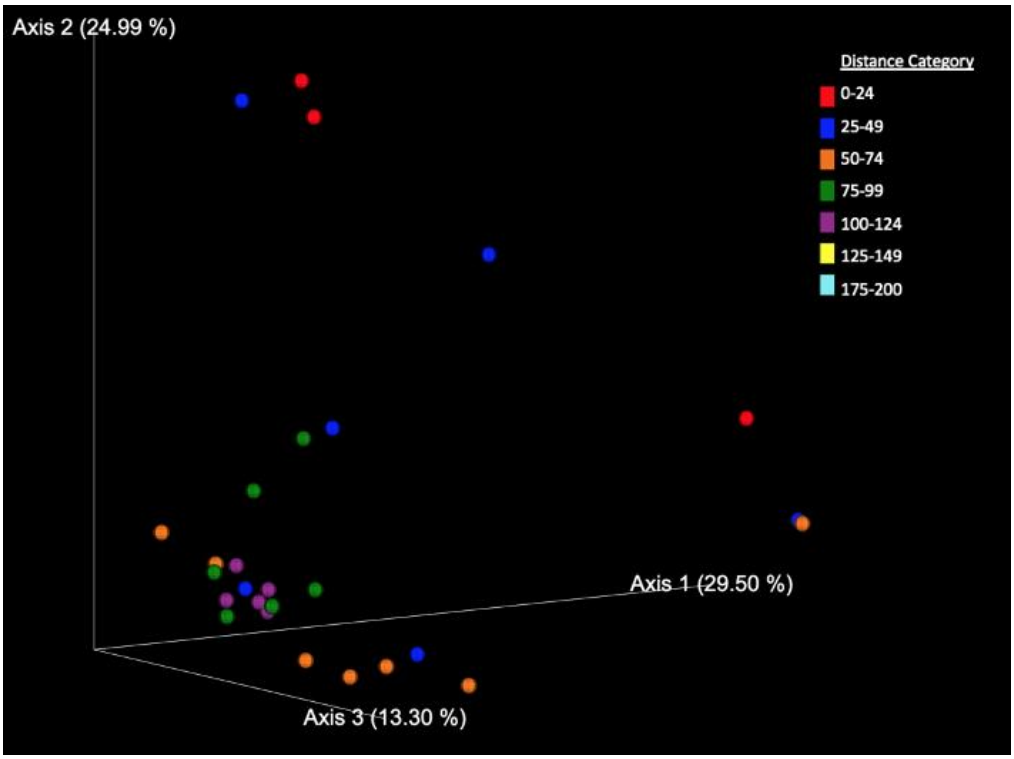

Figure A.51 UniFrac PCoA for fungi from Site 15711 pine samples.

UniFrac PCoA results reveal distance category groupings along Axes 1 and 2.

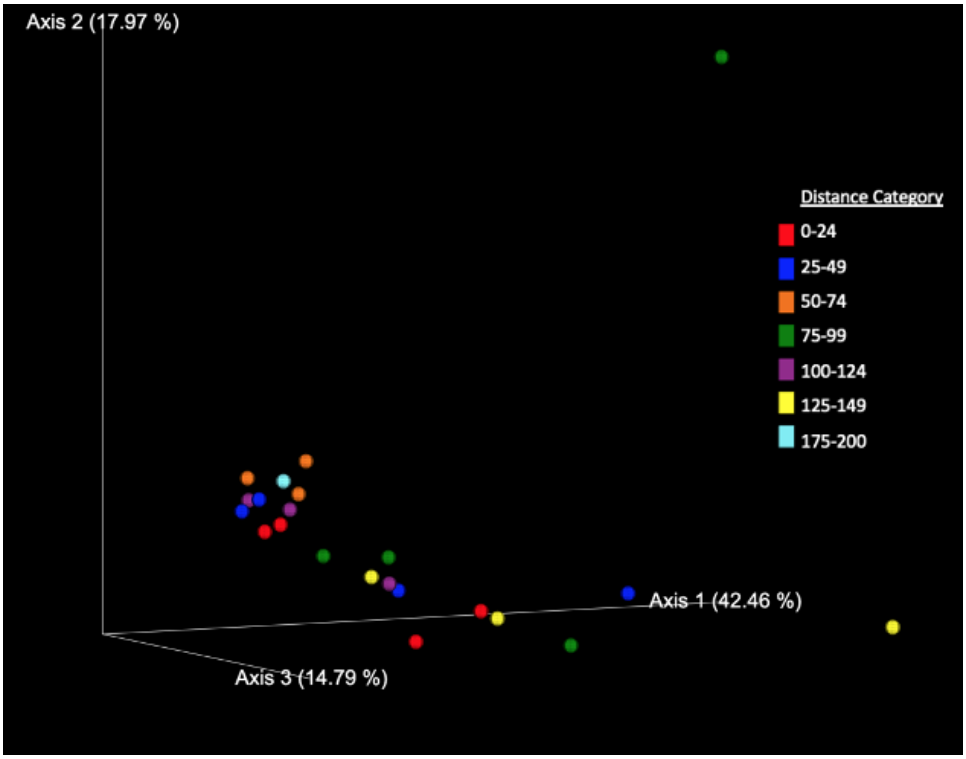

Figure A.52 UniFrac PCoA for fungi from Site 15470 pine samples.

UniFrac PCoA results reveal distance category groupings along Axis 1.

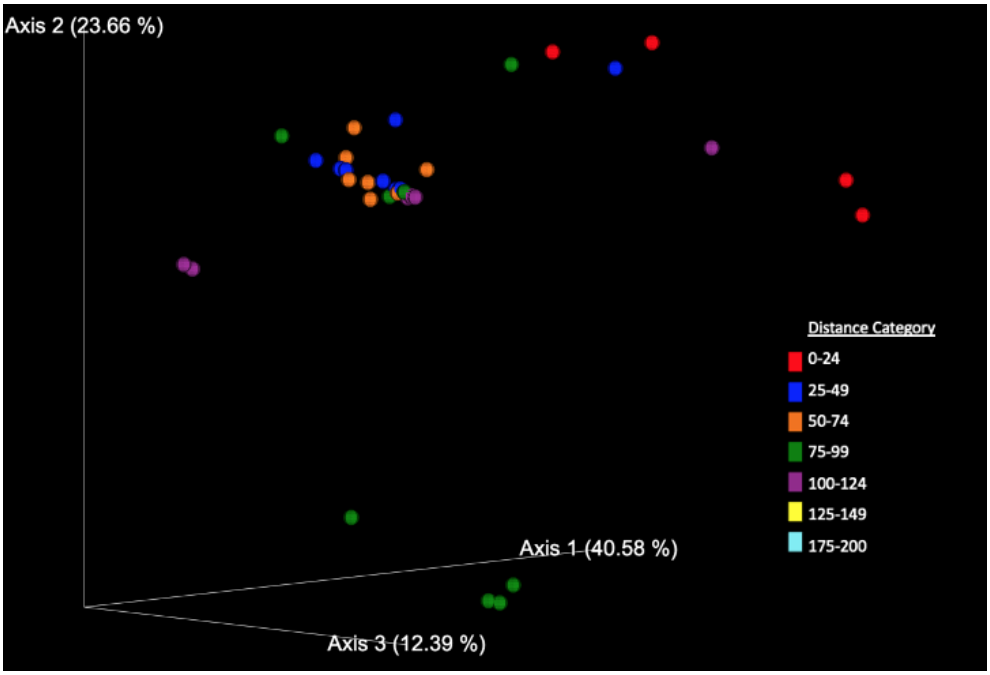

Figure A.53 *UniFrac PCoA for fungi from Site 15711 oak samples.*

UniFrac PCoA results reveal distance category groupings along Axis 1.

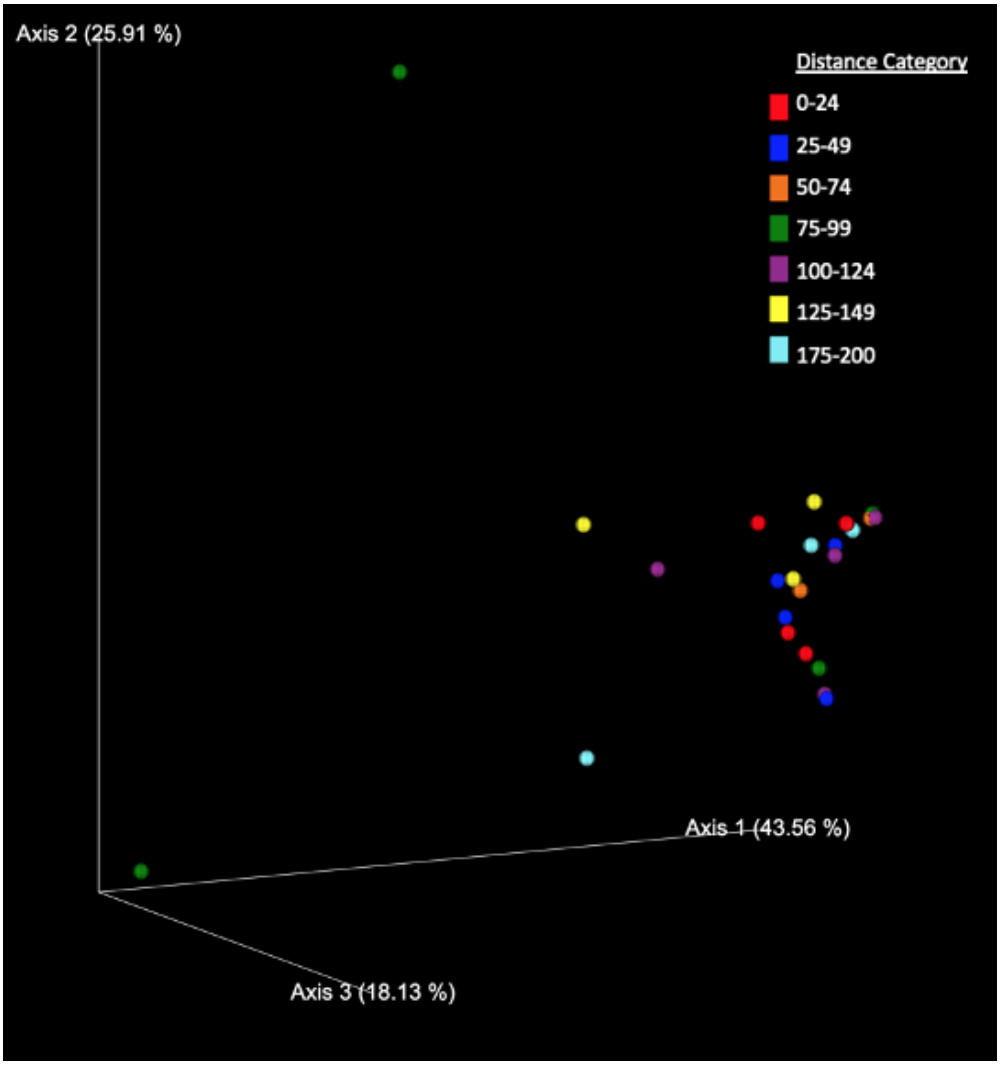

Figure A.54 UniFrac PCoA for fungi from Site 15470 oak samples.

UniFrac PCoA results reveal distance category groupings along Axis 1.

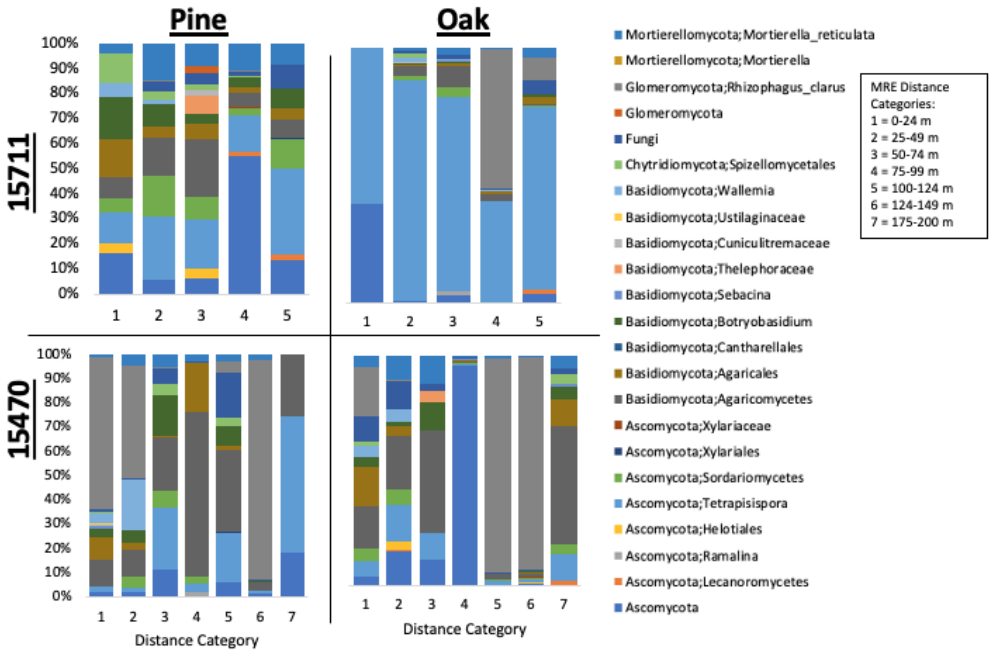

Figure A.55 *OTUs with greater than 1% relative abundance of the total fungi community at Level 7 classification for Sites 15711 and 15470.*

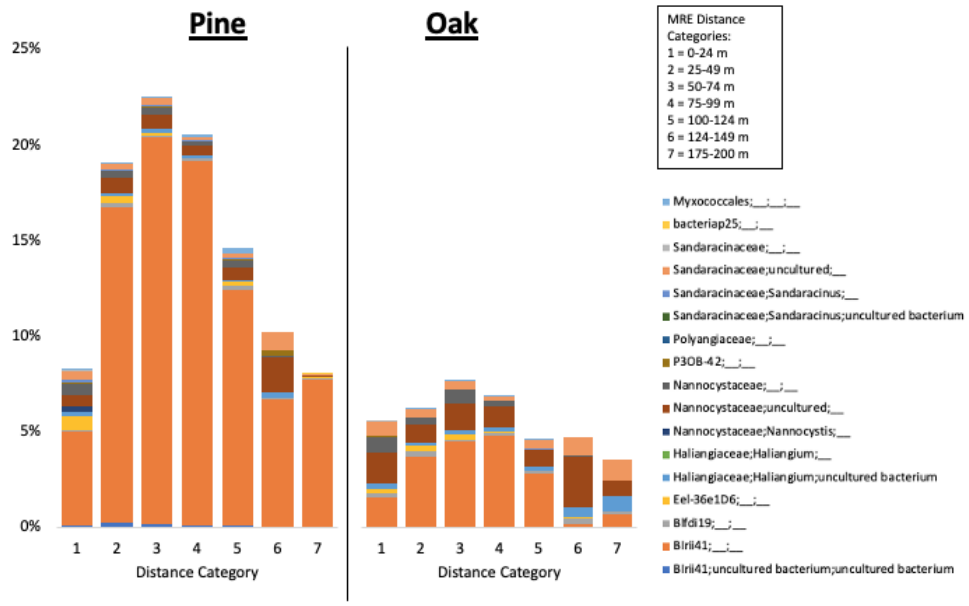

Figure A.56 *Bacterial OTUs from the order Myxococcales.*

REFERENCES

Anderson RE, Sogin ML & Baross JA (2015) Biogeography and ecology of the rare and abundant microbial lineages in deep-sea hydrothermal vents. *FEMS Microbiol Ecol* **91**: 1-11.

Auguet JC, Barberan A & Casamayor EO (2010) Global ecological patterns in uncultured Archaea. *ISME J* **4**: 182-190.

Baas-Becking, LGM (1934). Geobiologie of Inleiding Tot de Milieukunde *The Hague*.

Beijerinck, MW (1913) De infusies en de ontdekking der backteriën. *Jaarboek van de Koninklijke Akademie van Wetenschappen*.

Bell T, Ager D, Song JI, Newman JA, Thompson IP, Lilley AK & van der Gast CJ (2005) Larger islands house more bacterial taxa. *Science* **308**: 1884.

Bell E, Blake LI, Sherry A, Head IM & Hubert CRJ (2018) Distribution of thermophilic endospores in a temperate estuary indicate that dispersal history structures sediment microbial communities. *Environ Microbiol* **20**: 1134-1147.

Bienhold C, Pop Ristova P, Wenzhöfer F, Dittmar T, Boetius A (2013) How Deep-Sea Wood Falls Sustain Chemosynthetic Life. *PLoS ONE* **8**(1): e53590.

Bienhold C, Zinger L, Boetius A & Ramette A (2016) Diversity and Biogeography of Bathyal and Abyssal Seafloor Bacteria. *PLoS One* **11**: e0148016.

Callahan BJ, McMurdle PJ, Rosen MJ, Han AW, Johnson AJ, Holmes SP (2016) DADA2: High-resolution sample inference from Illumina amplicon data. *Nat Methods* **13**: 581-583.

Caporaso JG, Paszkiewicz K, Field D, Knight R & Gilbert JA (2012) The Western

English Channel contains a persistent microbial seed bank. *ISME J* **6**: 1089-1093.

Cho J & Tiedje JM (2000) Biogeography and Degree of Endmicity of Fluorescent *Pseudomonas* Strains in Soil. *American Society for Microbiology* **66**: 12.

Colwell FS & D'Hondt S (2013) Nature and Extent of the Deep Biosphere. *Reviews in Mineralogy and Geochemistry* **75**: 547-574.

Comeau AM, Vincent WF, Bernier L & Lovejoy C (2016) Novel chytrid lineages dominate fungal sequences in diverse marine and freshwater habitats. *Sci Rep* **6**: 30120.

Comeau AM, Li WK, Tremblay JE, Carmack EC & Lovejoy C (2011) Arctic Ocean microbial community structure before and after the 2007 record sea ice minimum. *PLoS One* **6**: e27492.

Comte J, Monier A, Crevecoeur S, Lovejoy C & Vincent WF (2016) Microbial biogeography of permafrost thaw ponds across the changing northern landscape. *Ecography* **39**: 609-618.

Comte J, Culley AI, Lovejoy C, & Vincent WF (2018) Microbial connectivity and sorting in a High Arctic watershed. *The ISME Journal* **12**: 2988-3000.

Damour M, Church R, Warren D, Horrell C, Hamdan L (2016) "Gulf of Mexico Shipwreck Corrosion`, Hydrocarbon Exposure`, Microbiology`, and Archaeology (GOM-SCHEMA) Project: Studying the Effects of a Major Oil Spill on Submerged Cultural Resources," in *Proceedings for Historical Archaeology Annual Conference*, (Germantown, MD: Society for Historical Archaeology), 51-61.

Darcy JL, Gendron EMS, Sommers P, Porazinska DL & Schmidt SK (2018) Island

Biogeography of Cryoconite Hole Bacteria in Antarctica's Taylor Valley and Around the World. *Frontiers in Ecology and Evolution* **6**

Dick GJ, Anantharaman K, Baker BJ, Li M, Reed DC & Sheik CS (2013) The microbiology of deep-sea hydrothermal vent plumes: ecological and biogeographic linkages to seafloor and water column habitats. *Front Microbiol* **4**: 124.

Distel DL, Altamia MA, Lin Z, *et al.* (2017) Discovery of chemoautotrophic symbiosis in the giant shipworm Kuphus polythalamia (Bivalvia: Teredinidae) extends wooden-steps theory. *Proc Natl Acad Sci U S A* **114**: E3652-E3658.

Distel DLB, A.R.; Chuang, E.; Morrill, W.; Cavanaugh, C.; Smith, C.R. (2000) Do mussels take wooden steps to deep-sea vents? *Nature* **403**: 725-726.

Faegervold, SK, Galand, PE, Zbinden M, Giall, F, Lebaron, P, Palacios, C (2012) Sunken woods on the ocean floor provide diverse specialized habitats for microorganisms. *FEMS Microbiol Ecol* **82**: 616-628.

Fenchel T (2003) Biogeography for Bacteria. *Science* **301**: 925-926.

Finlay BJ (2002) Global Dispersal of Free-Living Microbial Eukaryote Species. *Science* **296**: 1061-1063.

Galand PE, Potvin M, Casamayor EO & Lovejoy C (2010) Hydrography shapes bacterial biogeography of the deep Arctic Ocean. *ISME J* **4**: 564-576.

Garrett TR, Bhakoo M & Zhang Z (2008) Bacterial adhesion and biofilms on surfaces. *Progress in Natural Science* **18**: 1049-1056.

Goffredi SK & Orphan VJ (2010) Bacterial community shifts in taxa and diversity in

response to localized organic loading in the deep sea. *Environ Microbiol* **12**: 344-363.

Hamdan LJ, Coffin RB, Sikaroodi M, Greinert J, Treude T & Gillevet PM (2013) Ocean currents shape the microbiome of Arctic marine sediments. *ISME J* **7**: 685-696.

Hamdan LJ, Salerno JL, Reed A, Joye SB, Damour M (2018) The impact of the Deepwater Horizon blowout on historic shipwreck-associated sediment microbiomes in the northern Gulf of Mexico. *Sci Rep* **8**: 9057.

Hamilton P (2009) Topographic Rossby waves in the Gulf of Mexico. *J Phys Oceanogr* **20**: 1087-1104.

Hanson CA, Fuhrman JA, Horner-Devine MC, Martiny JBH (2012) Beyond biogeographic patterns: processes shaping the microbial landscape. *Nat Rev Microbiol.* **10**: 497-506.

Hedlund BP, Staley, JT (2004) Microbial Endemism and Biogeography. *Microbial Diversity and Bioprospecting*. Chapter 22.

Hoshino T, Doi H, Uramoto G, Wörmer L, Adhikari RR, Xiao N, *et al*., (2020) Global diversity of microbial communities in marine sediment. *PNAS* **117**: 27587-27597.

Huber JA, Welch DBM, Morrison HG, Huse SM, Neal PR, Butterfield DA, Sogin ML (2007) Microbial Population Structures in the Deep Marine Biosphere. *Science* **318**: 97-100.

Jadoon WA, Nakai R, Naganuma T (2012) Biogeographical note on Antacrctic microgloreae: Endemism and cosmoploitanism. *Geosci Fron* **4**: 633-646.

Kalenitchenko D, Fagervold SK, Pruski AM, Vétion G, Yücel M, Le Bris N, Galand PE (2015) Temporal and spatial constraints on community assembly during microbial

colonization of wood in seawater. *ISME J* **9**: 2657–2670.

Kallmeyer J, Pockalny R, Adhikari RR, Smith DC & D'Hondt S (2012) Global distribution of microbial abundance and biomass in subseafloor sediment. *Proc Natl Acad Sci U S A* **109**: 16213-16216.

Knights D, Kuczynski J, Charlson ES, Zaneveld J, Mozer MC, Collman RG, Bushman FD, Knight R & Kelley ST (2011) Bayesian community-wide culture-independent microbial source tracking. *Nat Methods* **8**: 761-763.

Levin LA, Baco AR, Bowden DA, Colaco A, *et al*., (2016) Hydrothermal Vents and Methane Seeps: Rethinking the Sphere of Influence. *Frontiers in Marine Science* **3**.

Leys C, Ley C, Klein O, Bernard P, & Licata L (2013) Detecting outliers: Do not use standard deviation around the mean, use absolute deviation around the mean. *Journal of Experimental Socail Psychology*.

Lindstrom ES & Lagenheder S (2011) Local and regional factors influencing bacterial community assembly. *Env Microbiol Rep* **4**: 1-9.

Lozupone C, Knight R (2005) UniFrac: a New Phylogenetic Meghod for Comparing Microbial Communites. *App Environ Micro* **71**(12): 8228-8235.

Macarthur RH, Wilson EO (1967) *The Theory of Island Biogeography*. Princeton University Press, Princeton, NJ.

Martiny JB, Bohannan BJ, Brown JH, *et al.* (2006) Microbial biogeography: putting microorganisms on the map. *Nat Rev Microbiol* **4**: 102-112.

Mason OU, Canter EJ, Gillies LE, Paisie TK, Roberts BJ (2016) Mississippi river plume enriches microbial diversity in the northern gulf of Mexico. *Front Microbiol* **7**.

Mugge RL, Brock ML, Salerno JL, Damour M, Church RA, Lee JS & Hamdan LJ (2019) Deep-Sea Biofilms, Historic Shipwreck Preservation and the Deepwater Horizon Spill. *Frontiers in Marine Science* **6**.

Op de Beeck M, Lievens B, Busschaert P, Declerck S, Vangronsveld J, Colpaert JV (2014) Comparison and validation of some ITS primer pairs useful for fungal metabarcoding studies. *PLOS One* **9**: e97629-e97629.

Orcutt BN, Sylvan JB, Knab NJ, Edwards KJ (2011) Microbial Ecology of the Darck Ocean above, at, and below the Seafloor. *Miicrobiology and Molecular Biology Reviews* **75**: 2.

Overholt WA, Schwing P, Raz KM, Hastings D, Hollander DJ, Kostka JE (2019) The core seafloor microbiome in the Gulf of Mexico is remarkably consistent and shows evidence of recovery from disturbance caused by major oil spills. *Environ Microbiol* **21**: 4316–4329.

Palacios C, Zbinden M, Pailleret M, Gaill F & Lebaron P (2009) Highly similar prokaryotic communities of sunken wood at shallow and deep-sea sites across the oceans. *Microb Ecol* **58**: 737-752.

Pedersen NB, Matthiesen H, Blanchette RA, Alfredsen G, Held BW, Westergaard-Nielsen A, Hollesen J (2020) Fungal attack on archaeological wooden artefacts in the Arctic- implications in a changing climate. *Scientific Reports* **10**: 14577.

Perez-Brunius P, Furey H, Bower A, Hamilton P, Candela J, Garcia-Carillo P, Leben R (2018) Dominant Circulation Patterns of the Deep Gulf of Mexico. *J Phys Oceanogr* **48**: 511-529.

Ristova P, Bienhold C, Wenzhöfer F, Rossel PE, Boetius A (2017) Temportal and

Spatial Variations of Bacterial and Faunal Communities Associated with Deep-Sea Wood Falls. *PLoS ONE* **12**(1): e0169906.

Ruff, S. E. *et al.* (2015) Global dispersion and local diversification of the methane seep microbiome. *P Natl Acad Sci USA* **112**, 4015-4020.

Sánchez-Soto Jiménez MF, Cerqueda-García D, Montero-Muñoz JL, Aguirre-Macedo ML, García-Maldonado JQ (2018) Assessment of the bacterial community structure in shallow and deep sediments of the Perdido Fold Belt region in the Gulf of Mexico. *Peer J* **6**: e5583

Smith CR, Kukert H, Wheatcroft RA, Jumars PA, Deming JW (1989) Vent fauna on whale remains. Nature **32**: 251-253.

Smith CR, Baco AR (2003) Ecology of Whale Falls at the Deep-Sea Floor. *Oceanography and Marine Biology: an Annual Review* **41**: 311-354.

Smith CR, Glover AG, Treude T, Higgs ND, Amon DJ (2015) Whale-Fall Ecosystems: Recent Insights into Ecology, Paleoecology, and Evolution. *Ann Rev Mar Sci* **7**: 571–596.

Storesund JE, Sandaa R, Thingstad TF, Asplin L, Albretsen J, Erga SR (2017) Linking bacterial community structure to advection and environmental impact along a coast-fjord gradient of the Sognefjord, western Norway. *Progress in Oceanography* **159**: 13-30.

Tolar BB, Reji L, Smith JM, Blum M, Pennington JT, Chavez FP, Francis CA (2020) Time series assessment of Thaumarchaeota ecotypes in Monterey Bay reveals the importance of water column position in predicting distribution–environment relationships. *Limnol Oceanogr* **65**: 2041–2055.

van der Gast CJ, Lilley AK, Ager D & Thompson IP (2005) Island size and bacterial diversity in an archipelago of engineering machines. *Environ Microbiol* **7**: 1220-1226.

Wolff T (1979) Macrofaunal Utilization of Plant Remains in the Deep Sea. *Sarsia* **64**: 117-136.

Zinger L, Amaral-Zettler LA, Fuhrman JA, Horner-Devine MC, Huse SM, Welch DBM, Martiny JBH, Sogin M, Boetius A, Ramette A (2011) Global patterns of bacterial beta-diversity in seafloor and seawater ecosystems. *PLoS One* **6**: 1–11.